Seismic stratigraphy and attribute analysis of the Mesozoic and Cenozoic of the Penobscot Area, offshore Nova Scotia

TAYLOR CAMPBELL

SUPERVISOR: DR.GRANT WACH

Submitted in Partial Fulfilment of the Requirements
for the Degree of Bachelor of Sciences, Honours
Department of Earth Sciences
Dalhousie University, Halifax, Nova Scotia
March 2014

Distribution License

DalSpace requires agreement to this non-exclusive distribution license before your item can appear on DalSpace.

NON-EXCLUSIVE DISTRIBUTION LICENSE

You (the author(s) or copyright owner) grant to Dalhousie University the non-exclusive right to reproduce and distribute your submission worldwide in any medium.

You agree that Dalhousie University may, without changing the content, reformat the submission for the purpose of preservation.

You also agree that Dalhousie University may keep more than one copy of this submission for purposes of security, back-up and preservation.

You agree that the submission is your original work, and that you have the right to grant the rights contained in this license. You also agree that your submission does not, to the best of your knowledge, infringe upon anyone's copyright.

If the submission contains material for which you do not hold copyright, you agree that you have obtained the unrestricted permission of the copyright owner to grant Dalhousie University the rights required by this license, and that such third-party owned material is clearly identified and acknowledged within the text or content of the submission.

If the submission is based upon work that has been sponsored or supported by an agency or organization other than Dalhousie University, you assert that you have fulfilled any right of review or other obligations required by such contract or agreement.

Dalhousie University will clearly identify your name(s) as the author(s) or owner(s) of the submission, and will not make any alteration to the content of the files that you have submitted.

If you have questions regarding this license please contact the repository manager at dalspace@dal.ca.

Grant the distribution license by signing and dating below.

_____ _____

Name of signatory Date

DALHOUSIE UNIVERSITY
Inspiring Minds

Department of Earth Sciences
Halifax, Nova Scotia
Canada B3H 4R2
(902) 494-2358
FAX (902) 494-6889

DATE: April, 16/2014

AUTHOR: Taylor Campbell

TITLE: Seismic Stratigraphy and attribute analysis of the Mesozic and Cenozoic of the Penobscot area, offshore Nova Scotia

Degree: B.Sc Convocation: May Year: 2014

DALHOUSIE UNIVERSITY

DEPARTMENT OF EARTH SCIENCES

The readers of this thesis entitled "Seismic Stratigraphy and attribute analysis of the Mesozoic and Cenozoic of the Penobscot area, offshore Nova Scotia" by Taylor Campbell in partial fulfillment of the requirements for the degree of Bachelors of Science are the following:

Supervisor: Dr. Grant Wach

Readers: Dr. Marcos Zentilli and Dr. Martin Gibling

ABSTRACT

The Penobscot Area is located within the Scotian Basin, northwest of Sable Island, offshore Nova Scotia and comprises geological formations with representative properties for petroleum system in the basin. The Penobscot dataset includes a 3D seismic survey covering 87 km^2, two well logs and corresponding cored intervals totaling nearly 52 m. The cored intervals provide a detailed analysis of the Abenaki and Lower Missisauga formations, both known reservoirs within the Scotian Basin. Penobscot L-30 and Penobscot B-41 are 2 of 180 exploratory wells that have been drilled in the Scotian Basin since 1980. Both wells had hydrocarbon shows, however were not considered to be economic.

This study has been designed to determine whether seismic inversion, in conjunction with 3D seismic and well datasets, provides a valuable analytical tool of the rock properties of strata in the Scotian Basin. The analysis of the 3D seismic is completed using geologic software (e.g. Petrel) to interpret the seismic facies, structure, stratigraphy, and seismic attribute analysis. The focus of this study is on seismic inversion that solves for acoustic and elastic properties from the 3D seismic data. Inverting the seismic data from a reflector to a layer property provides a clearer understanding of the subsurface geology and the potential hydrocarbon reservoirs within the survey. Seismic inversion is used to correlate the well logs across the seismic survey to define the reservoirs of interest. The cored intervals from both wells are studied, examining the characteristics of different lithofacies and their corresponding depositional environments. The lithofacies from the core are tied to the well logs to develop petrophysical facies, and then tied to the seismic data to define the seismic facies. The inversion result confirms the correlation of the lithofacies to the petrophysical facies and enables the geological properties to be known within the entire survey area.

Keywords: Penobscot survey area, seismic inversion, acoustic impedance, P-impedance, seismic facies, lithofacies.

TABLE OF CONTENTS

TABLE OF FIGURES

TABLE OF TABLES

ACKNOWLEDGEMENTS

I would like to acknowledge and thank my supervisor Dr. Grant Wach for the opportunity to work on such an intriguing and stimulating project as well as his suggestions, encouragement and sense of humor, which helped me through the researching and writing process of this honors thesis. I would also like to thank Dr. Grant Wach for allowing me to partake in so many amazing opportunities throughout the past two years. Thank you to James Johnson and Lamuail Bashir from Jason- a CGG Company who were both gracious and patient enough to teach me the ins and outs of the Jason Software. I would also like to thank Dr. Martin Gibling for all of his advice and help throughout the entire process. To all my colleagues at the Basin and Reservoir Lab, especially Ricardo Silva, Carlos Wong and Dawn Tobey who all were very willing to lend their knowledge and their time when needed, thank you. Furthermore I would like to thank all of my friends and colleagues in the Earth Sciences Department at Dalhousie University who allowed me to have an unforgettable four years.

CHAPTER ONE – INTRODUCTION

1.1 Objectives:

The purpose of this thesis is to define the seismic facies, structure, sequence stratigraphy and seismic attributes of the Mesozoic and Cenozoic of the Penobscot area, offshore Nova Scotia, to interpret the depositional setting. This analysis is based in part on a 3D seismic survey located on the Scotian Shelf, within the Scotian Basin (Figure 1.1). The Penobscot area covers 87 km^2, located southwest of mainland Nova Scotia (Figure. 1.1). The focus of the interpretation is on seismic inversion, the first non-proprietary analysis completed on the Scotian margin, with acoustic impedance, which solves for the acoustic and elastic properties of seismic data. Inverting seismic reflections to acoustic impedance provides a greater understanding of the subsurface geology in terms of strata and lithology. Seismic inversion also is valuable for determining hydrocarbon potential, and could assist future exploration projects within the Scotian Basin. Acoustic impedance also produces more accurate and detailed structural and stratigraphic interpretations than can be obtained from seismic interpretation. In this study, data derived from seismic inversion will answer the question of whether acoustic impedance, in conjunction with seismic and well data can determine and confirm lithologies within the Scotian Basin.

1.2 Scope of Study:

To understand the benefits of acoustic impedance, components of the Penobscot dataset are analysed and compared to the final inversion result. These components include well log data from two wells in the area, Penobscot L-30, which can be identified in figure 1.1. There are cored intervals from each well, two cores from Penobscot L-30 totaling 17m of core from the

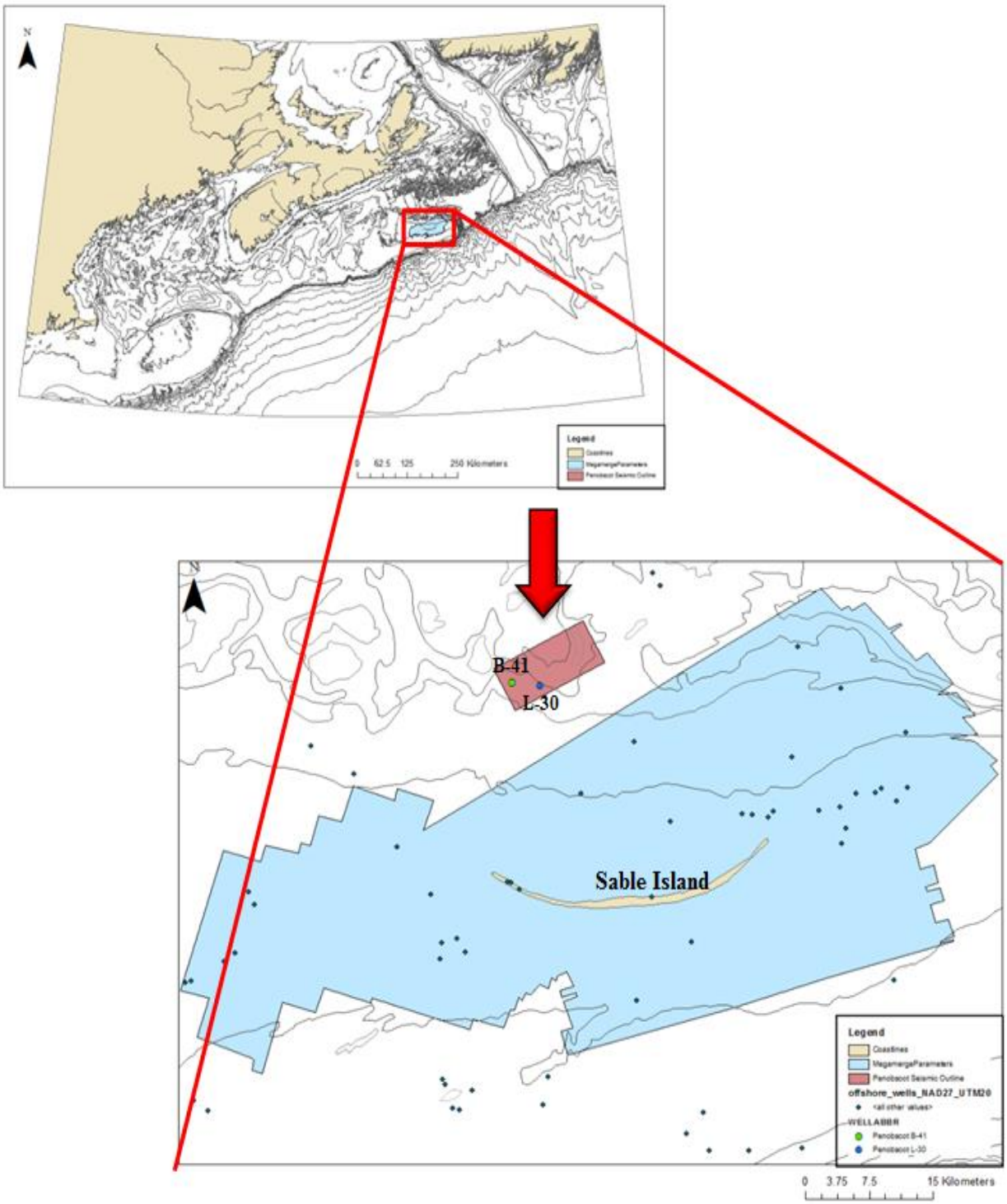

Figure 3.1: Location of Penobscot study area offshore Nova Scotia. Detail identifies the Penobscot area as the pink polygon and location of both wells within dataset (modified from Tobey, 2012, unpublished).

Abenaki Formation and four cores from Penobscot B-41 totaling 42 m of core from the Lower Missisauga Formation. There are accompanying wireline logs for each well which are analysed using geologic software including Petrel, Techlog and Jason. After the analysis of all the components of the Penobscot dataset, seismic inversion is used to correlate the well logs across the seismic survey to define the reservoirs of interest, and interpreting the depositional environment. The cored intervals from both wells were studied to interpret the characteristics of different lithofacies and infer their corresponding depositional environments. The lithofacies from the core were tied to the well logs to develop petrophysical facies, and then tied to the seismic data to define the seismic facies. This study is the first detailed study on the benefits of seismic inversion within the Scotian Basin.

1.2 Study Area:

The 3D marine seismic survey of the Penobscot area (Table 1.1) was acquired by Nova Scotia Resources Ltd. in 1992.

Table 1.1: Latitude and longitude coordinates of the corner points of the seismic survey located offshore Nova Scotia (CNOSPB, 2007).

Decimal Latitude	Decimal Longitude
44.08333	-59.87500
44.08333	-60.25000
44.25000	-60.25000
44.25000	-59.87500

The study area is located on the Scotian Shelf offshore Nova Scotia, Canada, close to Sable Island (Figure 1.1). The survey is 7.2 km long and 12.03 km wide making the total area 86.62 km^2. The inline range is from 1000 to 1600, the crossline range is 1000 to 1481 and the Z range in milliseconds 0 to 6000 (CNSOPB, 2008). There are a total of 241 seismic lines of very good resolution in the northeast to southwest direction that cover the entire survey area (Figure 1.2).

This amount of good quality seismic lines allows for clarity in interpreting the structural features of the subsurface geology (Crane and Clack 1992, p.7).

1.4 Exploration History in the Scotian Basin:

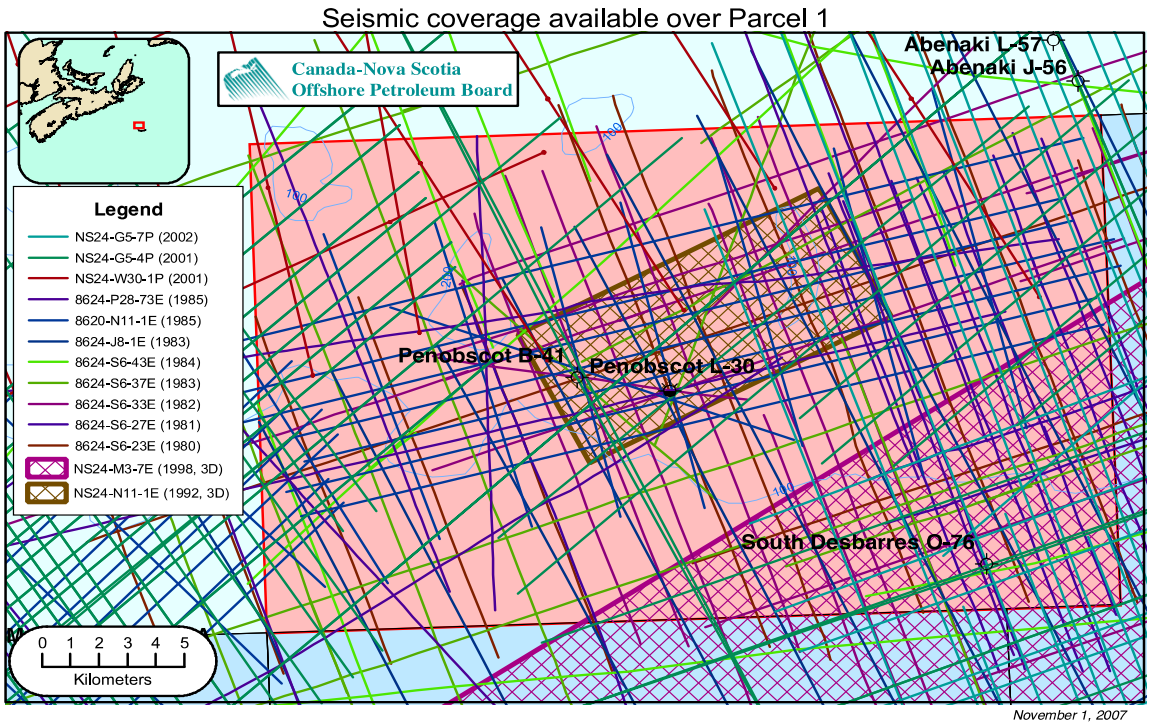

Figure 1.4 Locations of all seismic lines available for the Penobscot Area (CNSOPB, 2013).

Exploration in the Scotian Basin began in 1959 and now totals 207 wells drilled (CNSOPB, 2010). Given the large size of the Scotian Basin, it is virtually unexplored, for most of the wells drilled are located within the Sable Sub-basin (CNSOPB, 2010). To date, 23 hydrocarbon discoveries have been made offshore Nova Scotia, only eight of them being commercial discoveries and numerous others having oil and gas shows (CNSOPB, 2010). In total, 400,954 km of 2D seismic and 29,512km^2 of 3D seismic have been acquired (CNSOPB, 2010). Traps that have been tested within the Sable Sub-basin are rollover anticlines, with five fields currently under production within these trap configurations (CNSOPB, 2010). The Lower Cretaceous, Missisauga Formation has been host to some of the major producing fields to date, including Alma and North

Triumph, which comprise shelf-margin delta complexes (Cummings and Arnott, 2005). Both of these fields are part of the Sable Offshore Energy Project (SOEP), and have excellent sandstone reservoirs with high in-place gas reserves (CNSOPB, 2010). With advanced knowledge of seismic data and interpretation of the lithology of the area, distribution and the evolution of shelf-margin deltas in the Sable Delta complex can be better understood, and future prospects may be found.

Companies have explored for oil and gas reserves in the Scotian Basin since 1959, Mobil Oil Canada was the first to drill a well on Sable Island in 1967, demonstrating evidence of a thick Cenozoic-Mesozoic succession, including the Late Jurassic Sable Delta with oil and gas shows (CNSOPB, 2000). A total of 71 wells were drilled between 1967 and 1978, accompanied by over 140,000 km of 2D seismic (CNSOPB, 2010). Shell Canada then became interested in the oil and gas potential of the Scotian margin in 1969, as well as Petro-Canada, Husky-Bow Valley, Encana and BP Oil (CNSOPB, 2010).

The first major gas discovery was the Venture field just to the east of Sable Island in the Cretaceous and Jurassic sandstone reservoirs of the Sable Delta (CNSOPB, 2010). More gas discoveries continued throughout the 1980s at South Venture, West Venture, Olympia, West Olympia, Arcadia and South Sable (Mobil), Glenelg, Alma, North Triumph, Uniacke, Eagle (Shell), Banquereau (Petro-Canada) and Chebucto (Husky-Bow Valley) (CNSOPB, 2010). Exploration and development drilling continued until 2005 by numerous companies, some discovering gas reserves in the dolomitized limestones of the Late Jurassic Abenaki reef margin, although the fluvio-deltaic sands of the Missisauga Formation continued to have the most gas shows (CNSOPB, 2010). In 1998, Encana began drilling on shallow Scotian Shelf and deepwater Scotian Slope. These was named the Cohasset-Panuke Project, which targeted gas in a dolomitized

limestone of the Late Jurassic Abenaki reef margin. From 1999 to 2005 more wells were drilled in close proximity to define the areal extent of the Deep Panuke gas field (CNSOPB, 2008).

1.5 Practical Implications:

The present study has been designed to determine whether seismic inversion, in conjunction with seismic and well data, will provide a valuable analysis of strata in the Scotian Basin to aid in future exploration studies within the basin by easily distinguishing lithology with inverted acoustic impedance.

1.6 Previous Work:

Since 1960, approximately 180 exploratory wells have been drilled in the Scotian Basin (Mukhopadhyay et al., 2003) for the purpose of locating hydrocarbons. The hydrocarbons that were found in the Scotian Basin are mainly gas and condensates (Mukhopadhyay et al., 2003). Since 1995, more licenses have been issued for deep-water exploration on the Scotian Shelf and slope as a result of the spike in gas exploration in North America (Mukhopadhyay et al., 2003). Hydrocarbon exploration is cyclic and this has been the case offshore Nova Scotia.

Canada-Nova Scotia Offshore Petroleum Board (CNSOPB) conducted one notable publication for Nova Scotia Resources (Ventures) Ltd. in 1992 titled "Final Report on the 3D Seismic Survey on Penobscot E.L. 2353 Offshore Nova Scotia". The Penobscot area has two wells located in the southwest corner of the data set (Figure 1.2), neither of which have produced hydrocarbons. The easternmost well, Penobscot L-30, drilled in 1976 by Shell-PetroCanada (CNSOPB, 2008), had a minor showing of hydrocarbons. The westernmost well, Penobscot B-41, drilled a year later in 1977 by Shell- PetroCanada, did not show evidence of hydrocarbons (CNSOPB, 2008). Although the Penobscot Area is not producing, the lithologies present in the

area are producing in other parts of the Scotian Basin. This study is the first detailed analysis using seismic inversion within the Scotian Basin and by examining the Penobscot dataset, there will be applied knowledge of this method and its application to future studies.

The Canada-Nova Scotia Offshore Petroleum Board has collaborated with numerous companies including, Shell-PetroCanada, ExxonMobil, Husky and Chevron to examine the geology of the Sable Sub-Basin and the Scotian Shelf including the open source Penobscot 3D and 2D seismic dataset (CNSOPB, 2008).

CHAPTER TWO-GEOLOGICAL BACKGROUND

2.1 Regional Geology:

The study area is located on the Scotian Shelf, in the Scotian Basin, in the Sable sub-basin, and some of the Abenaki sub-basin. The Scotian Basin was a result of North American plate becoming separated from the African plate during the break-up of Pangaea. The basin is approximately 300,000 km^2 in area (Hansen et al, 2004), made up of four sub-basins and three plateaus that form a high to low topography from the southwest to the northeast: Shelburne sub-basin, La Have Platform, Sable and Abenaki sub-basins, Banquereau Platform, Orpheus Graben and Laurentian sub-basin (Mukhopadhyay et al, 2003). The layout of sub-basins and platforms within the Scotian Basin can be observed in figure 2.1.

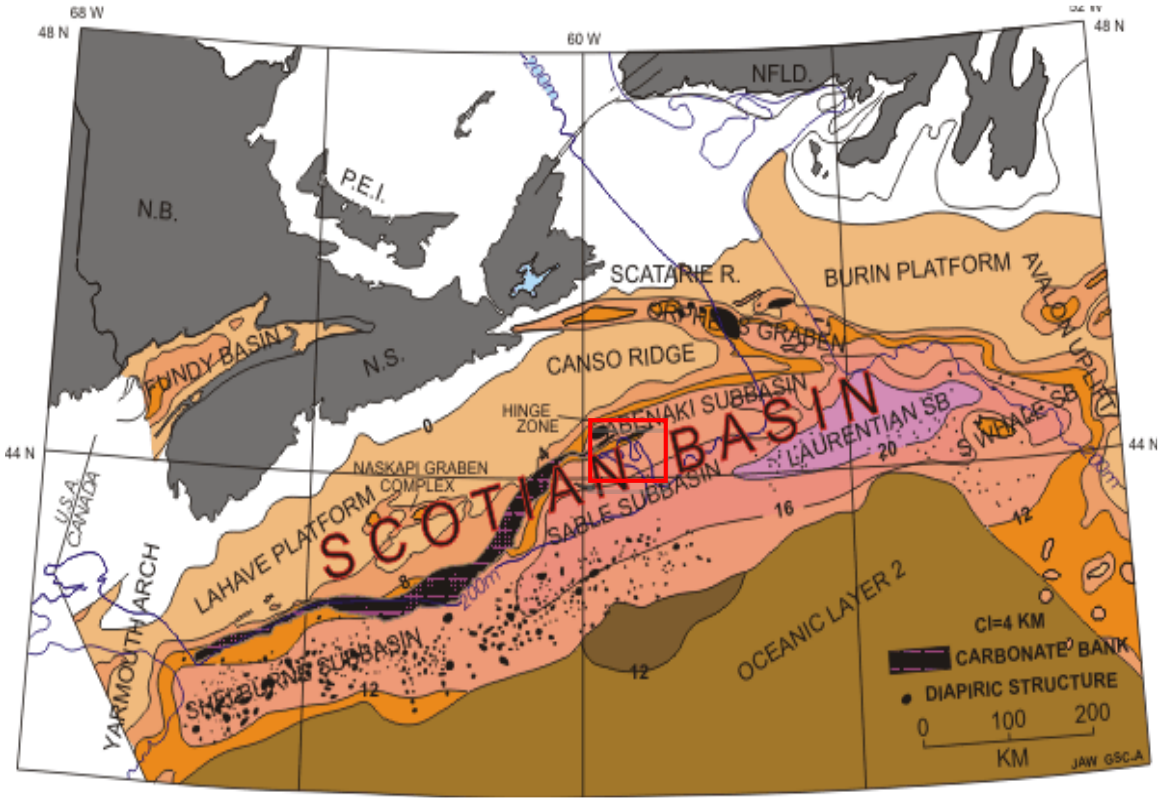

Figure 2.1: Locations of sub-basins and platforms that comprise the Scotian Basin. Red box indicates where the Penobscot area is located (Natural Resources Canada, 2010).

2.2. 1 Pre and syn-rifting of the Scotian Basin:

The separation of the North America from the African continent began in the Middle Triassic when the Nova Scotia region was located close to the equator. The initial rifting phase created many interconnected rift basins with fluvial red bed sediments infilling the basins, along with volcanic rocks associated with the rifting. Throughout the Middle Triassic to the Late Triassic, plate tectonics shifted North America and Africa northwards, positioning the Nova Scotia region in a sub-equatorial area that resulted in an arid climate. Rifting continued throughout the late Triassic when topographic barriers was breached, and marine water filled the basins, with deposition of the Eurydice Formation comprising siliclastic and carbonate sediments (CNSOPB, 2007). The sub-equatorial climate promoted evaporation of marine waters and created the Argo Formation of salt and anhydrite layers up to two km thick (CNSOPB, 2007). Paleographic reconstruction of the Scotian Basin during the Late Triassic, 210 Ma, is represented by figure 2.2. During the Late Triassic, the Fundy Basin located to the northwest of the Scotian Basin, was in a rifting phase. The rift created two grabens along the Scotian Basin, Mohican and Naskapi,

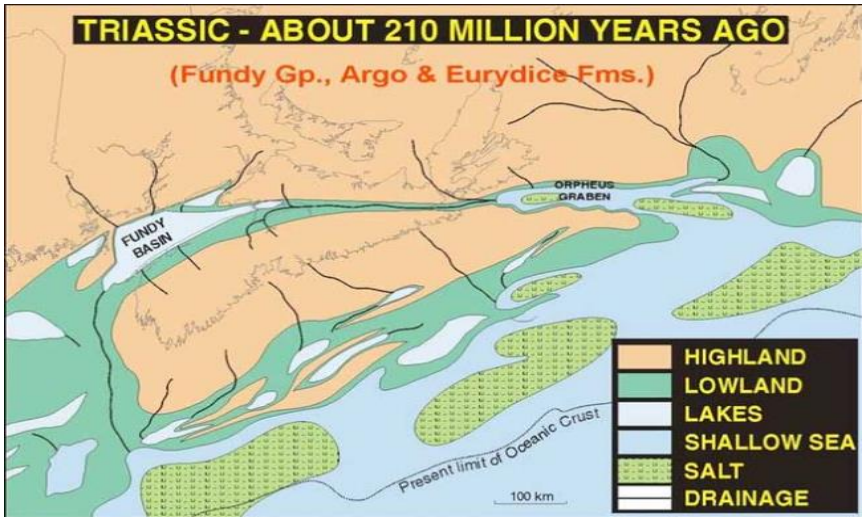

Figure 2.2: Paleographic reconstruction of the Scotian Basin during the Late Triassic during the deposition of the Argo Formation and the Eurydice Formation (Atlantic Geoscience Society, The Last Billion Years, 2001).

allowing sediment from mainland Nova Scotia to accumulate (Wade et al., 1995). In the Early Jurassic/ Late Triassic, tectonism continued, culminating in the formation of the Break-Up Unconformity, where North America and Africa separated completely, forming the proto- Atlantic Ocean (CNSOPB, 2007).

2.2.2 Post rifting of the Scotian Basin

After the Break-Up Unconformity, the basin was covered with a shallow sea allowing thin carbonates and clastics to form the Iroquois Formation. This was followed by deposition of the Mohican Formation, with thick beds of coarse, clastic fluvial sediments (Wade and MacLean, 1990). The Abenaki Formation (Figure 2.4), made up of thick carbonate beds located in the southwestern part of the basin, was deposited in the Jurassic- early Cretaceous as a result of basin subsidence due to spreading of the sea floor, forming a carbonate platform along the basin hinge zone and continued into deeper water, where clastics and muds were deposited. The Abenaki Formation is made up of three members: the oldest being the Scatarie Member, the Misaine Member and the Baccaro Member (CNSOPB, 2008).

The MicMac Formation (Figure 2.4), which consists of fluvio-deltaic sands interbedded with tongues of the prodelta shales of the Verrill Canyon Formation was deposited in the late Jurassic and marks the initial phase of uplift and delta progradation (CNSOPB, 2008). A paleographic reconstruction of the Scotian Basin during the Late Jurassic time, 150 Ma, is represented by figure 2.3. The deposition of fluvio-deltaic sediments continued into the early Cretaceous forming the Missisauga Formation (Jansa et al., 1990). This formation is one of the main reservoirs in the area. After deposition of the Missisauga Formation (Figure 2.4), deltaic sedimentation came to a halt and Logan Canyon sand beds interfingered with thick shale packages deposited during marine transgression (Wade and MacLean, 1990), resulting in source rocks and

seal (Mukhopadhyay et al, 2003). Marine transgression continued landward (Jansa et al., 1990) depositing thicker shale packages forming the Dawson Canyon Formation, which has not been identified as a source rock, however forms an appropriate seal.

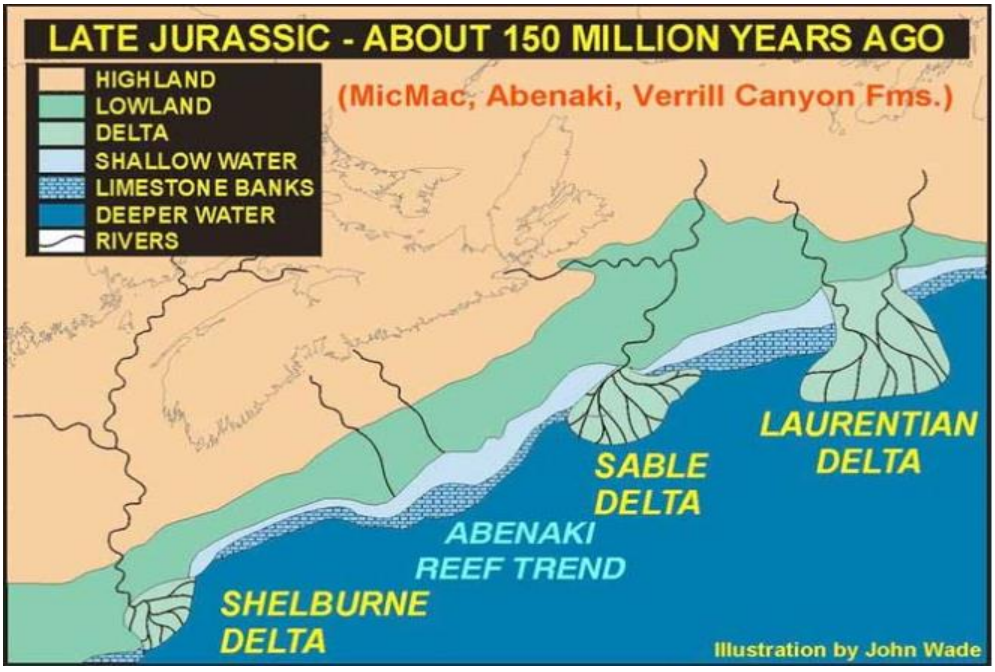

Figure 2.3: Paleographic reconstruction of the Scotian Basin during the Late Jurassic during the deposition of the MicMac, Abenaki and Verrill Canyon Formations. (Atlantic Geoscience Society, The Last Billion Years, 2001).

The chalks of the Wyandot Formation were a result of eustatic sea level rise in the Scotian Basin as well as subsidence creating additional accommodation space. The Wyandot has a high amount of bioturbation (Ings et al, 2005), which creates a good reservoir for hydrocarbons in areas to the southeast of Sable Island (Ings et al, 2005). During the Cenozoic, sea level fell, resulting in the creation of major unconformities. The Banquereau Formation (Figure 2.4), which overlies the Wyandot Formation, deposited by a suite of progradational deltas, and coarsens upwards from shale to sand and conglomerates (Hansen et al., 2004). The thickness of the Banquereau changes from very thick along the basin margin to more than 4 km thick beneath the continental slope with accommodation space formed due to salt withdrawal in the basin (Natural

Resources Canada, 2010).

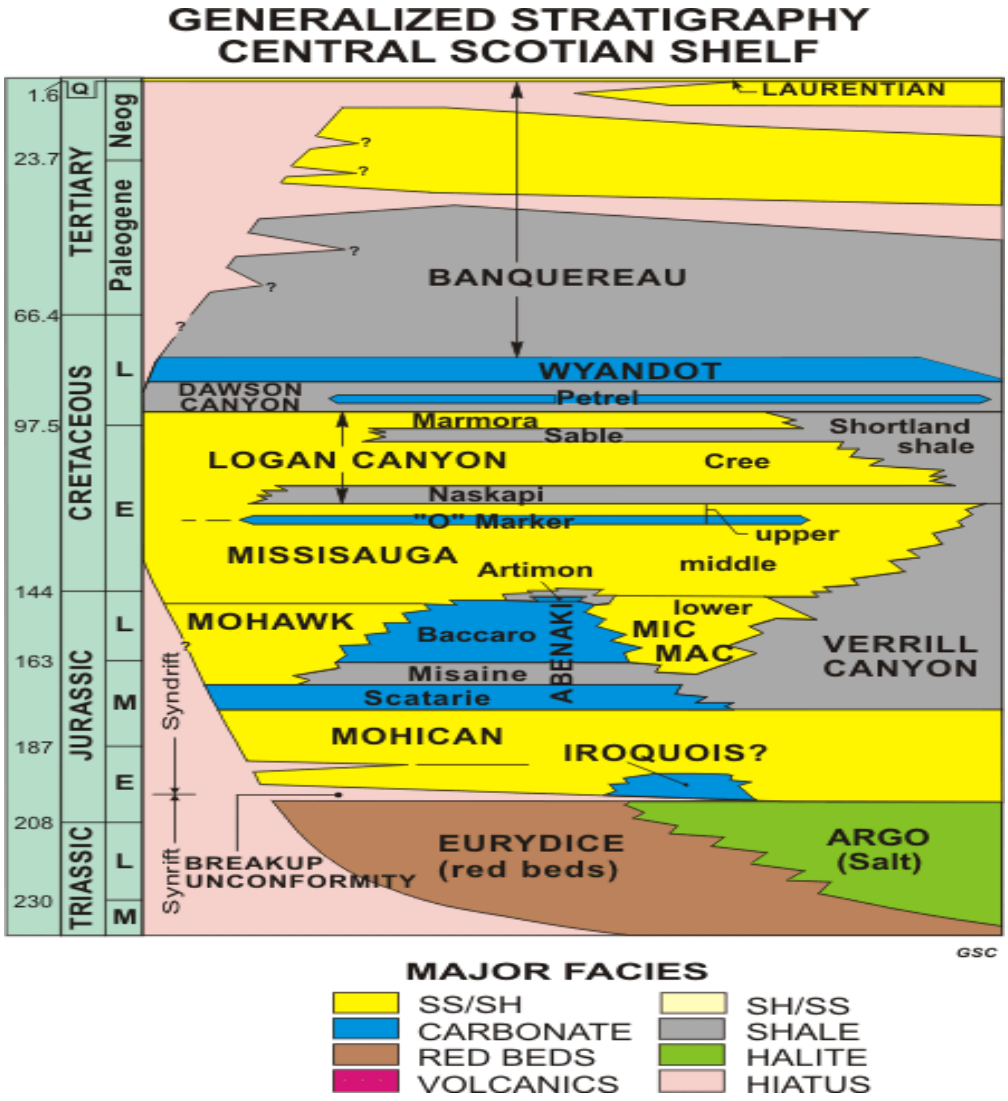

Figure 2.4: Generalized stratigraphic column of the Scotian Basin (modified by Natural Resources of Canada, Wade and MacLean, 1990).

CHAPTER THREE-METHODS

3.1 Data:

The data used in this research are an open-sourced 3D seismic survey known as the Penobscot dataset contributed by the Nova Scotia Department of Energy and Canada Nova Scotia Offshore Petroleum Board. Within the survey area of 87 km^2 the signal is strong until approximately 3.0 seconds, or 5 km depth. The survey includes 3D and 2D seismic data, however only 3D seismic data was used for the purpose of this study. The dataset also includes stacking velocities, horizon data and well log data.

3.2 Seismic acquisition:

To collect seismic data, an impulse source, this for marine data is typically an air gun that releases highly compressed air, sending acoustic energy into the Earth (Mondol, 2010). The acoustic energy propagates in different directions and gets reflected or refracted when it reaches boundaries between two geological layers of variable density (Mondol, 2010). Seismic receivers, such as hydrophones are designed to detect seismic energy in the form of pressure changes in the water during marine acquisition, are placed on the surface of the water and measure the reflected or refracted acoustic energy (Mondol, 2010). The hydrophones are combined to form streamers that trail behind the seismic acquisition vessel. Typically, the length of the steamer is about 4-6 km long with approximately 96 hydrophones along a 75 m long receiving section. The receivers convert the acoustic energy into an electrical signal that typically consists of seismic frequencies in the range of 5-100 Hz (Mondol, 2010). A seismic trace is recorded that is derived from a convolution (*) of the source signal and the reflectivity sequence of the Earth, plus noise. This is represented by the equation 3.1:

Equation 3.1: $S = W * R + Noise$

In this equation, S represents the recorded seismic trace, R is the reflectivity, and W is the wavelet (Mondol, 2010). The wavelet is a mathematical function that is used to divide a specific function into different frequencies, allowing the operator to study each component with a resolution that matches its scale (Mondol, 2010). Seismic data represents changes in acoustic impedance (AI), which is the product of density (ρ) and velocity (V), within the subsurface, demonstrated in Equation 3.2:

Equation 3.2: AI = ρ ● V, in kg/m^3 ● m/s or g/cc ● ft/s

whereas seismic reflections (reflection coefficients, RC) are caused by contrasts in the AI (acoustic impedance) between layers, demonstrated in Equation 3.3.

Equation 3.3: $RC_1 = \frac{AI_2 - AI_1}{AI_2 + AI_1}$ (Jason – a CGG Company, 2013).

Figure 3.1 demonstrates the convolutional model, which is how the seismic is arrived at from the reflection coefficients and the wavelet.

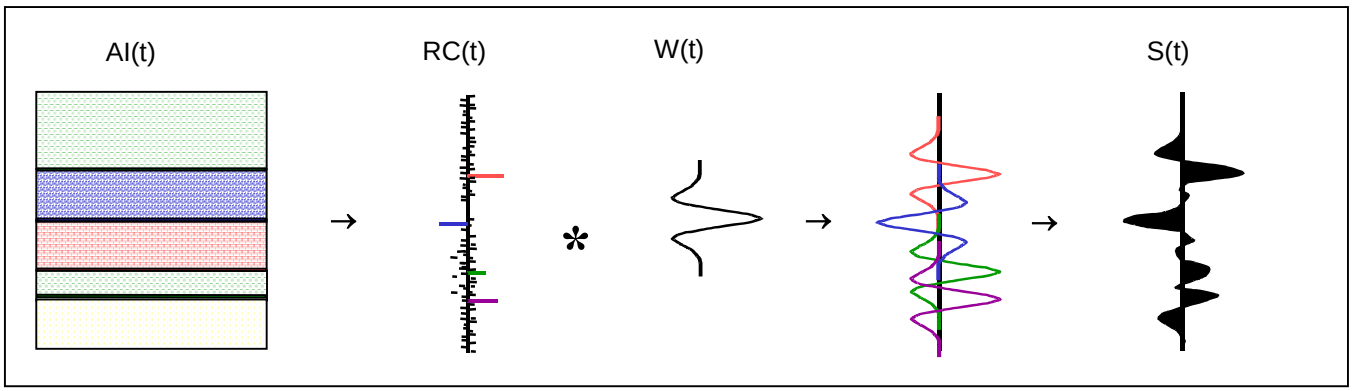

Figure 3.1: Process of acquiring a seismic trace. The reflectivity coefficients are derived from the contrasts in acoustic impedance, convoluted by an initial wavelet (Jason-a CGG Company 2013).

Accurate wavelet estimation is crucial to obtain satisfactory inversion results. The shape of the wavelet will strongly alter the seismic inversion results and subsequent assessments of the reservoir quality (Mondol, 2010).

A seismic trace is a time measurement that corresponds to one source-receiver pair and an offset represents the distance between the source and the receiver for a given trace (Mondol, 2010). The traces from one source are simultaneously recorded at several receivers, the sources and the receivers then are moved along the survey line and other recordings are made. The travel time it takes for the seismic waves to travel from the source to a reflector (geological boundary) and then back to the receiver is known as the two-way travel time (Mondol, 2010). All of the traces that correspond to the same source firing are defined as a gather, for the Penobscot survey the traces were sorted by collecting the traces that have the same midpoint, which is a process called common midpoint gather. These common midpoints then are stacked vertically and the number to which they are stacked is known as a fold (Mondol, 2010). This method reduces the signal-to-noise ratio to make the seismic trace easy to see. Figure 3.2 represents the common midpoint gather method.

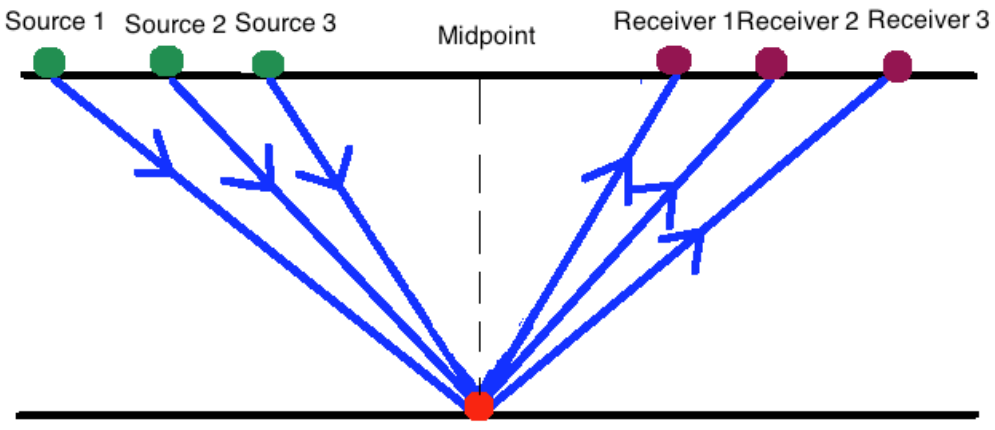

Figure 3.2: Common midpoint gather method (modified from Burger et al., 2006).

In marine acquisition, a 3D seismic survey vessel that tows up to 20 streamers at the same time has multiple arrays of air guns and will be more capable of producing more accurate images of reflected waves because it uses multiple points of observation (Mondol, 2010), illustrated by figure 3.3. After seismic processing, the data can be represented as a 3D volume image of the subsurface.

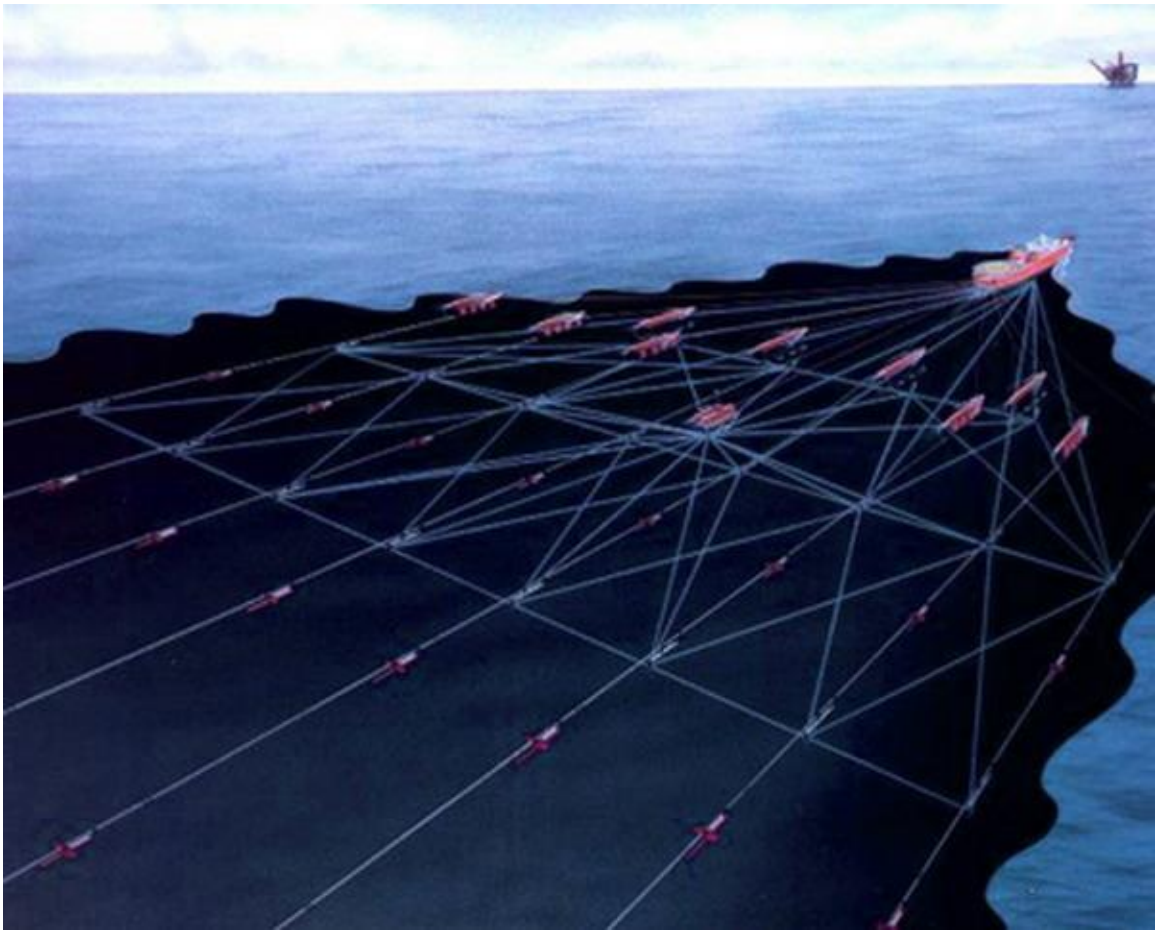

Figure 3.3: Towed streamer for 3D seismic acquisition (ION Geophysical, 2010).

Once seismic data is acquired, seismic facies and structure of the subsurface were analyzed, such as horizons and faults, using different geological software.

3.3 Petrel Software:

Petrel software has several modules, including a module to interpret seismic data, allowing interpretation of seismic facies, structure, seismic sequence stratigraphy, and seismic attributes, all used to help with the interpretation of a petroleum system. Inlines, crosslines and z-lines for the 3D seismic dataset were provided and imported into Petrel and then interpreted. For the purpose of this thesis, Petrel was used primarily to perform structural and stratigraphic interpretations, as well as to create a time-to-depth relation with the provided well log data and seismic data. To create horizon surfaces, the same reflection was mapped throughout the whole 3D package, and the software analysis was then extrapolated between the 2D horizons to create a 3D surface. This process was also done for creating fault surfaces. The two well logs were correlated with well top markers to be able to correlate seismic horizons throughout the survey area and petrophysical facies were then interpreted.

3.4 Jason Software:

Jason is a reservoir characterization software that allows for more knowledge to be known and understood of reservoirs through integrating seismic, well and horizon data into accurate reservoir models. The software solves for different solutions in petrophysics and rock physics, interpretation and analysis, model building, seismic inversion and geostatistical inversion (Jason- a CGG Company, 2013). This thesis focuses on seismic inversion specifically acoustic impedance inversion (InverTrace Plus), which transforms seismic reflection data to P-impedance layer data.

The inversion type that was used during this study was the constrained sparse spike inversion (CSSI). CSSI is a method that integrates different aspects of a seismic dataset including, full stack seismic data, geological interpretation (horizons and faults) and well log data in order to

generate acoustic impedance that has a higher resolution than the input seismic data (Jason- a CGG Company, 2013).

The benefit of using acoustic impedance is that inverted impedance gives a clearer image of the actual subsurface geology than what can be seen from seismic reflections. When acoustic impedance is compared directly to the wells, it can be extensive over a large area. Acoustic impedance also assists in interpreting horizons, faults and stratigraphic units by allowing layers to be seen as opposed to interfaces from seismic data. The seismic inversion process also attenuates wavelet effects, reduces side-lobes and tuning effects, and gives the possibility of extending beyond the seismic band. By using an acoustic impedance inversion, well ties must be made and therefore understood since the inversion process integrates the information known at the wells across the entire survey area. The final inversion result can then be analysed in detail and quantitative predictions of reservoir properties can be made (Jason – a CGG Company, 2013).

Inverted acoustic impedance can be used as a lithology indicator to map lithology/flow units accurately, serving as a porosity indicator as well as a hydrocarbon indicator. Seismic inversion is basically the reverse of seismic acquisition. Seismic acquisition (as discussed in 3.2) is the convolution of the relfection coefficients of the Earth by the wavelet, which gives seismic amplitudes. Seismic inversion is then the deconvolution of the seismic amplitudes by the wavelet, which gives acoustic impedance. Acoustic impedance allows a clearer image of actual earth properties to be seen, compared to seismic, because it is related to geological layers, not interfaces (Jason – A CGG Company, 2013). This process is represented in Figure 3.4.

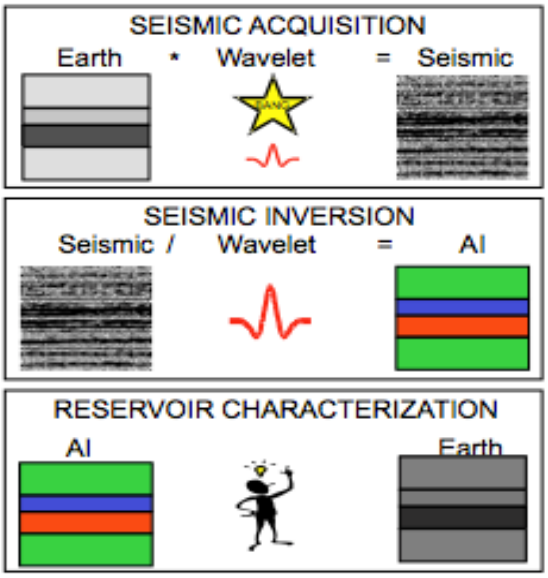

Figure 3.4: Brief schematic explanation of the process to obtain inverted acoustic impedance (modified from Jason- a CGG Company, 2013).

3.5 InverTrace Plus Workflow:

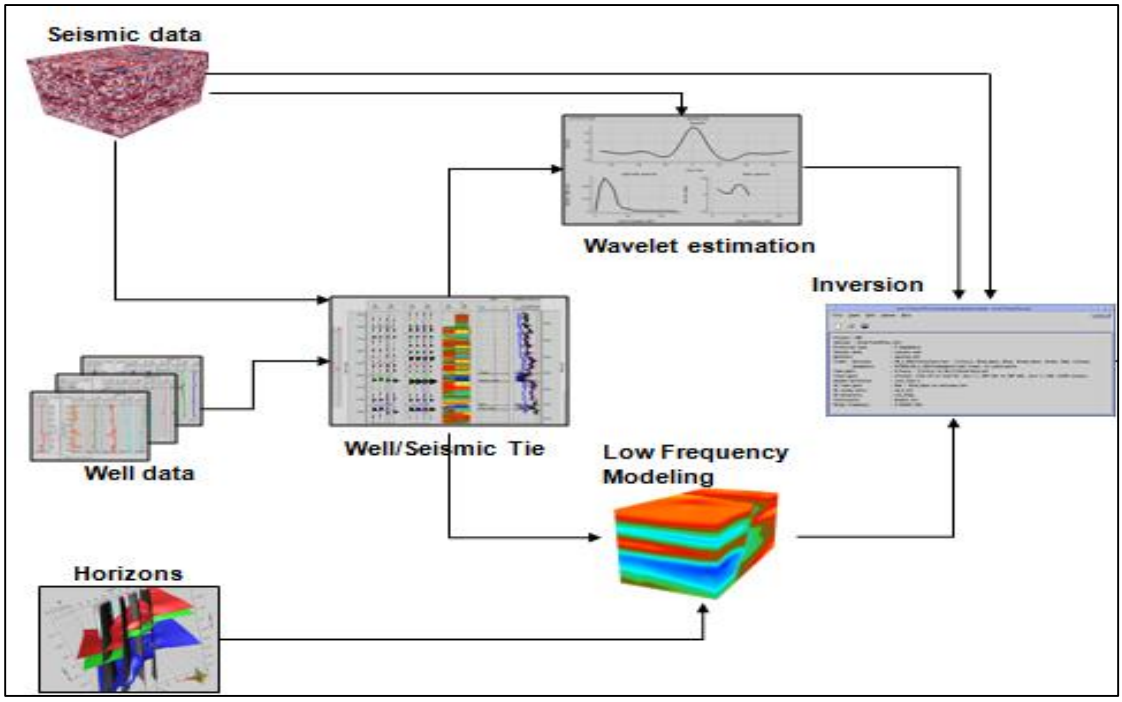

Figure 3.5: InverTrace Plus workflow.

Several steps need to be performed in order to obtain the best possible inversion result, using seismic, well and horizon data. This order of steps is demonstrated in figure 3.5. From imported seismic and horizon data, a grid is created and coordinates and survey definitions are

stored within the grid. The seismic property, 2D or 3D, is imported as trace data and all well information is imported into one file, including the logs, tops, tracks and the time-to-depth relationship (as a time log) (Jason – a CGG Company, 2013).

The next step is to test the data, known as a feasibility study. By looking at the well data, the frequency range required for the objective and whether acoustic impedance inversion is the right choice can be determined. To do this, a cross-plot of logs is created to see if a P-impedance cutoff will identify reservoir zones in the log plots. It is then important to cross-plot filtered logs to see if a P-Impedance cutoff will still identify reservoir zones on the log plots at seismic resolution (Jason – a CGG Company, 2013).

Once the zones of interest are determined, a time-to-depth relationship can be created using seismic and well data. The method used to create a time-to-depth relationship for the Penobscot dataset is known as Sonic (Backus Averaged). Sonic (Backus Averaged) uses analytical equations to estimate elastic properties of well logs that are used in seismic data analysis (Kumar, 2013). The sonic is backus averaged by choosing a time and depth from the seismic that is believed to be located in the proper place within the seismic. The time and depth position has been chosen to create an initial tie and then it gets integrated away from the datum point by entering a new, known time and depth (Jason – a CGG Company, 2013).

After the wells are tied to the seismic, a wavelet for each well can be estimated to create a synthetic log at every trace of the seismic. Wavelet estimation is done at the well location, where impedance, thus the reflection coefficients, and the seismic record are all known. Signifying, both the geophysical and petrophysical data is already known and has been properly correlated.The inversion process then estimates reflection coefficients at each trace of the seismic using the

information known and taken from the wells, far away from the wells, using the seismic and the estimated wavelet (Jason – a CGG Company, 2013).

The next step is to create models that contain geological information that is used in the inversion. The first model needs to be created from the: Model Builder, which builds its models with the use of the seismic data. Essentially the Model Builder makes synthetic logs at every trace of the seismic survey using the information from the input well logs. The model is made up of stacked layers that form a cube, which is defined by the seismic laterally and a chosen time/depth gate vertically, typically enclosing the zones of interest. The layers are formed by the input horizons. For the purpose of this study, all of the horizons were loaded into the Model Builder because the entire Penobscot survey area was the area of interest. The result of the Model Builder is a "Solid Model". The Solid Model is a parametric model, which contains all the information for next model that needs to be created, which creates an actual volume, known as the Model Generator. The Solid Model is a basic model for the geological structures (Jason – A CGG Company, 2013). As previously stated, the next model to be created through the Model Generator and is called the Low Frequency Model. The Model Generator takes the information from the Solid Model and create values for every sample in a volume over the selected vertical gate. It can generate a volume from any logs or other 1D function. It creates the low frequency model, which fills in the frequency "gap" between the wells and the seismic. The size of the frequency gap between the wells and the seismic depends on whether the dataset is offshore data or onshore data. Offshore data have a gap of 6Hz while onshore data have a gap of 10Hz, this is because there is more noise generated from onshore data due to more interferences from subsurface features, such as overburden. In simple terms, the low frequency model accounts for the frequency data that was lost during seismic acquisition (Jason – a CGG Company, 2013).

After all the steps are performed, the inversion can be run. Good inversion results allows for improved speed and quality of the interpretation at a higher resolution, compared to seismic. Acoustic impedance inversion can also reduce drilling risks and can give an accurate positioning and realistic reserve estimates (Jason – A CGG Company, 2013).

3.6 Core Description:

The Canada Nova Scotia Petroleum Board in Dartmouth, Nova Scotia provided access to six cored intervals from two separate wells. Well Penobscot L-30 comprises two cored intervals making up approximately 17 m of core. Table 3.1 represents the depth intervals from which the cores were taken. Both consist of carbonates from the Abenaki Formation, the first core is from the Baccaro Member and the second from the Scatarie Member. The core locations are shown in figure 3.6. Both cores are described in Chapter 4. Dunhams Classification (1962), revised by Embry and Klovan (1971), and then again by Wright (1992) were used to distinguish the name of the carbonate lithofacies of Penobscot L-30.

The second well, Penobscot B-41, is represented by four cored intervals making up approximately 42 m total. All four cores represent the Middle Missisauga Formation from the Early Cretaceous. Table 3.2 represents the depth intervals from which the cores were taken,

Table 3.2: Penobscot L-30 cored intervals:

Core Number:	Depth Interval:
Core #1	3,424.8m – 3,432.6m
Core #2	4,050.3m – 4,059.6m

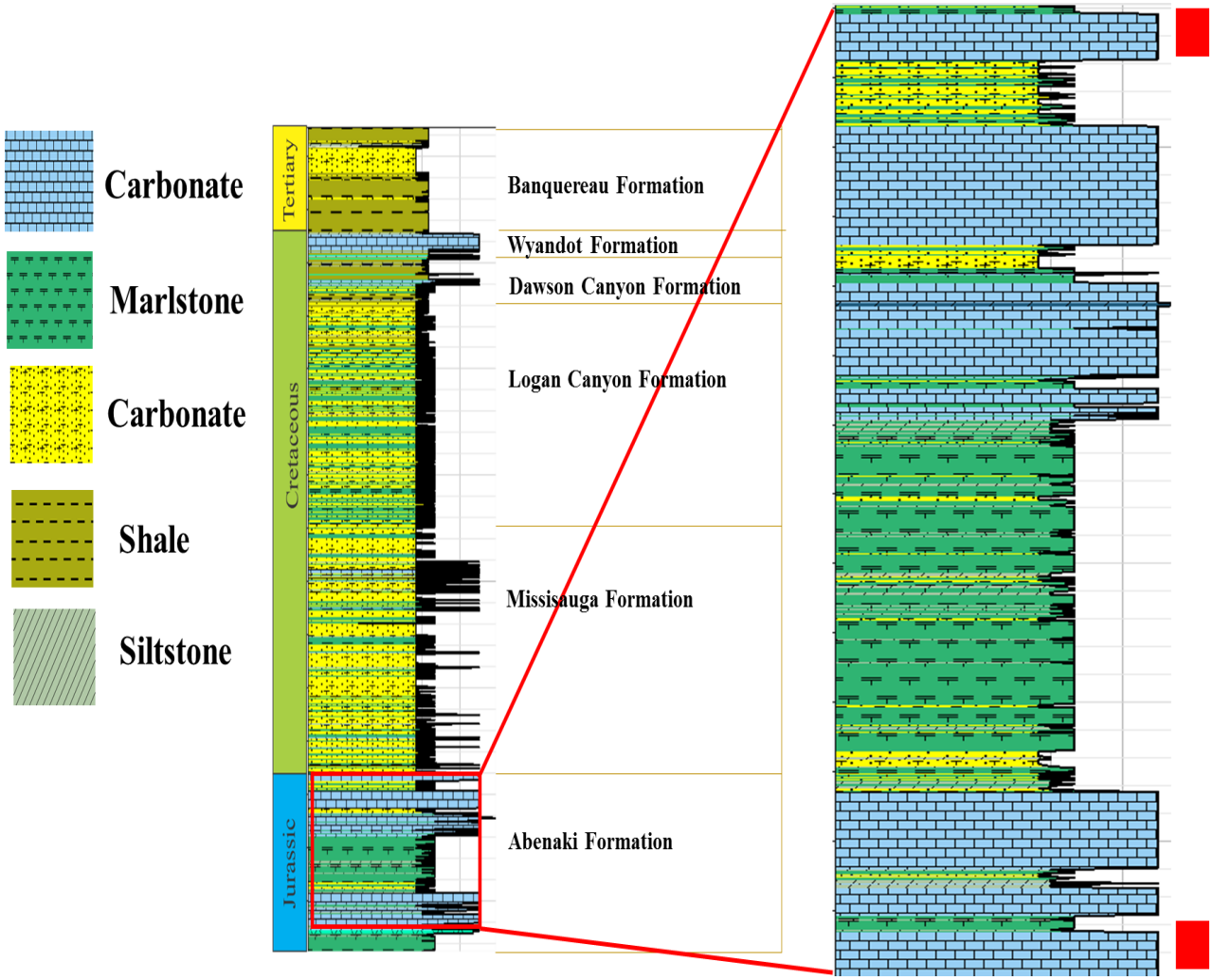

Figure 3.6: Lithological log for well Penobscot L-30. Red box represents zoomed in area, whereas the red solid rectangle represents where the core was taken from (modifed from Wade and MacLean, 1

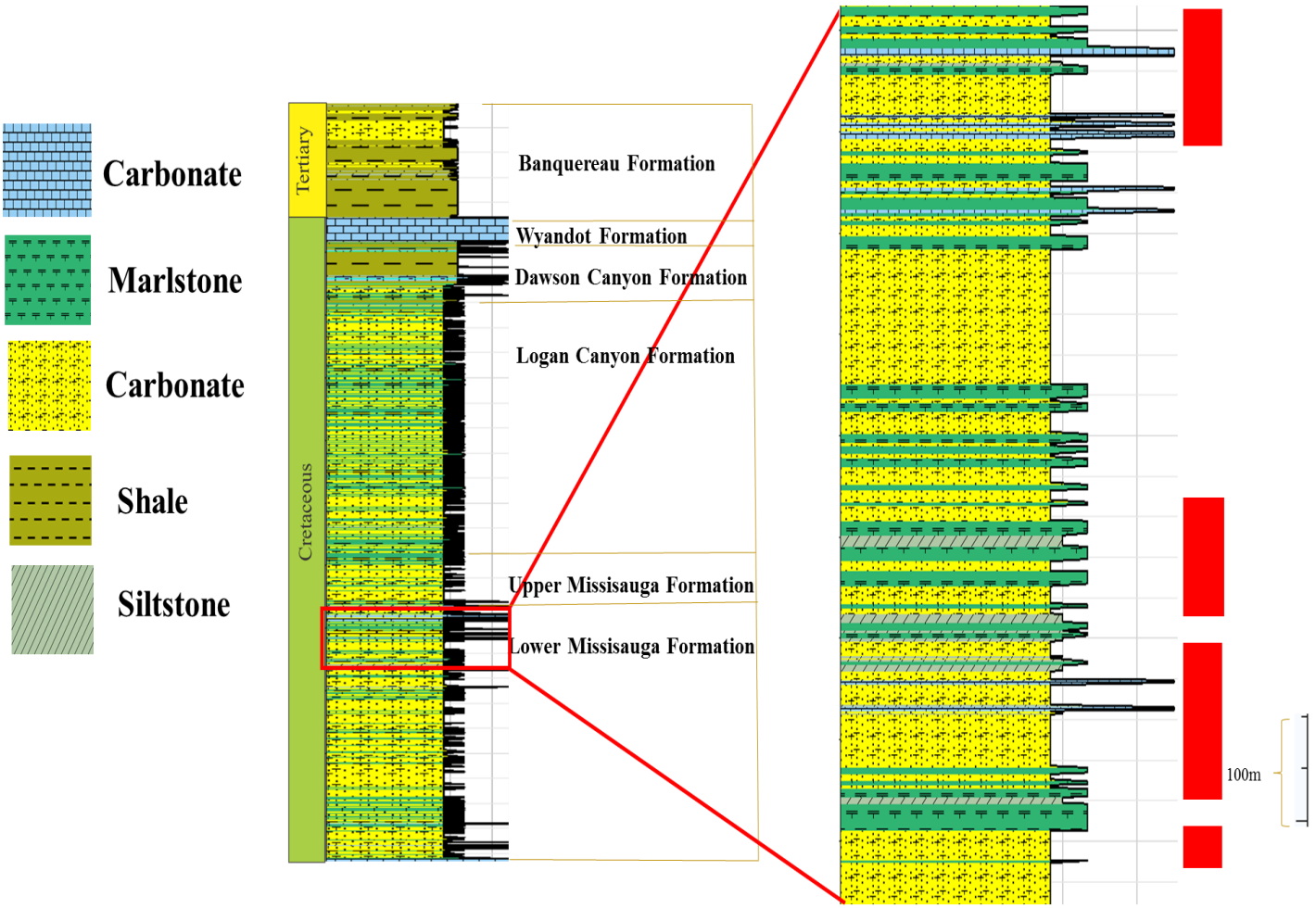

Figure 3.7: Lithological log for well Penobscot B-41. Red box represents zoomed in area, whereas the red solid rectangle represents where the core was taken from (modified from Wade and MacLean, 1993).

Table 3.2: Penobscot B-41 cored intervals:

Core Number:	Depth Interval:
Core #1	2,500.0 m - 2,517.4 m
Core #2	2,643.3 m - 2,657.6 m
Core #3	2,661.6 m - 2,669.8 m
Core #4	2,699.7 m – 2,702.7 m

In core four, there are intervals missing and broken. Description of the core is in Chapter 4. Figure 3.7 also represents where amongst the well all four cores were taken from.

3.7 Wireline log analysis:

The information presented in section 3.7 is from Bjorlykke, 2010. Well logs record the physical properties of the rocks that are penetrated by a well. Shell Canada Resources Limited, the operator, drilled the two wells for the Penobscot area as wildcat wells. A borehole is logged by lowering a probe with different instruments down the borehole to measure different properties. The wireline logs that were given include depth, caliper-density and caliper-sonic, delta rho, sonic, gamma ray-density and gamma ray-sonic, deep induction standard processed and medium induction standard processed (both of which are resistivity logs), neutron porosity for a limestone matrix and neutron porosity for a sandstone matrix, bulk density and spontaneous potential. The logs that were studied were sonic, gamma ray-density and sonic, resistivity, neutron porosity for limestone and sandstone matrix, density and spontaneous potential.

A sonic log measures how fast sound travels through rocks and provide valuable information about the porosity and whether a liquid or a gas is present. It does this by sending out acoustic pulses that travel through the surrounding rock and the velocity of the sound of the rock gets recorded.

Gamma ray logs measure the natural radioactivity within the rock surrounding the well. The elements of interest that produce gamma radiation in typical sedimentary rocks include potassium, thorium and uranium. Generally, shale contains most of these elements and therefore the gamma ray reading of shale is typically larger than that of sandstone. Gamma ray logs can provide an indication of potential source rock intervals by examining the decay chain of the three

elements: potassium, thorium and uranium, and the log response in which they form. Since these elements are found in shales, the higher log responses on a gamma ray log could potentially represent source rock intervals.

Resistivity logs measure the resistance between two and four electrodes, which are in contact with the rocks surrounding the well. Measured resistivity is a function of water saturation, the percentage of the porosity that is filled with water. If oil or gas is present in the rock, resistivity will be higher than if just water is present. Although, to be sure if the fluid is hydrocarbons the use of other well logs, such as gamma ray, is necessary.

Neutron porosity is measured by the release of neutrons from a probe that gets lowered down the borehole at high velocity. Absorption of neutron radiation is a function of hydrogen concentration, and the water present in the rock due to the collisions with atomic nuclei absorbs neutron rays. The collision frequency of the neutrons is recorded by measuring the secondary X-ray radiation that is created when neutron radiation gets absorbed. Neutron logs can demonstrate the water content of a rock, therefore determining the rock's porosity. It is useful to determine the porosity of shales and distinguish whether it is oil or gas that is present since gas has fewer hydrogen atoms. Neutron porosity for limestone gives a more reliable reading since there are not many hydrogen atoms present in carbonate rocks.

Density logs measure the density of the rocks and their pore fluid by measuring the electrodensity of a rock. A strong radioactive source emits high-energy gamma rays down the borehole, and with every collision with an electron the gamma rays loses energy and some eventually get absorbed when their energy gets too low (Watson, 2013). The gamma rays that get returned back to the detectors are measured and the formation's density is determined. Formations

with a high gamma ray count have lower densities then those with a low gamma ray count (Watson, 2013).

Spontaneous potential logs measure the currents that are generated naturally in the rocks by the difference in the compositions of the pore fluids. It is a continuous recording of the difference in potential between a moving electrode in the borehole and a fixed potential surface electrode (Watson, 2013). It determines the boundaries between different beds as well as helping to correlate between wells (Watson, 2013). It also helps to determine the water resistivity of a formation and gives an indication of where shale is located (Watson, 2013).

CHAPTER FOUR – LITHOFACIES DESCRIPTION AND DEPOSTIONAL SETTING

4.1 Core Descriptions of Penobscot L-30:

Core 1 from Penobscot L-30 consists of 8.4 m of core from the Baccaro Member, the uppermost member of the Abenaki Formation. The core consists of a packstone with clay seams facies. The lithofacies is described in detail in section 4.1.1. Table 4.1.describes core 1 in detail and what exactly can be seen throughout the entire lithofacies as well as the associated mineral assemblages and structures found within the core.

Core 2 from Penobscot L-30 consists of 9.3 m of core from the Scatarie Member, the middle member of the Abenaki Formation. The core consists of two lithofacies, lithofacies B, which is a grainstone and lithofacies C described as shale to marl, with the contact boundary between the two at approximately 4054.4m depth. Table 4.2 depicts the summary of core 2 and the defining mineral assemblage as well as distinct structures. The two lithofacies found in core 2 are described in detail in section 4.1.3 and 4. 1.4

4.1.1 Lithofacies A: Packstone with clay seams:

This lithofacies (Figure 4.1) is characterized by medium grey packstone, defined by being grain supported with the interstices containing mud as defined by Dunham (1962). This lithofacies can be seen within an approximate 8.5 m interval from 3423.21 m depth to 3431.74m. It is fossil rich, consisting of branching tubular coral and bivalve fragments and other bioclastic material in a mixed fine-grained groundmass with occasional spar (Dunham, 1962). It has pelletal material and dark grey-black ooids throughout the lithofacies. Organic-rich material is observed within clay seams throughout the upper part of this lithofacies interval. There are large calcite-filled vugs present throughout the lithofacies as well as crystalline calcite nodules. The argillaceous seams present throughout do not react with HCL, suggesting a

lower amount of carbonate material. The porosity of this lithofacies is hard to see, suggesting that there is little porosity throughout this lime grainstone. There is also no indication of hydrocarbons.

Figure 4.1: Lithofacies A: Packstone, lower part of core 1 from Penobscot B-41, darker interval near the end of core represents the argillaceous rich interval.

4.1.2 Depositional environment of core 1 from Penobscot L-30.

Strata in Core 1 from the Baccaro Member of the Abenaki Formation were deposited during the Late Jurassic on a carbonate shelf (Kidston et al., 2005). The presence of lime mud suggests low energy depositional conditions. Lithofacies A was deposited on the relatively shallow part of the carbonate shelf, most likely in the restricted interior platform area, where restricted circulations favors deposition of lime mud, and where bioclastic material is often found (Flügel, 2010).

4.1.3 Lithofacies B: Wackestone-Packstone:

This lithofacies (Figure 4.2) is characterized as a dark grey, wackestone-packstone, based on Dunham's classification (1962) due to being matrix supported, with less than 10% grains, although containing approximately 20% of bioclastic material. Intraclasts are observed throughout the lithofacies in a fine-grained matrix. Clay is present throughout the lithofacies and an abundance of vugs 3-4 cm in

diameter, some calcite-filled. Fractures and veins are abundant with no preferred orientation. Stylolites are also observed throughout the lithofacies, in no preferred orientation. Bioclastic material is rare to common within the lithofacies. The entire wackestone-packstone reacts to HCL.

Figure 4.2: Lithofacies B: Wackestone-packstone with intraclasts in a microcrystalline matrix.

4.1.4 Lithofacies C: Calcareous shale to marl:

Lithofacies C (Figure 4.3) changes quite drastically from lithofacies B. The lithofacies is dark grey in color and is characterized by containing a matrix made up of carbonate material with calcite nodules less than or equal to 0.64 cm in diameter. Stylolites are also common throughout the lithofacies, in no preferred orientation. There are occasional pyrite masses found throughout, evident from rusty areas. The entire lithofacies reacts to HCL.

Figure 4.3: Lithofacies C: Calcareous shale to marl.

4.1.5 Depositional environment of core 2 from Penobscot L-30:

The basal Scatarie Member of the Abenaki Formation, deposited during the mid-Jurassic, is also a part of the carbonate shelf (Kidston et al., 2005). The intraclasts and variable grain size throughout lithofacies B, as well as being fossiliferous suggest that this lithofacies was deposited on the slope of the carbonate shelf. This depositional environment then would have altered to the deep shelf (Flügel, 2010), depositing the shale to marl lithofacie C, demonstrating a more calm (below storm wave base) depositional environment than that of B.

Table 4.1: Detailed log description specifically for lithofacies A: Packstone

Well: Penobscot L-30, Core 1 **Sheet:** 1 of 1

Depth (m):	Mineral Assemblage:	Structures:	Notes:
3423.88m-3423.9m	Calcite, clay-argillite (20-25%), lime mud.	Fossils, (tubular coral), BC < 1cm	Medium gray, BC is beige/white.
3423.9m- 3424.5m	Calcite, clay-argillite (20%), 30 cm section of sparite filled voids/ cracks.	BC=0.6-1.3cm	
3424.5m- 3425.3m	Calcite, clay argillite (15%), lime mud.	Crystalline calcite, sparite filled vugs. BC=< 1cm	
3425.3m- 3426.0m	Calcite, clay-argillite (10-15%), lime mud.	BC (<1cm) crystalline calcite concretion (2cm) Minor sparite	Very fine grained mud
3426.0m- 3426.7m	Calcite, clay-argillite (5%)	Large calcite filled vug (2cm) BC (minor amounts). Minor sparite,.	Very fine grained mud
3426.7m- 3427.4m	Calcite	BC =< 0.3cm, Minor sparite, .	Very fine grained mud
3427.4m- 3428.2m	Calcite, clay argillite (<10%).	Minor amounts of BC =< 0.3cm	Very fine grained mud
3428.2m- 3428.9m	Calcite.	Calcite filled veins. Minor sparite, (grey-black with ooids).	Gray, Very fine grained mud
3428.9m- 3429.6m	Calcite, clay argillite (<2%)	Minor sparite, , pelletal material last 14cm. Less BC.	Tan gray, Very fine grained mud
3429.6m- 3430.2m	Calcite.	Minor sparite, =<1.3cm, minimal BC.	Very fine grained mud
3430.2m- 3431.0m	Calcite, clay-argillite (=<5%), sparite.	Minimal BC <0.15cm, small calcite viens.	Very fine grained mud
3431.0m- 3431.7m	Calcite, clay argillite (=<5%)	Minor sparite, calcite filled vugs.	Very fine grained mud

A

BC=Bioclastic material

Table 4.2: Detailed description of lithofacies B and C denoted by the corresponding B and C on the table.

Well: Penobscot L-30, Core 2 **Sheet: 1 of 1**

	Depth (m):	Mineral Assemblage:	Structures:	Notes:
B	4049.3m-4050.0m	Calcite (lime mud)	Abundance of calcite filled vugs.	Medium/dark gray, minimal BC.
	4050.0m- 4050.7m	Calcite (lime mud, sparite)	Calcite filled vugs. Stylolites.	Microcrystalline, minimal BC.
	4050.7m- 4052.9m	Calcite (lime mud, sparite)	Same as above.	Same as above.
	4052.9m- 4053.6m	Calcite (lime mud, sparite)	Less amounts of calcite filled vuggs. Stylolites.	Microcrystalline. Small amounts of BC.
	4053.6m- 4054.4m	Calcite (lime mud, sparite)	Minimal amounts of stylolites. Calcite filled vugs and veins very common. Fine grained siltstone clasts (rounded) in last 13cm of core.	Fining downwards. Dark gray. Microcrystalline.
C	4054.4m – 4055.1m	Calcite, organic material	Very fine grained and calcareous 0.6 cm round clasts (small amount).	Dark gray to black. Shale to siltstone.
	4055.1m- 4057.3m	Calcite, very calcareous stylolites.	Fine grained clasts =<1cm of siltstone. Rounded.	Shale, dark gray, microcrystalline.
	4057.3m- 4058.6m	Calcite, calcareous stylolites, silt, pyrite.		Dark gray to black. Mircocrystalline, fissile.

BC= Bioclastic material

4.2 Core Description of Penobscot B-41:

The four cores from Penobscot B-41 are from the lower Missisauga Formation deposited during the Early Cretaceous. In total, Penobscot B-41 recovered 42.9m of core, of which six distinct lithofacies were interpreted, some repeating throughout the cored intervals. The stratigraphic log containing all four cored intervals can be observed in Figure 4.4 A to C, which shows the location of these lithofacies as well as their relative grain size, lithology and laminae geometry, and if any bioturbation exists. This stratigraphic log will be mentioned throughout this

section to put into prospective where the lithofacies are located and if they reoccur. The lithofacies for Penobscot B-41 will be termed Lithofacies one through six with their appropriate name.

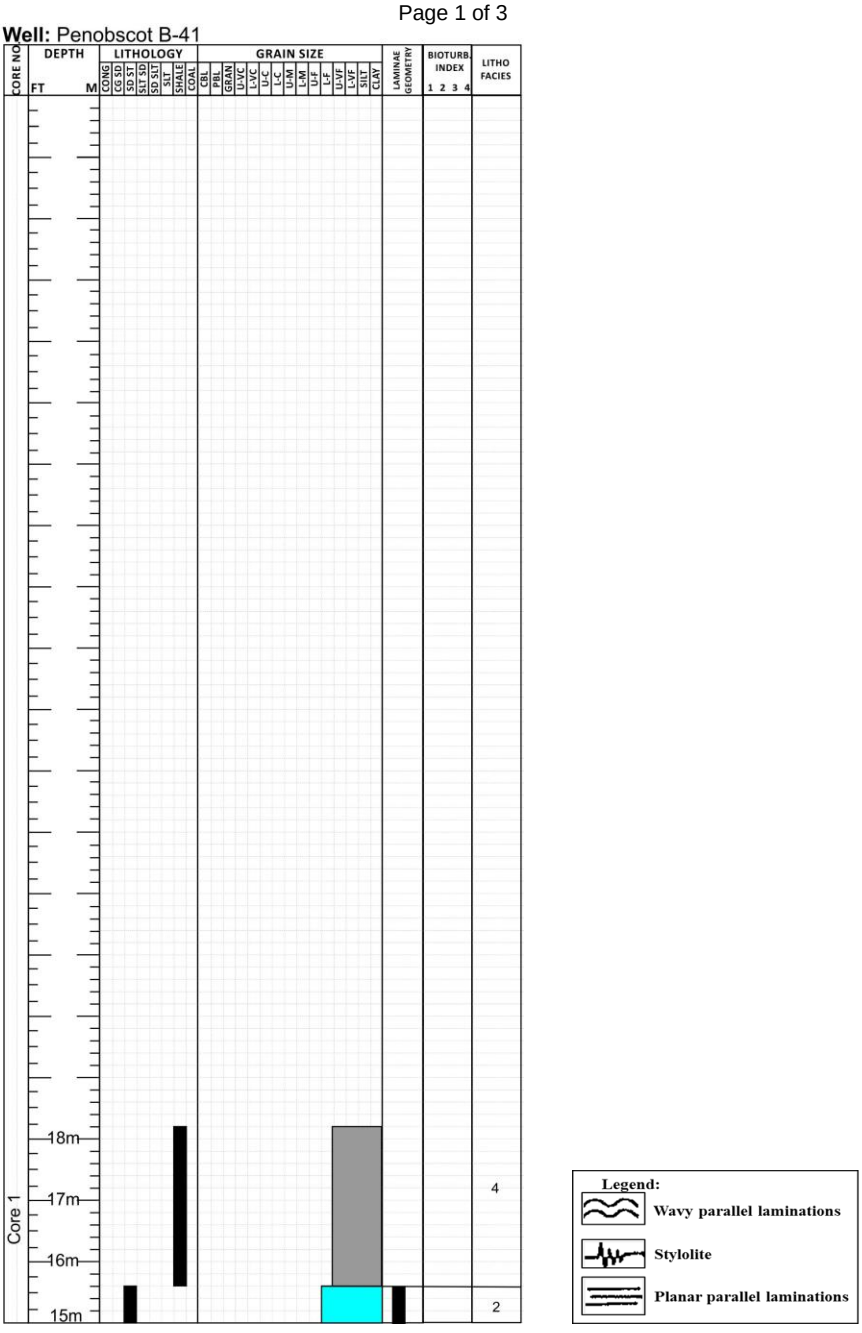

Figure 4.4 A: Stratigraphic column of Penobscot B-41, page 1 of 3. Lithofacies 2 represented by the color blue and lithofacies 4 represented by the color grey.

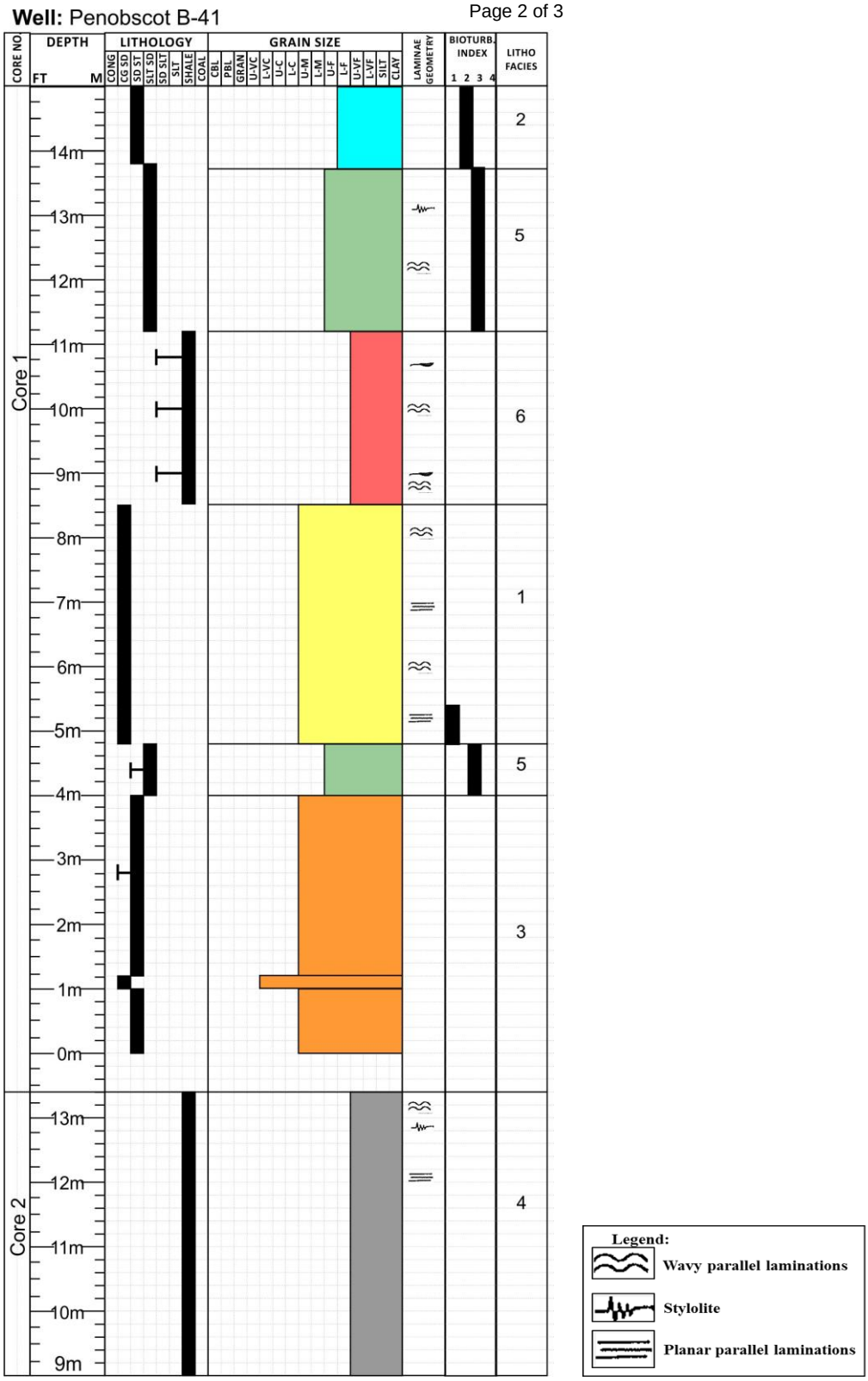

Figure 4.4 B: Stratigraphic column of Penobscot B-41, page 2 of 3. Lithofacies 1 represented by yellow, lithofacies 2 represented by blue and lithofacies 4 represented by grey, Lithofacies 5 represented by green and lithofacies 6 represented by red.

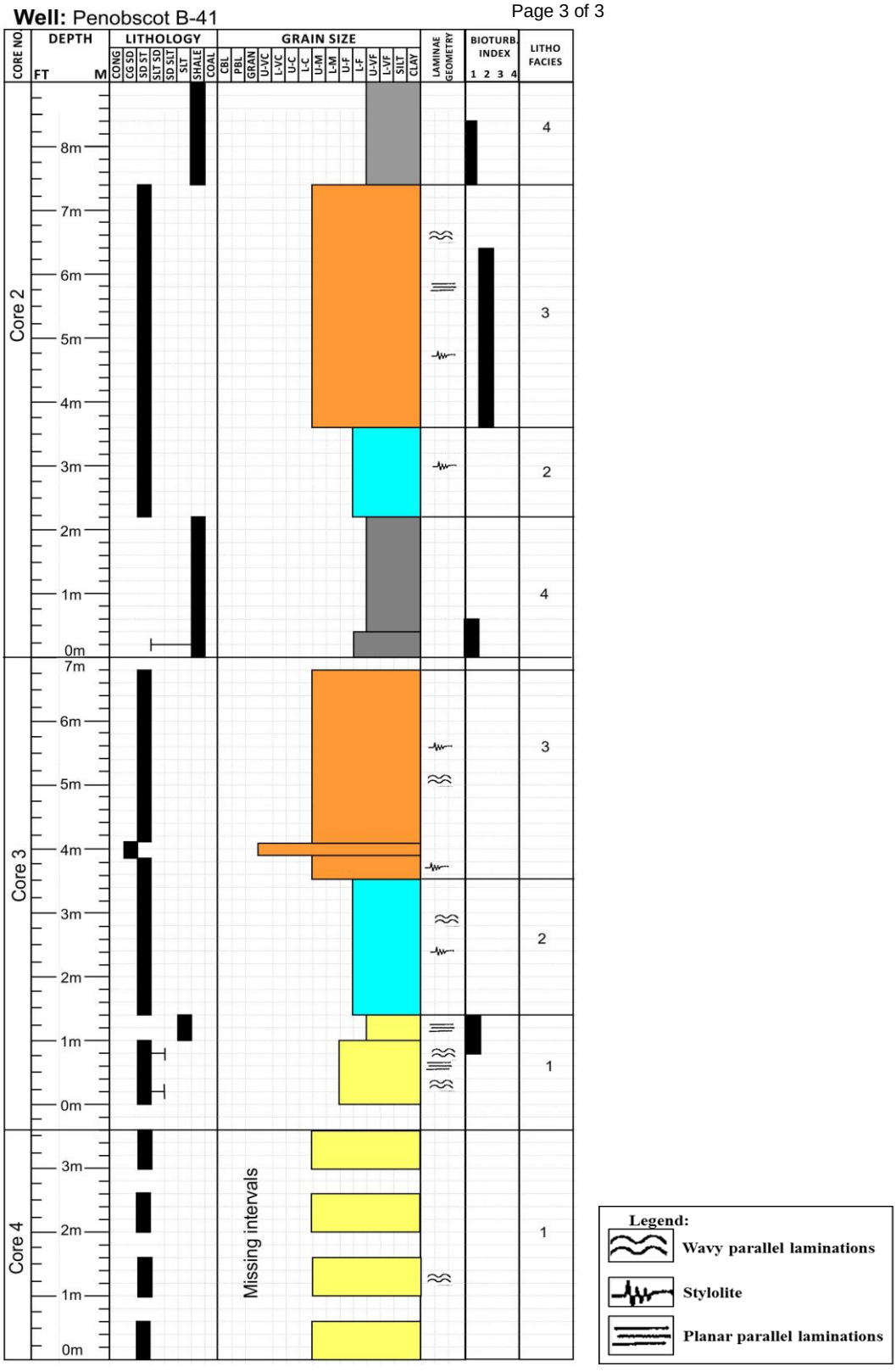

Figure 4.4 C: Stratigraphic column of Penobscot B-41, page 3 of 3. Lithofacies 1 represented by yellow, lithofacies 2 represented by blue and lithofacies 4 represented by grey.

4.2.1 Lithofacie 1: Medium grained beige sandstone:

Lithofacie 1 (Figure 4.5 A, B and C) comprises wavy parallel and planar parallel silt laminations within a medium grained consolidated sandstone. There are thin conglomerate intervals with coarse grained quartz and feldspar clasts, sub-rounded and well sorted. Lithofacies 1 can be observed twice throughout the core intervals of Penobscot B-41, demonstrated in figure 4.4 A to C. It occurs from 2702.1m depth to 2668.5m depth and again at 2511.9m to 2508.2m depth. When lithofacie 1 occurs at the shallower depth, the bottom is mixed with red clay, as well as contains red clay clasts up to 3cm in diameter. Lithofacies 1 is represented by yellow in figure 4.

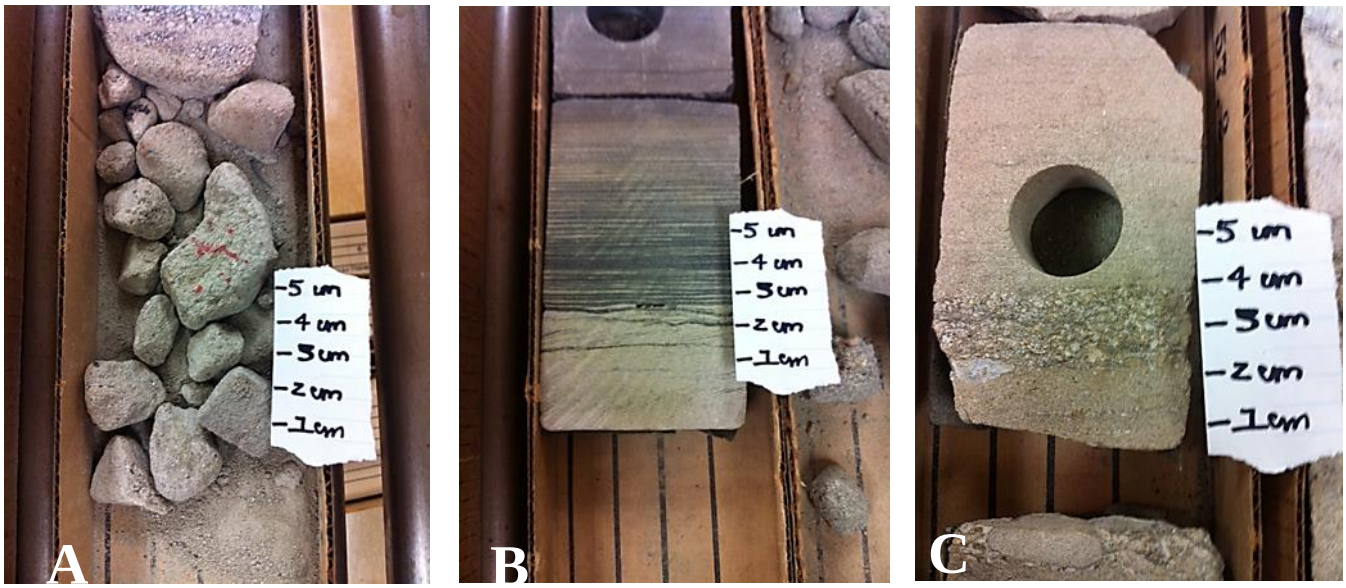

Figure 4.5: Lithofacies 1: Medium grained beige sandstone. A: Broken up section demonstrating lithology. B: Planar parallel silt laminations present throughout lithofacies. C: Conglomeratic interval with quartz and feldspar clasts.

4.2.2 Lithofacies 2: Fossiliferous calcareous cemented sandstone:

Lithofacies 2 (Figure 4.6 A and B) occurs throughout three intervals of the Penobscot B-41 core, the deepest depth at 2668.5m to 2664.3m, the second interval 2653.9m to 2653.0m depth, and the last occurrence at 2503.3m to 2501.5m depth. The lithofacies is composed of fine grained sand, fining upwards throughout the lithofacies, with abundant shell fragments. There is

also an abundance of crinoid fossils with occasional ooids throughout. Argillaceous material occurs throughout the lithofacies in layer intervals up to 0.5cm thick, with increasing amounts towards the top of the lithofacies. There is a strong reaction for HCL throughout the entire lithofacies, indicating carbonate material. Examination with an optical microscope concluded that the calcareous material was acting as cement, binding the quartz grains together. There is minor bioturbation throughout and contains the early onset of stylolites. There are also pyrite grains randomly dispersed throughout the lithofacies. In the second and third occurrences of this lithofacies, there are more shell fragments and the sandstone is redder in color indicating iron oxidation taking place. Lithofacies 2 is represented by the color blue in figure 4.4 A to C.

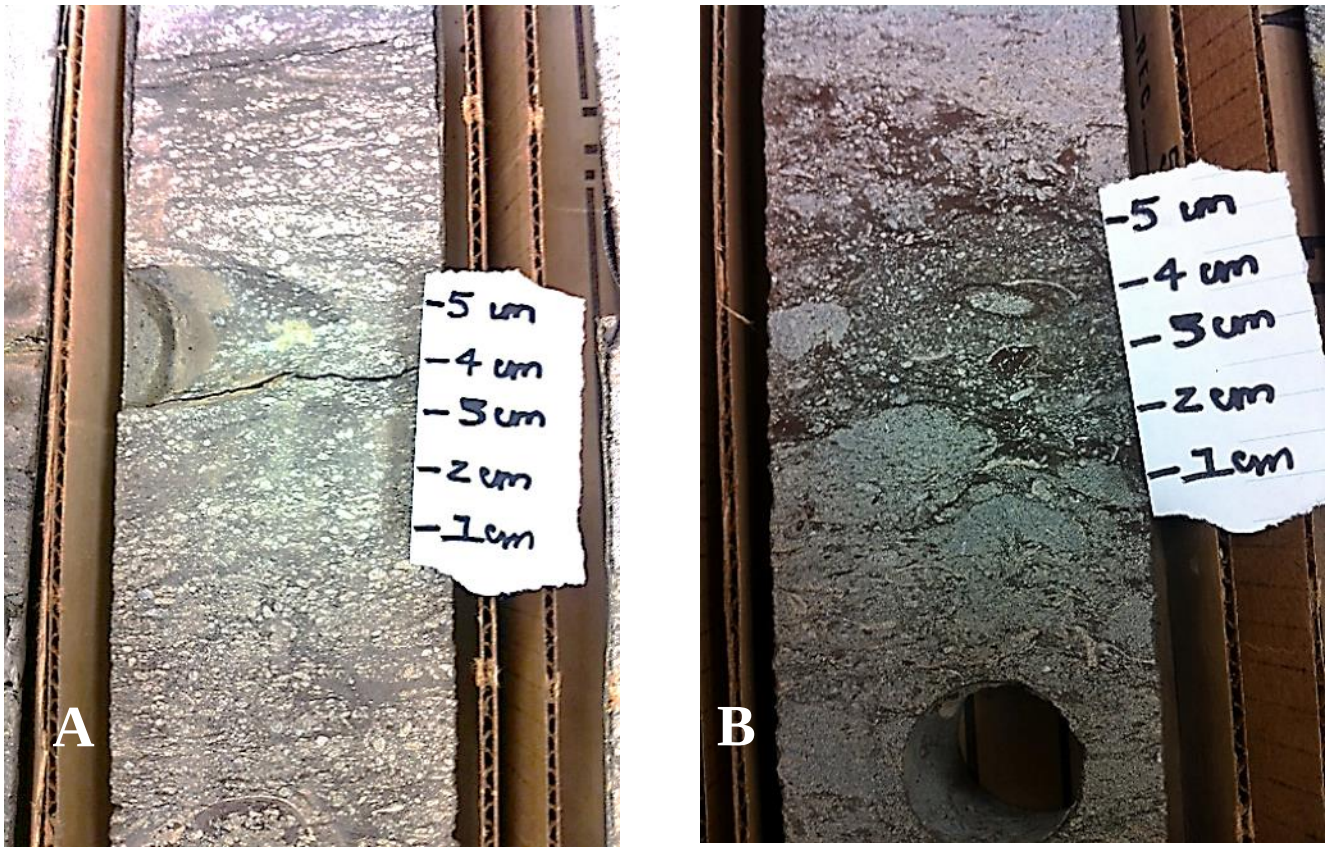

Figure 4.6: Lithofacies 2: Fossiliferous calcareous cemented sandstone. A: First occurance of lithofacies demonstrating grey color, shell fragments abundance of crinoid fossils. B: Representative of the second and third occurance, demonstrating red color and crinoid fossils.

4.2.3 Lithofacies 3: Calcareous cemented sandstone with black organic material:

Lithofacies 3 (Figure 4.7) occurs in three different intervals throughout the Penobscot B-41 core, the deepest occurrence at 2664.3m to 2661.5m depth. Lithofacies 3 occurred again at 2653.0m to 8648.7m depth. The final occurrence was at 2516.7m to 2512.8m depth. Lithofacies 3 is very similar to lithofacies 1, however it contains an abundance of organic-rich intervals and fragments throughout the entire lithofacies. This lithofacies is characterized as being beige in color, with quartz clasts cemented with calcite.It has polymictric conglomerate intervals up to 10cm thick containing rounded to sub-rounded, well sorted clasts smaller than or equal to 1cm. The lithofacies is medium grained and contains red clay clasts up to 1cm. There are stylolites present throughout the calcareous cemented sandstone composed of argillaceous material. In the second occurrence of this lithofacies, more bioturbation, with an index of 2 is present and there are pyrite clasts randomly dispersed throughout. Lithofacies 3 is represented by the color orange in figure 4.4 A to C.

Figure 4.7: Lithofacies 3: Calcareous cemented sandstone. Figure is representative of the overall lithofacies containing thick conglomeritic intervals.

4.2.4 Lithofacies 4: Grey fissile shale:

Lithofacies 4 (Figure 4.8 A and B) occurred throughout three different intervals, the deepest occurrence at 2656.3m to 2653.0m depth. The second appearance is at 2648.7m to 2643.2m depth, the third at 2501.5m to 2500.0m depth. Lithofacies 4 comprises very fine grained, dark grey fissile shale with shell fragments towards the top of the lithofacies. There are also crinoid fossils towards the bottom of the lithofacies in the first occurrence, demonstrating mixing with lithofacies 3. The lithofacies does not react to HCL, indicating no calcareous material present. There is minor bioturbation throughout and contains random sand lenses. There are also pyrite clasts dispersed throughout lithofacies. There are also occasional wavy parallel silt laminations. Lithofacies 4 is represented by the color grey in figure 4.4 A to C.

Figure 4. 8: Lithofacies 4: Grey fissile shale. A and B representative of how lithofacies 4 appears at all occurrences.

4.2.5 Lithofacies 5: Silty sandstone:

Lithofacies 5 (Figure 4.9) appears twice throughout the Penobscot B-41 cores. The deepest occurrence at 2512.8m to 2511.9m depth and the second occurrence at 2505.5m to 2503.3m depth. Lithofacies 5 is characterized as a heavily bioturbated fine grained sandstone, grey in color and contains abundant crinoid and shell fossils. The silt component of the lithofacies is very fine grained and black in color. There are red clay layer intervals throughout the lithofacies up to 5cm thick. Stylolites are present throughout the lithofacies as well. Lithofacies 5 is presented by the color green in figure 4.4 A to C.

Figure 4.9: Lithofacies 5: Silty sandstone. Figure demonstrates high amounts of bioturbation and presence of stylolites and shell fragments.

4.2.6 Lithofacies 6: Lenticular red shale:

Lithofacies 6 (Figure 4.10) occurs once throughout all four core of Penobscot B-41. This depth interval is 2508.2m to 2505.5m. It comprises lenticular laminations of lithofacies 1 in very fine grained red shale. There are four pyrite clasts up to 5 cm in diameter. There are also clay intevals throughout the lithofacies. The sand component of this lithofacies also occurs as wavy parallel laminations as well as wavy non-parallel. There are pyritized intervals, which can be seen as the rust color in Figure 4.10. Lithofacies 6 is represented by the color red in figure 4.4 A to C.

Figure 4.10: Lithofacies 6: Lenticular red shale. White material is lithofacies 1 being mixed with lithofacies 6 and occurring as lenses throughout the lithofacies. Rust color indicates pyrite clasts.

4.2.7 Depositional Environment of Penobscot B-41:

All lithofacies described in the cores from Penobscot B-41 represent the Middle Missisauga Formation deposited during Early Cretaceous (Kidston et al., 2005). Based on the above

descriptions, the depositional environment changed frequently from nearshore to offshore, and four distinct cycles of transgression, indicating sea level would rise, and then fall over short periods of time can be distinguished. The first cycle represented by lithofacies 1 comprising medium grained sandstone to lithofacies 4 a very fine grained shale. The second cycle is represented by lithofacies 2, a fossiliferous calcareous cemented sandstone to lithofacies 4, demonstrating another transgressive system. The third cycle is represented by lithofacies 3, a calcareous cemented sandstone to lithofacies 6, a lenticular red shale. This cycle demonstrates an oxidizingg system, since the shale of lithofacies 6 is red in color. The final cycle is represented by lithofacies 5 to lithofacies 4, with lithofacies 2 in between, containing bioturbation and abundant shell fossils. This change in sea level possibly represents a prograding fluvio-deltaic succession composed of siliclastic material. All of the shell fragments, bioclastic material and ooids represent a shallow marine environment.

CHAPTER FIVE – SEISMIC AND WELL DATA

5.1 Geology observed within the Penobscot dataset:

The geological formations that can be identified within the Penobscot survey area can be identified in Figure 5.1. These include: the Abenaki Formation and Lower Missisauga Formation separated from the Upper Missisauga Formation by the limestone O-Marker, Logan Canyon, Dawson Canyon, Wyandot and the Banquereau formations.

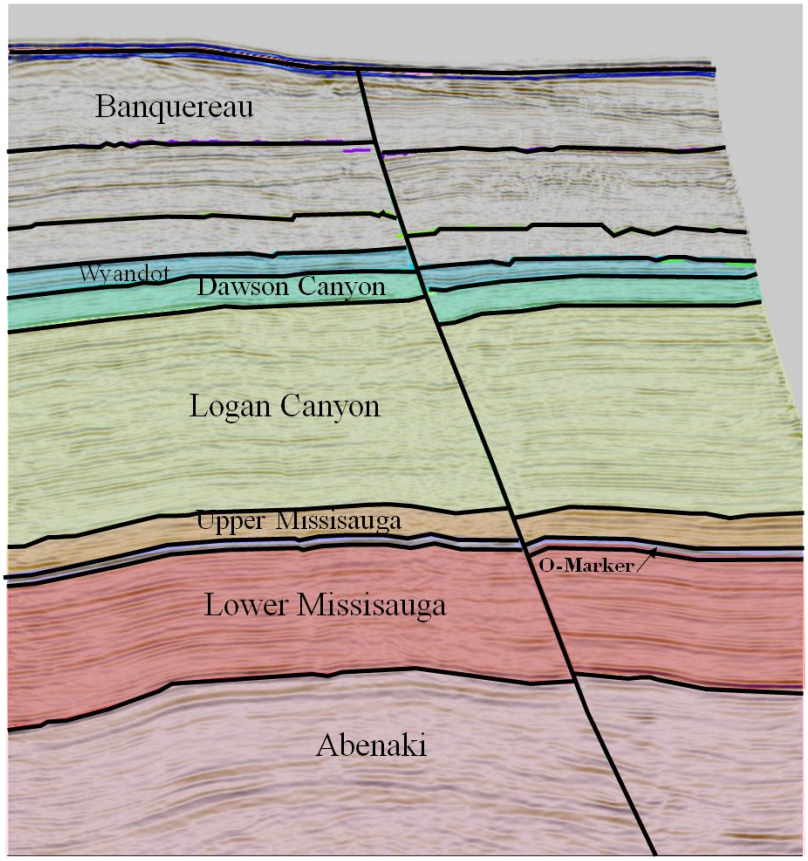

Figure 5.1: Xline1255 demonstrating the stratigraphic facies within the Penobscot Area that can be identified in the 3D seismic data.

The Abenaki Formation is Jurassic in age, the Missisauga, Logan Canyon, Dawson Canyon, and Wyandot formations are all of Cretaceous age. The Banquereau Formation is topmost Cretaceous to Cenozoic in age (Figure 2.4) (Ings et al, 2005).

5.2 Methods of interpretation:

The primary methods of geological investigation for this study were the interpretation of seismic reflections with the use of the 241 seismic lines collected to create a 3D seismic dataset. The methods of interpretation include Petrel software that was used to interpret seismic facies, structure and stratigraphy. Jason software was used to perform an attribute analysis on the seismic, which was correlated to the interpreted results of Petrel.

Petrel, Jason and Techlog were also used to analyze the well logs and create petrophysical facies, that were compared to the lithologies previously interpreted.

5.3 Seismic stratigraphy:

Seismic stratigraphy is an interpretation technique that uses knowledge of seismic reflections and general stratigraphic concepts to infer the depositional sequence (Vail et al., 1977). Seismic reflections are generated at changes in acoustic impedance (previously described in chapter 3), impedance being defined by the changes in the bulk rock properties of the velocity and density of the subsurface. Seismic reflection data consist of different attributes including the amplitude, phase, frequency and coherency, which when used in combination form the basis of seismic interpretation (Stoker et al., 1997).

5.3.1 Seismic facies:

The stratigraphy interpreted for the Penobscot dataset has been described for each formation based on the internal seismic characteristics and the strong seismic reflectors separating specific boundaries. The analysis of seismic facies is the process that involves the interpretation of geometry, amplitude, frequency, velocity and continuity (Sangree and Widmier, 1979). The reflection geometries are divided into distinct packages of reflections, described as parallel

(concordant), sub-parallel (discordant), divergent, clinoform (sigmoidal, oblique, or shingled), reflection free, wavy, chaotic, hummocky or contorted (Mitchum et al., 1977). Within the Penobscot 3D survey, four different seismic facies were identified. These can be observed in figure 5.2 labeled A, B, C, and D.

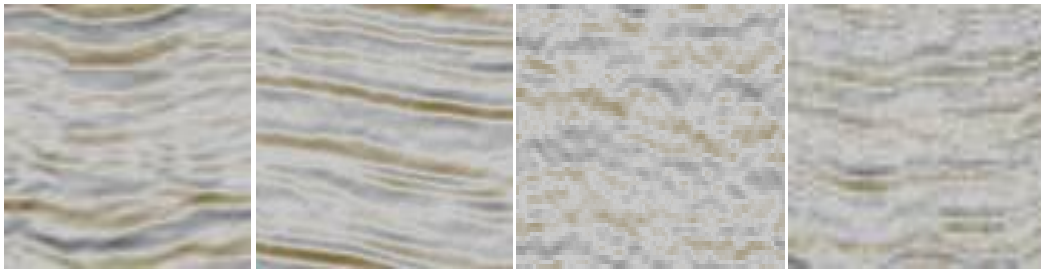

Facies A: Parallel-concordant, high amplitude reflectors.	Facies B: Parallel, high amplitude reflectors.	Facies C: Chaotic-discontinuous, amplitude incoherent reflectors.	Facies D: Sub-parallel, continuous high amplitude reflectors.

Figure 5.2: Characteristics for seismic facies A, B, C and D.

5.3.2 Seismic Horizons and Reflectors:

Six key seismic reflection horizons were chosen throughout the Penobscot area based on their continuity across the area. The six horizons identified have been used to separate 7 units identified within the study area and were named based on knowledge of the stratigraphy in the area, as well as the known location of the formation tops within Penobscot L-30 and Penobscot B-41. Figures 5.3 and 5.4 are two seismic lines (Inline 1254 and Xline 1255 respectively) from the Penboscot 3D survey identifying the tops of all 6 horizons.

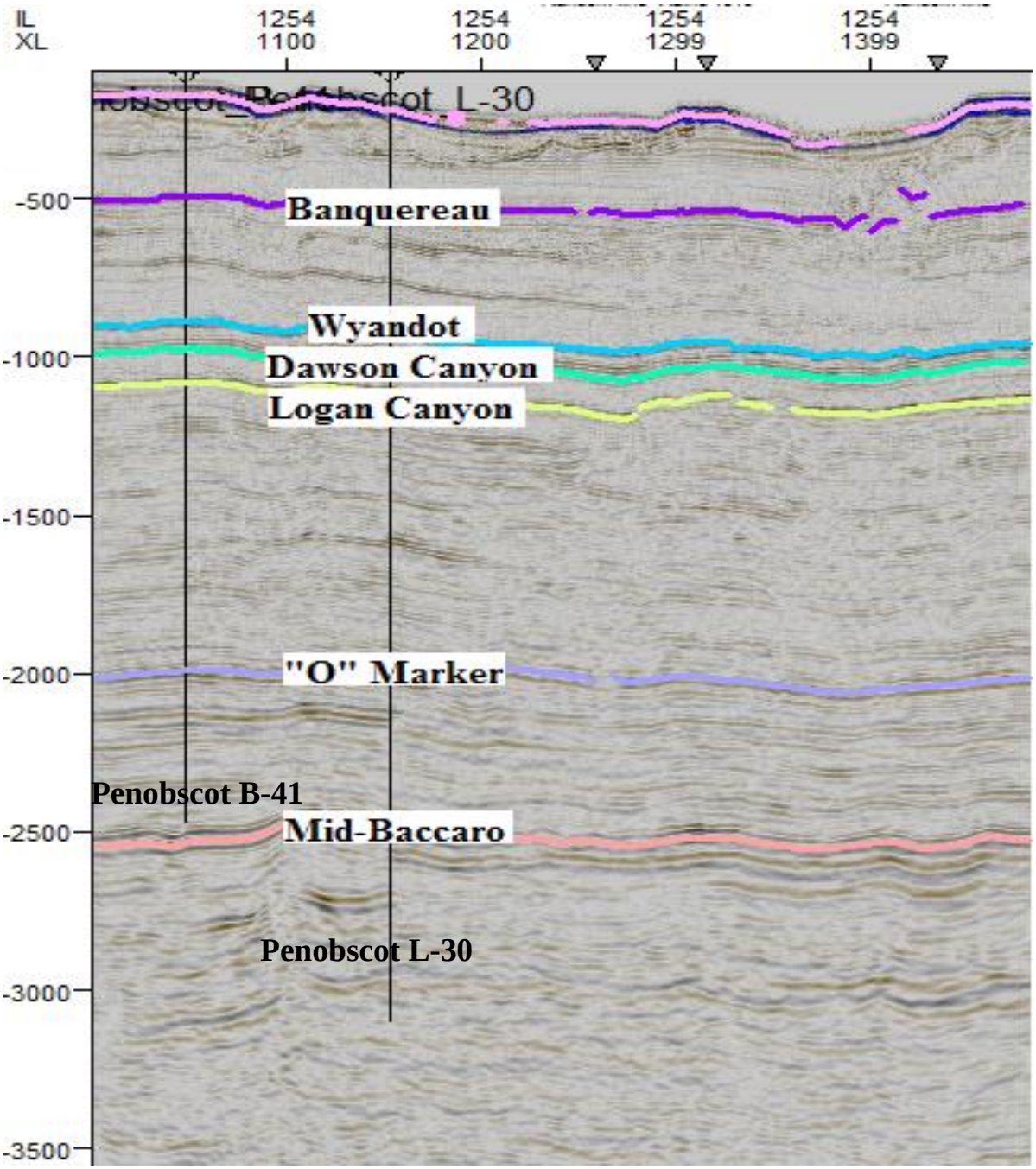

Figure 5.3: Inline 1254 demonstrating the seismic characteristics for the interpreted formations based off of the chosen formation tops (colorful horizontal lines). Penobscot L-30 is the black vertical line furthest to the right, whereas Penobscot B-41 is the black vertical line furthest to the left.

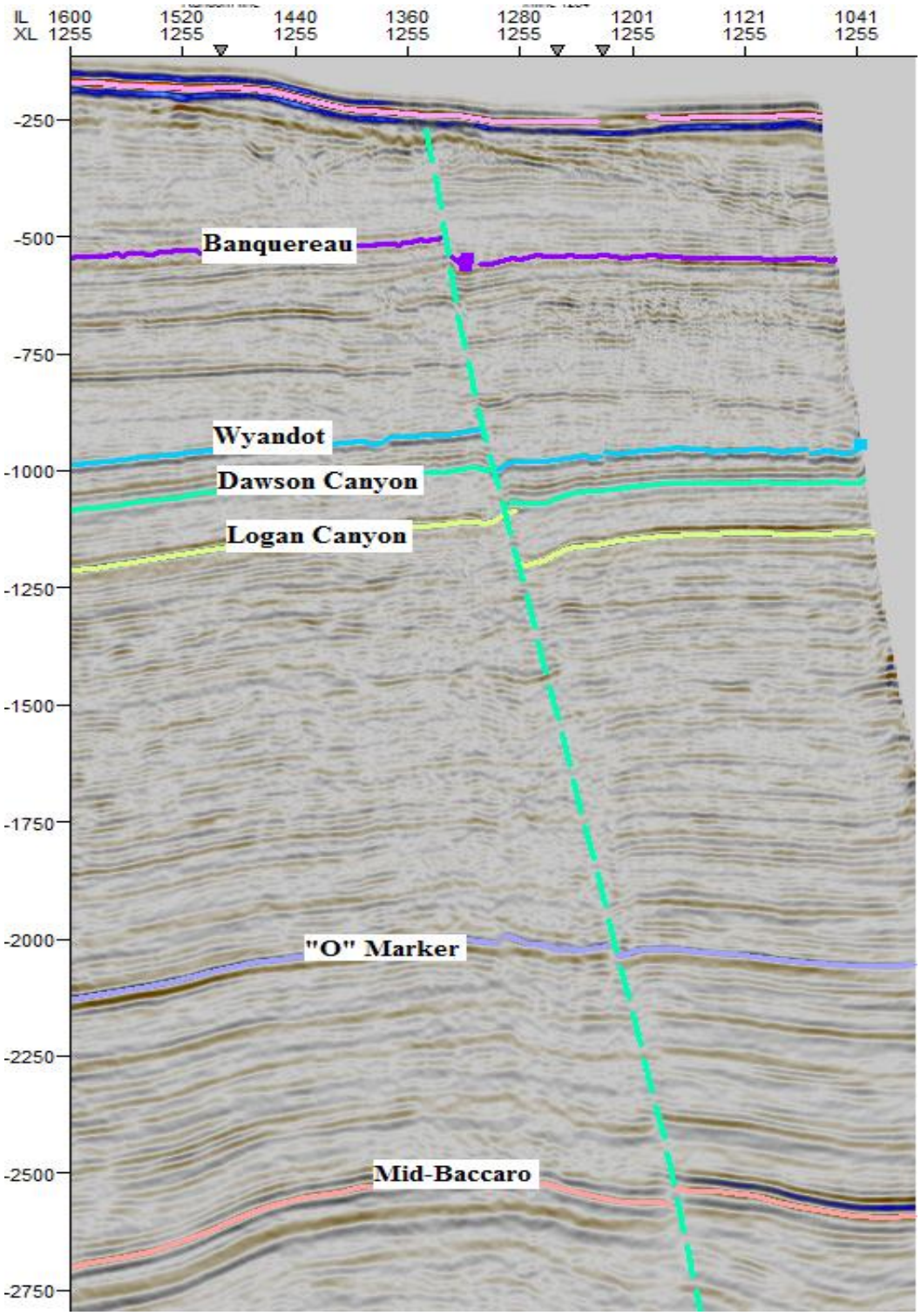

Figure 5.4: Xline 1255 demonstrating seismic characteristic for each interpreted formations based off of the chosen formation tops (colored horizontal lines) and location of one of the major normal listric faults.

Abenaki Formation: Mid-Baccaro Member (Late Jurassic):

The top of the Mid-Baccaro member of the Abenaki Formation is identified as a strong continuous reflector across the whole area, at approximately 2.55 seconds. The strong reflector at the top of the member can be correlated from the Penobscot L-30 well (Figure 5.3). The reflectors below the top of Mid-Baccaro are primarily facies A and B, although they are also chaotic reflectors, facies C, further down the unit, potentially due to decrease of frequency within the seismic section. On the inlines the reflector is relatively straight over the entire area; however in the xline, the member top is offset as a result of one of the two major normal listric faults in the area (Figure 5.4). The top of the Mid-Baccaro Member can be seen in figure 5.5. The color represents elevation time, demonstrating that there is a low area is the north-northwest corner gradually getting higher moving to the south. The large dark maroon angular areas in the middle of the figure are the two large normal listric faults that are creating a minor offset that can be seen when closely examining the color change on either side of the faults.

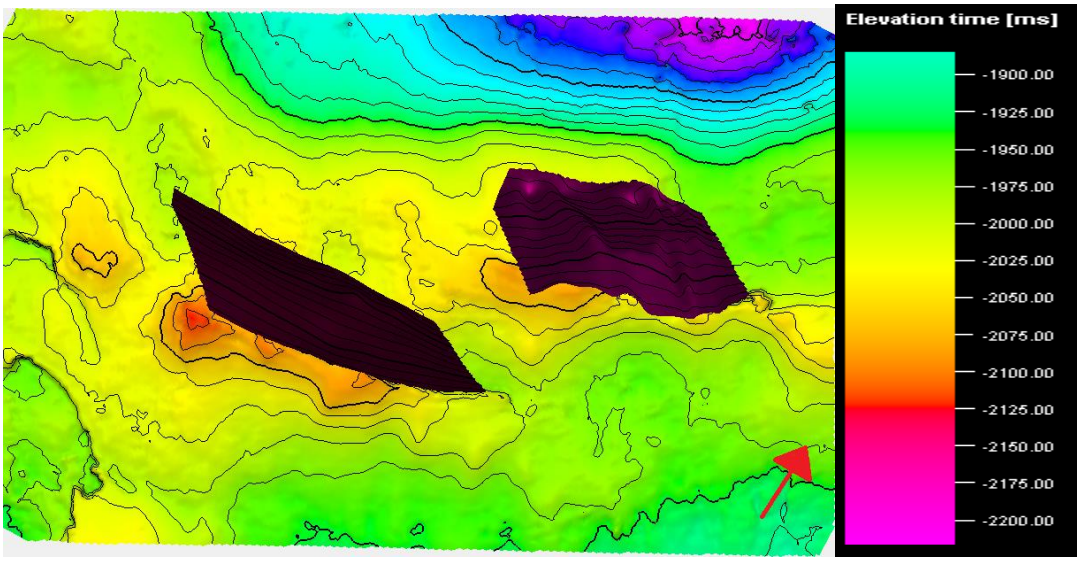

Figure 5.5: Top of the Mid-Baccaro Member, faults represented by two dark maroon areas. Color axis represents elevation in time. Red arrow represents north.

Missisauga Formation (Late Jurassic – Early Cretaceous):

The Lower Missisauga Formation, overlying the Mid-Baccaro, is the deepest formation that both Penobscot L-30 and Penobscot B-41 penetrate, allowing accurate correlation across the section. The formation is characterized by facies B and D that become discontinuous in certain areas. The main reflector interpreted across the entire section represents The "O" marker characterized by oolitic to skeletal and sandy limestone beds (Wade and MacLean, 1990) in the upper part of the Missisauga Formation. The "O" Marker is an excellent regional seismic marker horizon. Below The "O" Marker is the lower part of the Missisauga Formation that is characterized by more continuous parallel reflectors. The Missisauga Formation is cross-cut by both of the main normal listric faults in the xline (Figure 5.3 and Figure 5.4). The top of The "O" Marker can be seen in figure 5.6. The same characteristics can be observed in figure 5.6 as what was observed in figure 5.5. There is a low is the north-northwest area, gradually increasing in elevation moving to the south and being offset by the two large faults in the middle of the figure.

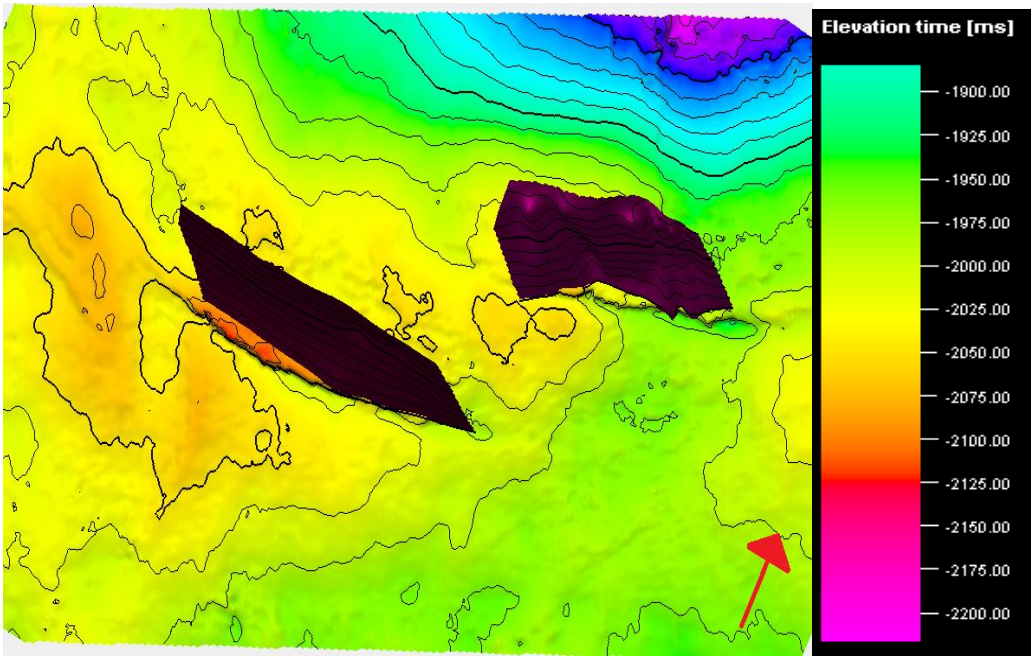

Figure 5.6: Top of the "O" Marker. Color axis represents elevation in time. Red arrow represents north.

Logan Canyon Formation (Early – Late Cretaceous):

The seismic response for the Logan Canyon Formation, made up of interbedded coarse clastics and shales, is characterized by facies B and D that become weaker seaward (right-hand side of Figures 5.3 and 5.4) The strong reflector that marks the top of the Logan Canyon is characterized by the contrast in velocity of the shales of the Dawson Canyon Formation above, to the sands of the Logan Canyon Formation. The Logan Canyon Formation is offset by both normal listric faults through the section that can be identified in the xlines. Top of the Logan Canyon can be seen in figure 5.7 and it can be observed that there is beginning to be more of a contrast in elevation is specific areas compared to figure 5.5 and 5.6. The north-northwest corner is not quite as shallow, it is still gradually increasing in elevation, however the offsets that the two faults create appear to be larger demonstrated by the elevation being approximately 2050ms on the northern side of the faults, jumping to 2200ms on the southern side of the faults.

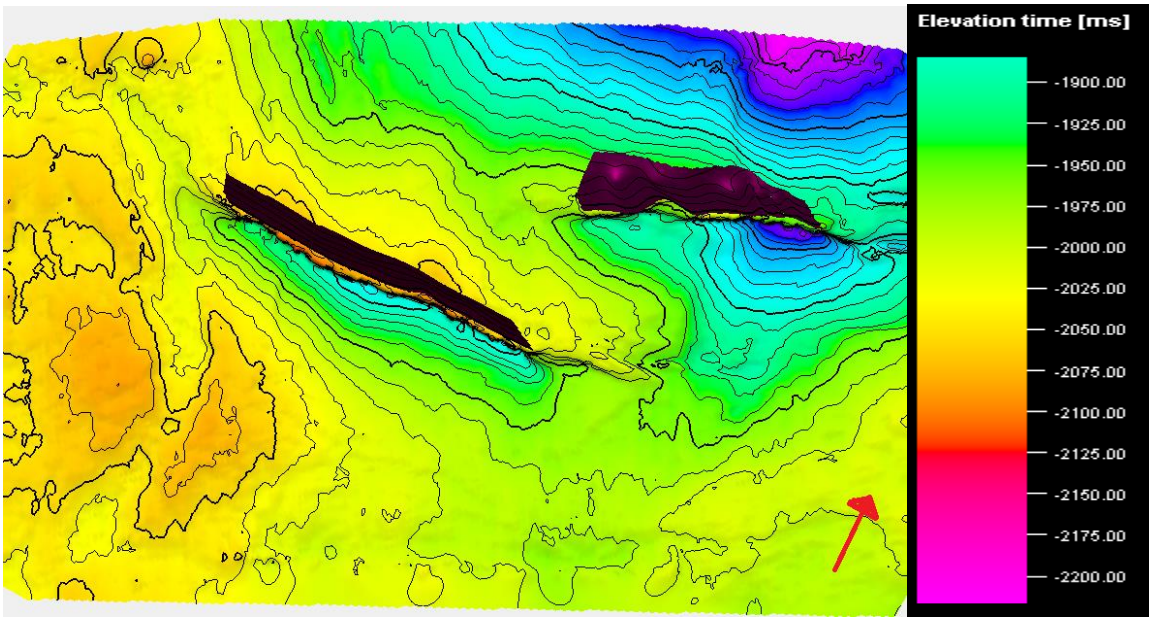

Figure 5.7: Top of Logan Canyon Formation. Color axis represents elevation in time. Red arrow represents north.

Dawson Canyon Formation (Late Cretaceous):

The top of the Dawson Canyon Formation is a strong clean reflection that can be correlated across the entire area. It is characterized by facies B made up of deep marine shales and limestone (Figure 5.3). Dawson Canyon Formation is offset as result of both normal listric faults (Figure 5.4) through the section. Top of the Dawson Canyon Formation can be seen in figure 5.8. The elevation change is still quite drastic for the eastern most normal fault, although the western most faults offset is decreasing. There also appears to be a low elevation area beginning to emerge in the western corner, represented by the color red.

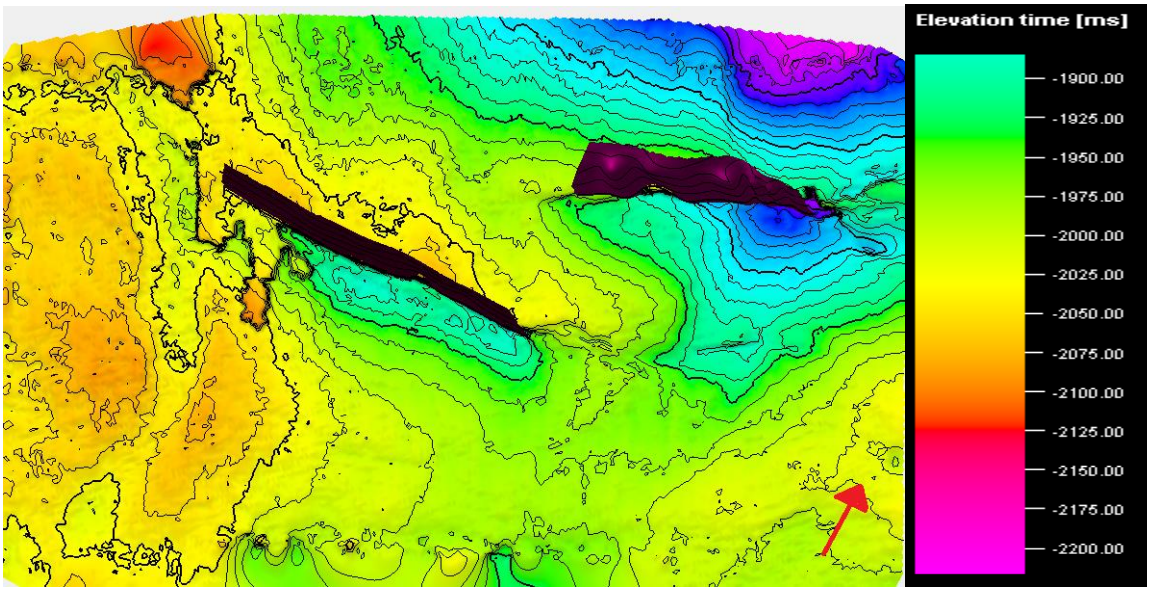

Figure 5.8: Top of Dawson Canyon Formation. Color axis represents elevation in time. Red arrow represents north.

Wyandot Formation (Late Cretaceous):

The Wyandot Formation, also deposited during the Late Cretaceous conformably on top of the Dawson Canyon Formation, comprises marine marls and chalky mudstones that create strong, clean and continuous reflectors across the entire area. The reflectors are made up of facies B and D, with amplitudes weaker in certain areas. The Wyandot Formation is offset by both normal listric

faults throughout the area. The top of the Wyandot can be seen in figure 5.9. The elevation of the area has changed quite when comparing the Mid-Baccaro to the top of the Wyandot Formation. There is still the low elevation area in the north-northwest corner, although there is also more topographic lows throughout the western area, represented by the red color. The western most fault is not causing as large of an offset, and the offset of the eastern most fault is also decreasing.

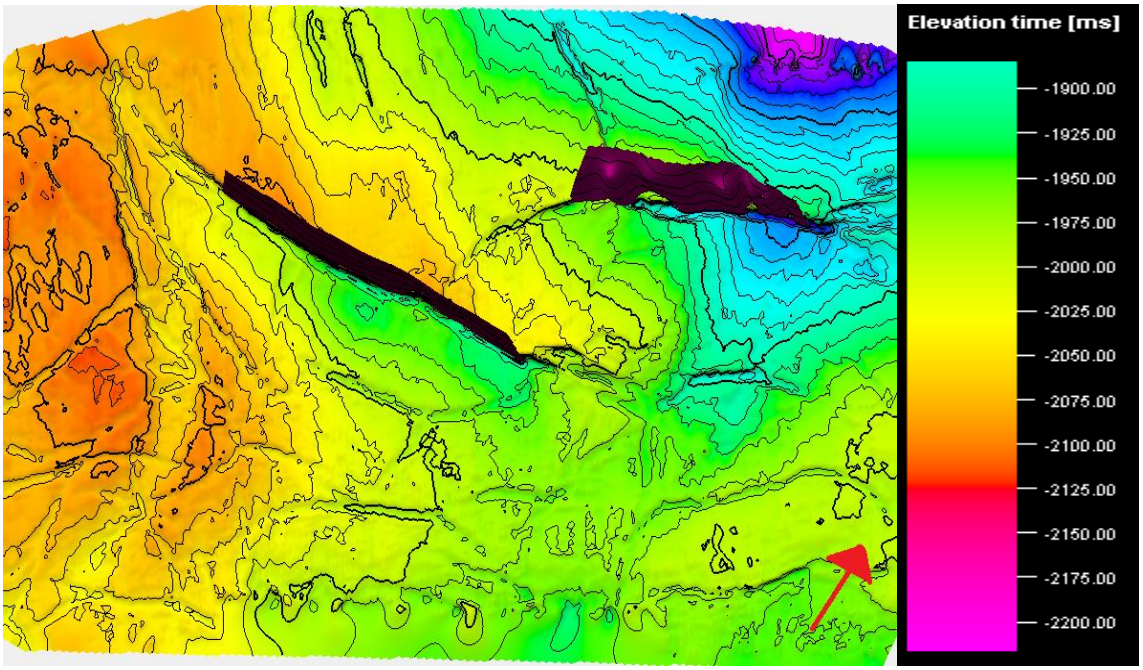

Figure 5.9: Top of the Wyandot Formation. Color axis represents elevation in time. Red arrow represents north.

Banquereau Formation (Late Cretaceous – Present):

The seismic reflectors of the Banquereau Formation are characterized by very strong, continuous reflections, made up mostly of facies A and B throughout the mudstones, sandstones and thin chalk layers. Slumping occurs as sediment was deposited basinward, (left-hand side of Figures 5.3 and 5.4), creating chaotic seismic reflectors. The two normal listric faults in the area create an offset of the Banquereau Formation, which can be seen in figure 5.4. Top of the Banquereau can be seen in figure 5.9. Slumping within the area making the correlation across all

of the seismic lines difficult causes the artifact in figure 5.9, in the eastern area. The top of the Banquereau Formation does not have many topographic changes, although the tops of both normal listric faults are still seen, not creating any offset.

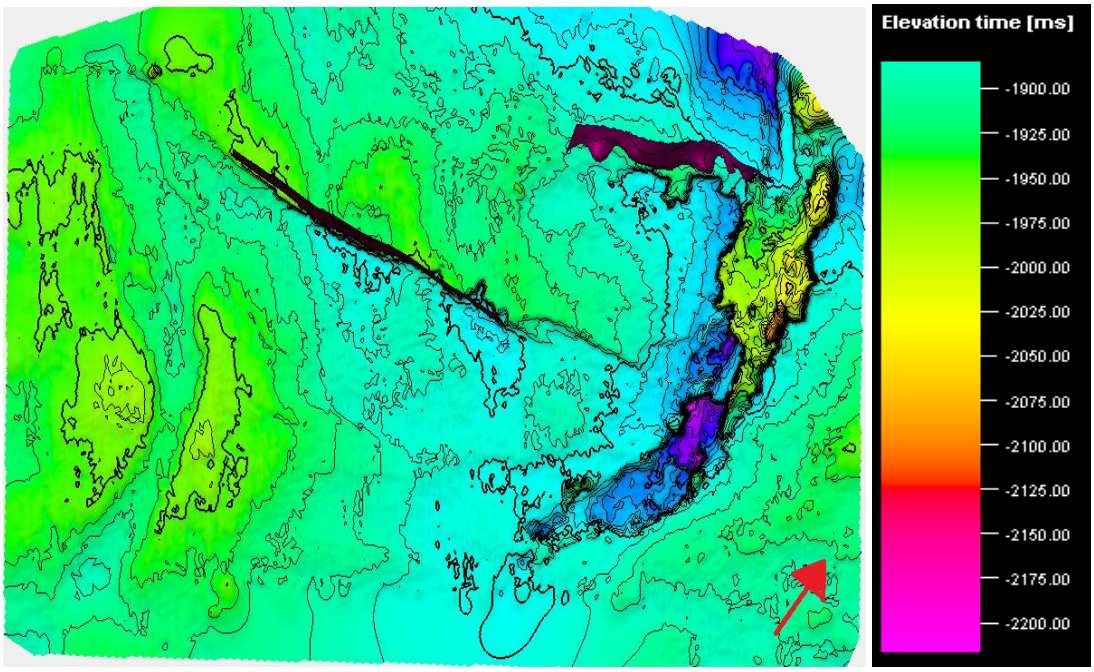

Figure 5.10: Top of the Banquereau Formation. Color axis represents elevation in time. Red arrow represents north.

5.4 Jason Software Results:

The method of running an inversion, described in detail in Chapter 3, was carried out and the results obtained with Jason were slightly different than the results obtained with Petrel. For Jason, the four horizons (chosen reflectors) given with the seismic dataset were used instead of indentifying the six reflectors previously interpreted and mentioned above with Petrel. This was done because the purpose of using Jason was to use seismic inversion, and not make reflection and structural interpretations, for that was already done with the use of Petrel.

5.4.1 Tying the Wells:

Tying the wells to the seismic is an important step in the inversion process. If the wells do not have a time-to-depth relationship, the inversion results will have no significance because the area of interest will be known amongst the wells; however the location within the seismic data will not be known. The inversion process requires carefully tied wells to derive a proper wavelet that determines the quality of the final inversion result. To tie Penobscot L-30 and B-41 to the seismic, a synthetic seismic log, which is derived from the initial given wavelet and the P-impedance log (sonic/density), was created to interpret petrophysical logs at every trace of the seismic. By matching key reflectors from the original seismic, to those of the synthetic log, with different stretching and squeezing techniques (as described in Chapter 3), a tie between the seismic and wells was created. The correlation between the geophysical and petrophysiscal data was satisfactory with Penobscot L-30 having a correlation of approximately 50% and Penobscot B-41 having a correlation of approximately 60%.

5.4.2 Estimating wavelets:

After the time-to-depth relationship between the wells and seismic was made, new wavelets were estimated from the wells. Without using data from the wells for wavelet estimation, the wavelet would be based on statistical techniques (Jason-a CGG Company). The inferred shape to the seismic wavelet can strongly influence the reservoir quality assessment; therefore it is important a proper shaped wavelet is created. The wavelets created for Penobscot L-30 and B-41 were very similar in shape, as they should be to create an accurate multi-well wavelet. The wavelets created for both wells can be seen in figures 5.11A and 5.11B. The multi-well wavelet, explained in greater detail in Chapter 3, is the final wavelet that is used during the inversion process. It is used to create a better tie between the two wells and can be observed in figure 5.12.

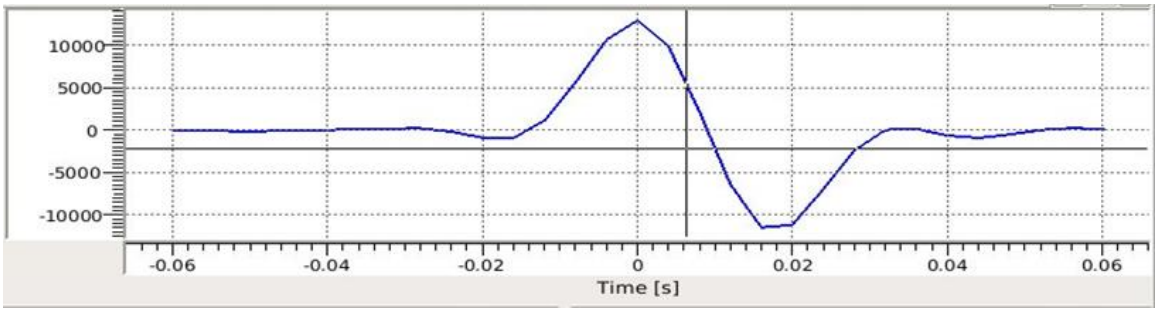

Figure 5.11 A: Estimated wavelet for Penobscot L-30.

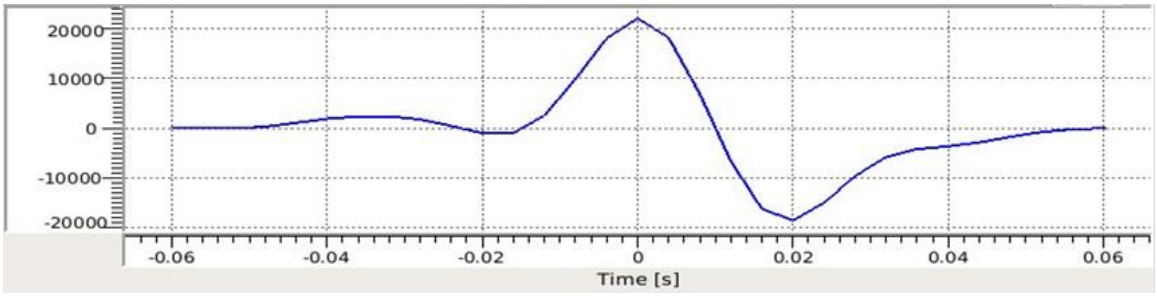

Figure 5.11 B: Estimated wavelet for Penobscot B-41.

In figures 5.11 A and 5.11 B, it can be observed that both wavelets are very similar in shape, both are centered on 0 seconds, and both of them taper off the 0 on the y-axis. The shape of both wavelets is known as a 45º phase.

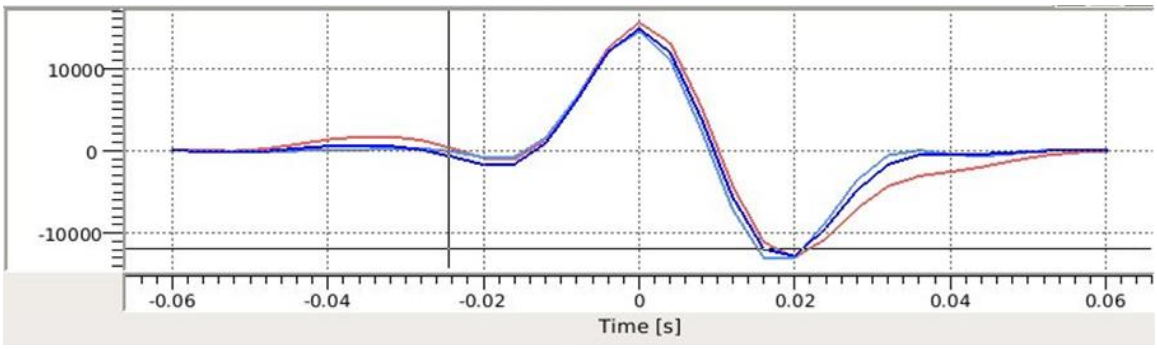

Figure 5.12: Multi-well wavelet.

In figure 5.12, the graph is shown with three wavelets. These wavelets represent the wavelet for both wells, and the multi-well wavelet. It can be seen that the wavelets from both wells fit nicely over the top of one another, this is ideal to run a successful inversion.

5.4.3 Solid Model:

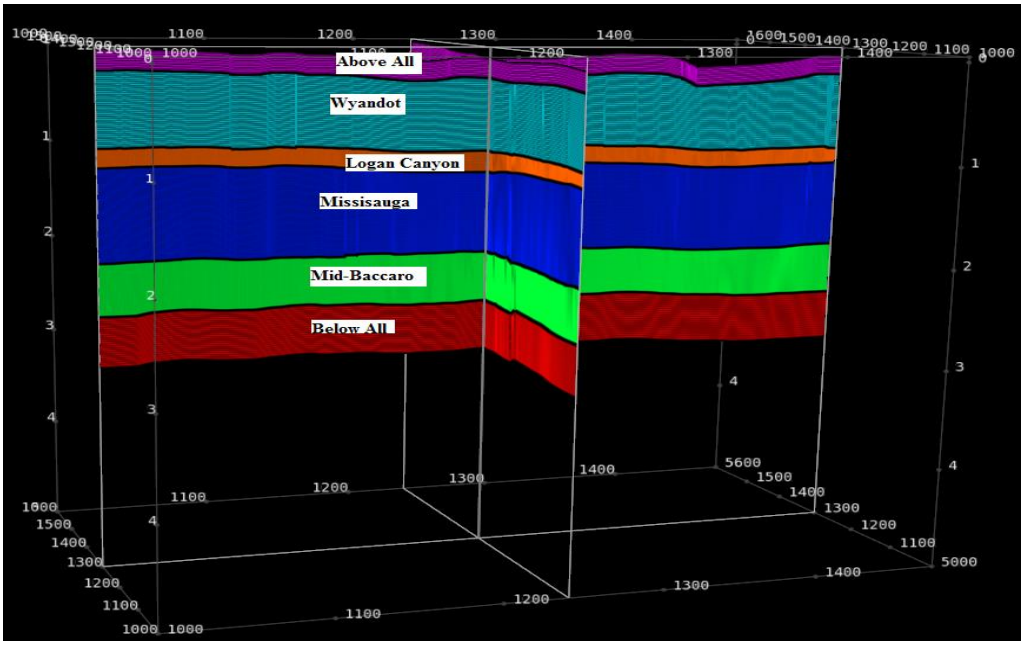

Figure 5.13: Constructed Solid Model with a 20 times exaggeration on the Y-axis. The Solid Model represents the geological information that is inputted into the Low Frequency Model, and then used in the final inversion. The colored layers represent formation thicknesses in time.

As mentioned in Chapter 3, the Solid Model creates a basic geological model with the given horizons that will be used in the final seismic inversion. It encloses the area of interest that the inversion will focus on. For the purpose of this study, all of the horizons were input into the Solid Model. Figure 5.13 shows the 3D view of the created Solid model. The different colored layers within figure 5.13 represent the formations that were given with the seismic dataset. The layers labeled "above all" and "below all" represent values that were input into the Solid model to enclose a larger space. Without these two layers, the Solid Model would not enclose below the Mid-Baccaro, a formation to which Penobscot L-30 reaches, therefore there would be no data beyond the Mid-Baccaro Member in the final inversion and no geological properties would be known. The two normal listric faults in the area would typically appear in the Solid Model;

however they were not needed for the purpose of this inversion since the focus of the inversion is on determining lithology and not structural elements.

5.4.4 Low Frequency Model:

After the Solid Model is created, the next step, described in chapter 3, is to create a Low Frequency Model that fills in the frequency "gap" that is missing between the petrophysical data, and the geophysical data. The Low Frequency Model created can be seen in figure 5.14. The Low Frequency Model should be very similar to the final inverted acoustic impedance results since low frequencies are the most critical to determining rock properties (Jason – a CGG Company, 2013). The Low Frequency Model, as seen in figure 5.14 is defined by a cube of interpolated impedance logs across the entire area of interest, in this case, the entire survey. In the Penobscot survey, the horizons are generally all flat-lying beds without much structure. The two normal listric faults would typically be shown in the Low Frequency Model, however since they were not used in the Solid Model, the model which contains all geological interpretations, they would not appear in the Low Frequency Model.

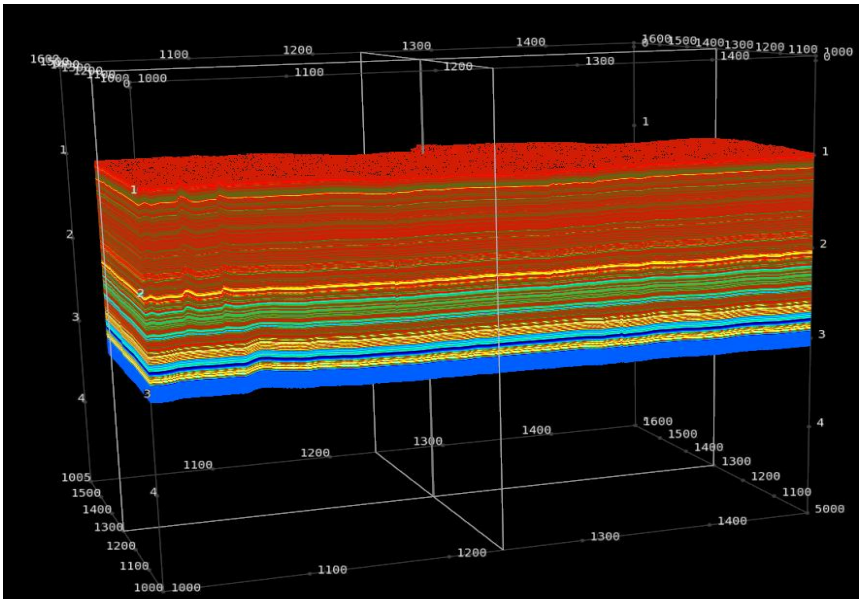

Figure 5.14: Low frequency model created using the inputted data from the Solid Model of the Penobscot 3D seismic survey. The Low Frequency Model represents the ideal version of the geological properties throughout the area; it should be very similar to the final inversion results.

5.4.3 Inversion Results:

The acoustic impedance inversion resolution has been determined by the frequency content of the input data, as you can see in figure 5.15, which in the entire Penobscot 3D survey area is represented by acoustic impedance and it closely resembles figure 5.14 but is more detailed. The resolution also is determined by the shape of the wavelet. Figure 5.15 demonstrates how continuous and parallel the lithologies are across the section. The acoustic impedance results that were obtained show the same units that were chosen with the use of Petrel and they represent real geological properties as opposed to seismic reflections. The colors of the acoustic impedance results represent specific lithological properties that will be further discussed in chapter 6.

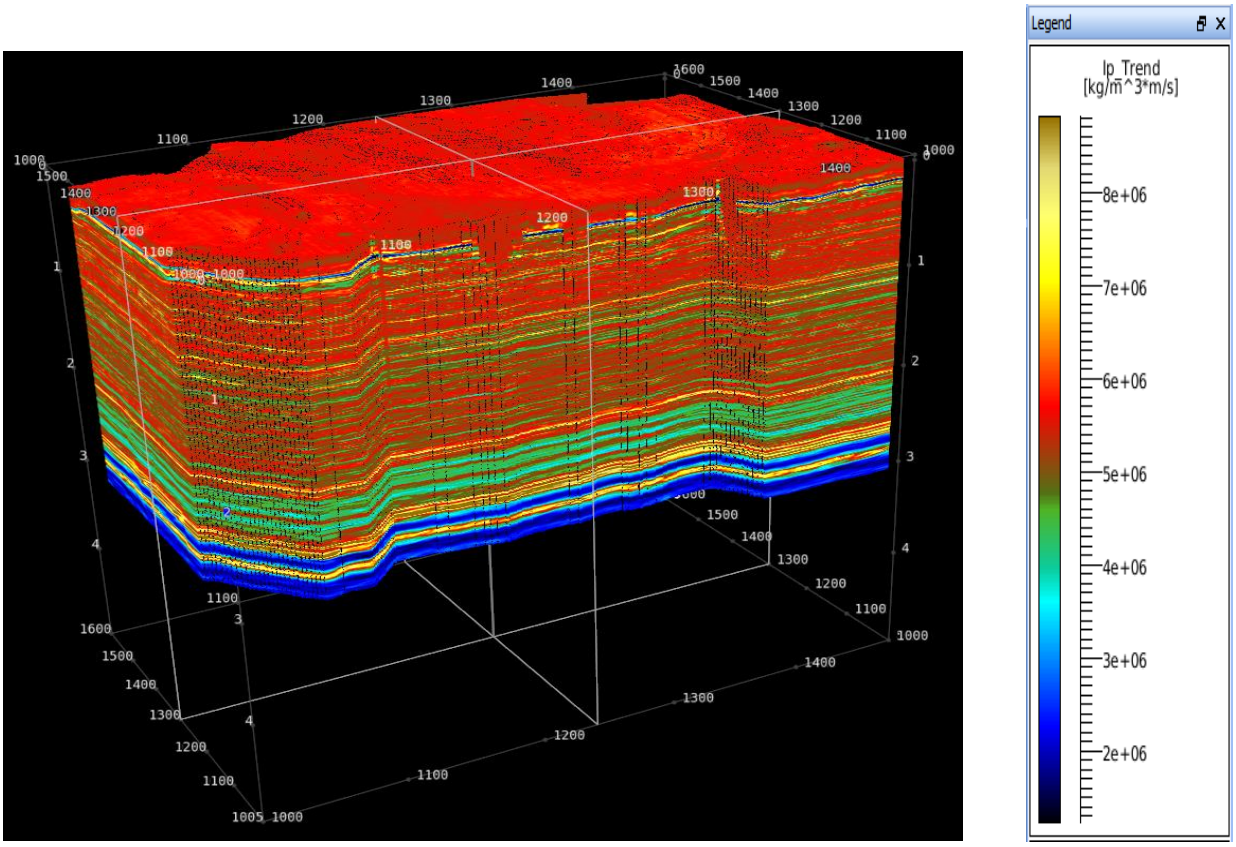

Figure 5.15: 3D view of entire Penobscot survey area with acoustic impedance. Geological properties can be observed, such as; the approximate thicknesses of the formations, the extent to which they extend and where the are located. The color represents the acoustic impedance values, determined by the velocity and density of each formation.

5.5 Wireline logs:

Penobscot L-30 and Penobscot B-41 were examined with the use of Petrel and the Jason Software. The two logs of interest for this study were the gamma ray log, and the resistivity log. From these two logs, nine formation tops were chosen on Penobscot L-30 and eight formation tops on Penobscot B-41, including the location of the cored interval in Penobscot B-41. These two logs were mainly studied for the purpose of identifying lithological units and correlating them with the cored intervals. Figure 5.17 illustrates the gamma ray log (green, yellow and brown logs) over the top of the caliper log, the shallow resistivity log over the top of the deep resistivity log (middle column) and the delta rho log over the top of the neutron porosity sandstone for Penobscot B-41 and limestone for Penobscot L-30 (blue, gray and black logs), although the first two columns were the only ones studied in detail for the purposes of this study.

The seven units that were identified by selecting horizons are identified in the well logs in figure 5.16, the units being; the sea floor - Wyandot Formation, Wyandot Formation-Dawson Canyon Formation, Dawson Canyon Formation-Logan Canyon Formation, Logan Canyon-Base "O" Marker, and Base "O" Marker-Mid-Baccaro. The Upper and Lower Missisauga tops were chosen by knowledge of stratigraphy of the area and the abrupt change of lithology observed on both the gamma-ray logs. Well logs will be discussed in more detail in Chapter 6.

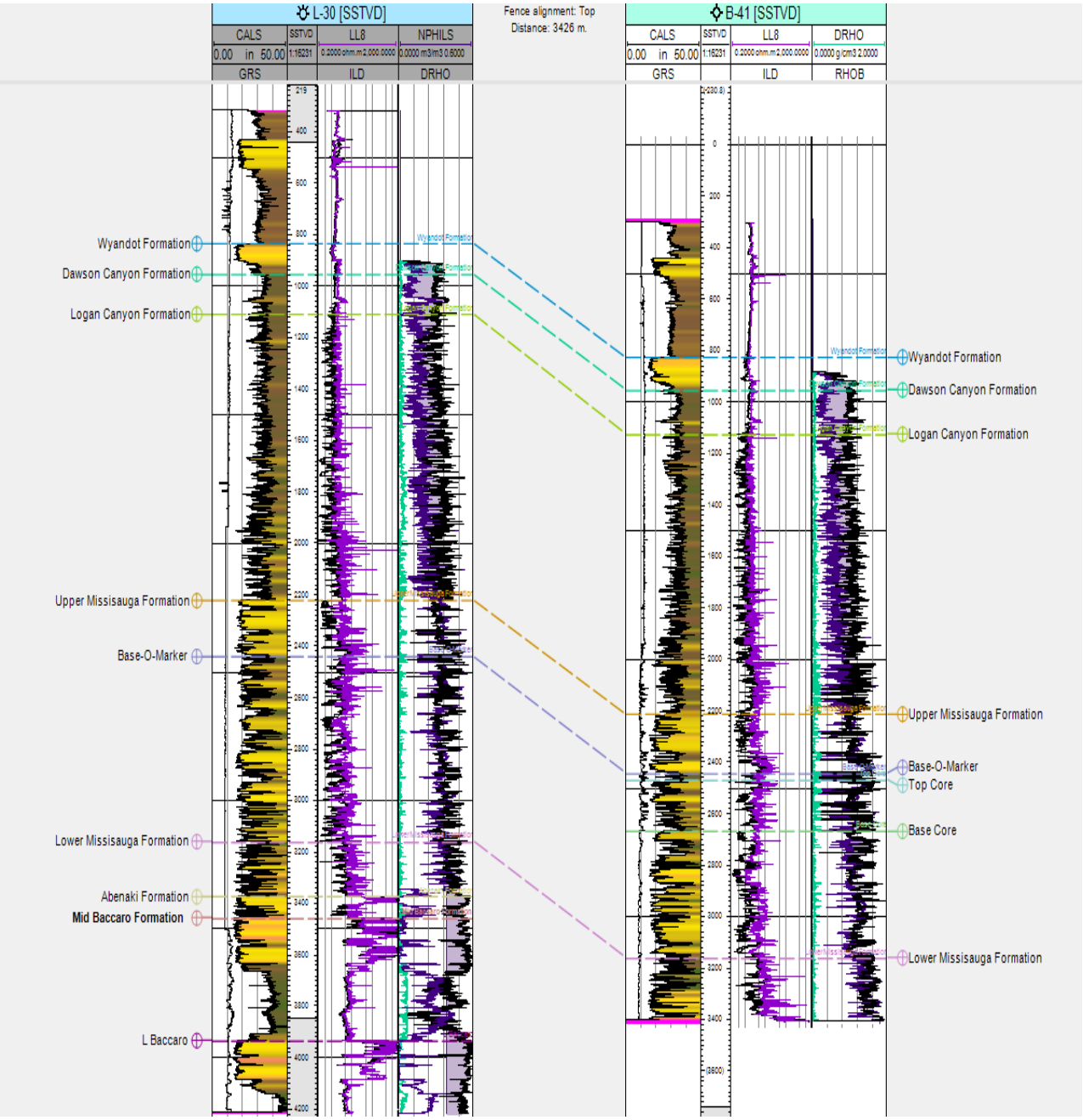

Figure 5.16: Penobscot B-41 and Penobscot L-30 wireline logs with formation tops. The formation tops were chosen on Penobscot L-30 primarily, and then correlated to Penobscot B-41 with the use of the gamma ray log, identified as the yellow, green and brown log. This is demonstrating that all well logs were examined and correlated, however primarily only the gamma ray log and sonic log were used throughout the study.

CHAPTER SIX- DICUSSION

6.1 Lithological and stratigraphic interpretations:

The Baccaro Member horizon of the Abenaki represents the Top Tithonian boundary of the Upper Jurassic. Beneath this horizon the Penobscot L-30 well shows beds of grey lime packstone, which were identified in the core taken from the Baccaro member and explained in Chapter 4. The strong reflector is due to the velocity contrast between the overlying sandstones and siltstones of the Missisauga Formation and the carbonates that make up the Baccaro Member. Based on Wade and MacLean (1993), the Baccaro Member is interpreted as carbonate interbedded with marlstone and sandstone, although only the carbonate interval was cored. It comes into contact with the shales and marlstones of the Misane Member (approximately 350 m deeper) (Figure 6.1). The transgressive shales, sandstones and marlstones of the Misane continue for another 250 m approximately until the well encounters the Scatarie Member of the Abenaki, made up of primarily oolitic limestone, with lesser quantities of sandstones and shales, which can be confirmed from the core description of core 2 of Penobscot L-30 in Chapter 4, as well as interpreted by Wade and McLean (1993), demonstrated by a lithological log in figure 6.1.

The Missisauga Formation marks the beginning of the Cretaceous with primarily sandstone, grading into a shale-rich unit seaward, as interpreted by Wade and MacLean in1993. The Missisauga horizon is a strong reflector that is interpreted to be associated with the "O" Marker, made up of limestone, near the top of the Missisauga Formation, before the transition into the sandstones of the Logan Canyon Formation. This is also be confirmed with the core description in Chapter 4 of core 1 from Penobscot B-41 (Figure 4.4 B and C) The Missisauga Formation is also composed thin siltstone and marlstone beds, as seen in figure 6.2 (Wade and MacLean, 1993).

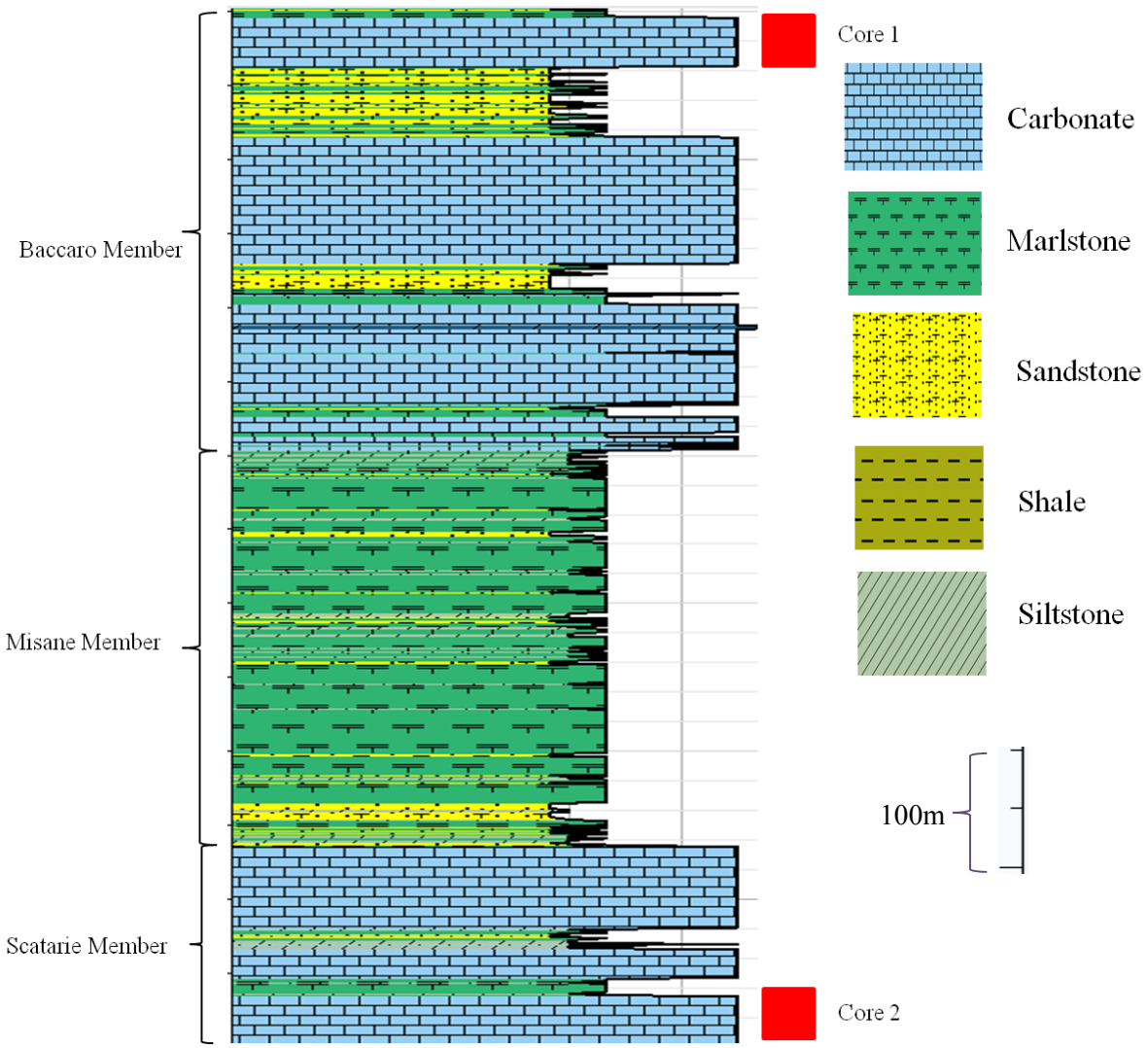

Figure 6.1: Lithological log from Penobscot L-30 identifying the locations the two cored intervals were taken, along with their corresponding lithologies (based on data from Wade and MacLean, 1993).

Logan Canyon horizon marks the top of the Cenomanian age of the Cretaceous, identifying the top of the Logan Canyon Formation. The Logan Canyon Formation is interpreted to be composed of sandstones deposited on the shelf, as well as shale deposited further off the shelf, closer to the top of the formation (Wade and MacLean, 1993). The seismic facies which make up the Logan Canyon Formation correspond to these lithologies, as seen in figure 5.4. They are parallel to sub-parallel, interpreted as flat lying beds of shales and sandstones.

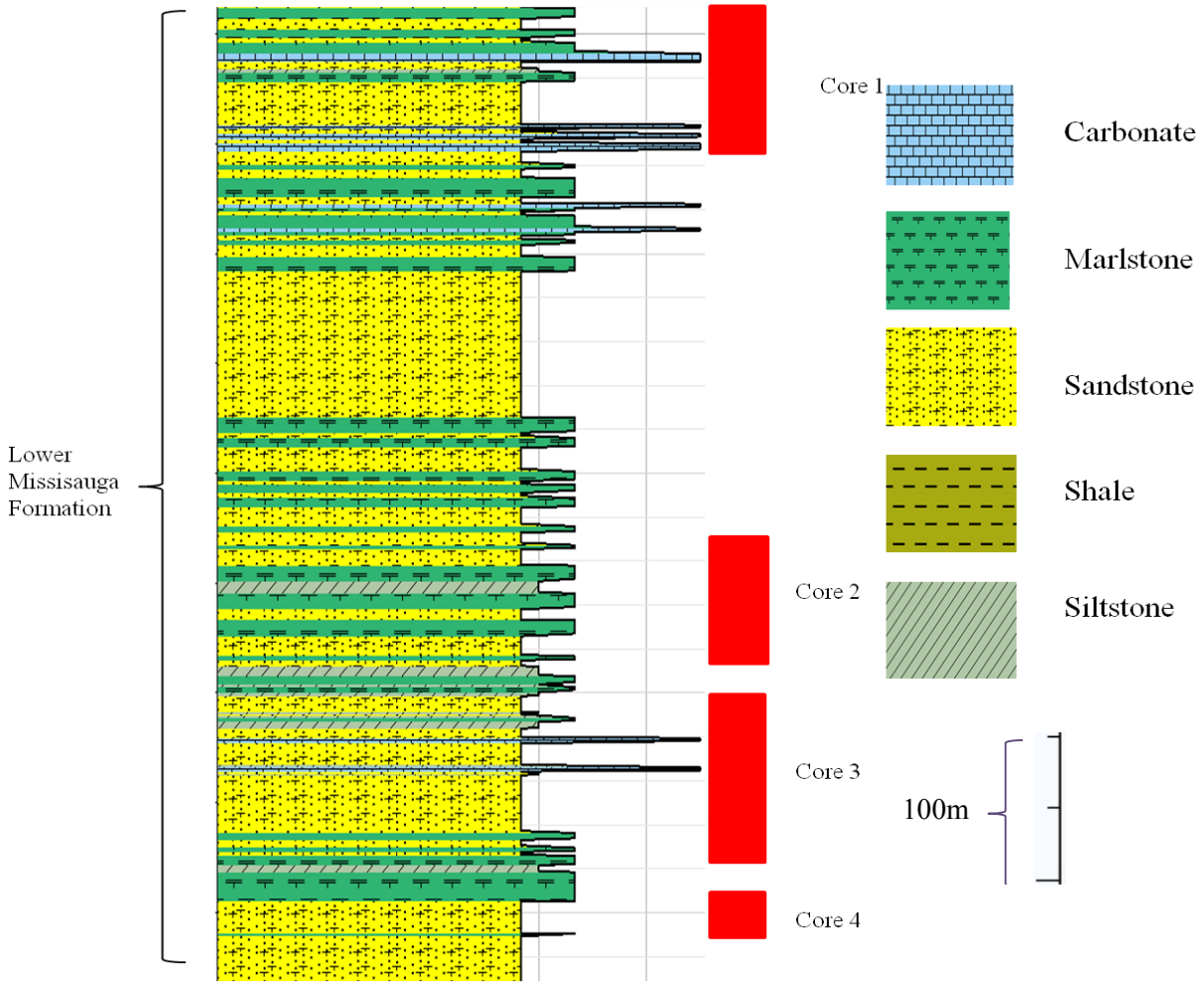

Figure 6.2: Lithological log from Penobscot B-41 identifying the locations the four cored intervals were taken, along with their corresponding lithologies (based on data from Wade and MacLean, 1993).

The Dawson Canyon horizon is represented by the strong reflector caused by the velocity change of the sandstones of the Logan Canyon Formation and the marine shales comprising the Dawson Canyon Formation. This is confirmed with the Dawson Canyon Formation comprising mainly seismic facies B (parallel reflectors), signifying shale beds. Wade and MacLean, 1993 also interpreted the Dawson Canyon Formation to contain minor amounts of chalk and limestone beds.

The Wyandot horizon is interpreted to be the top of the Lower Campanian age strata. The Wyandot Formation is composed of chalk, therefore creating a strong reflector. Overlying the Wyandot horizon is the Banquereau Formation consisting almost entirely of shales and sandstones,

with some thin siltstone beds (Wade and MacLean, 1993). This is also indicative of the sub-parallel- chaotic seismic facies due to overburden, seen throughout the Banquereau Formation.

6.2 Petrophysical Facies:

The lithofacies determined from the cored intervals of Penobscot L-30 and Penobscot B-41, as described in Chapter 4 represent important intervals within the Penobscot area. The Abenaki Formation represents an important reservoir and source of the Scotian Basin, and can be found in the Penobscot L-30 well. The cored intervals of the Baccaro Member and Scatarie Member were broken into three distinct lithofacies and then compared to the gamma log and sonic log to determine petrophysical facies, characteristic to those of the three lithofacies. When examining the gamma ray log in the locations of where the core was taken, at approximately 3424m (2.5s) and 4049m (2.65s), there are very large spikes (Figure 6.3) indicating quite low gamma response, approximately 15gAPI, alternating to 125 gAPI within the next 0.05s. This response is quite unusual, and the interpreted reasoning being that it is within the last 0.3s of the log therefore the results could have been potentially skewed as the tool was being brought back up the borehole. Therefore petrophysical facies for this log were not made, for there are no other similar gamma ray responses within the log. If the gamma ray readings were indeed correct, a large spike in gamma corresponding to approximately 15 gAPI jumping to 125 gAPI would represent the petrophysical facies.

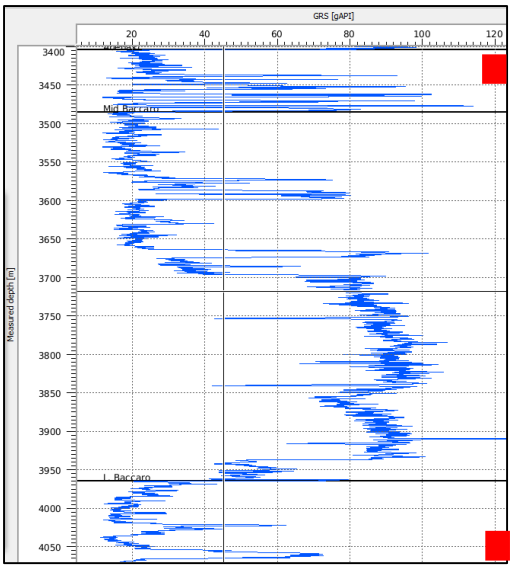

Figure 6.3: Zoom in of gamma ray log for Penobscot L-30 indicating intervals of the two cores (red boxes). The gamma ray response is believed to be an artificial low, changing quickly to a high gamma ray response. The entire gamma log from which this was taken can be seen in appendix 1.

The petrophysical facies for Penobscot B-41 were determined, with the use of the gamma ray and sonic logs for this well, modified from Robertson (2000). The lithofacies that were described in Chapter 4 were plotted on a stratigraphic log and correlated with the approximated depths of the gamma ray and sonic logs (Figure 6.4 A to C). The depths of the lithofacies are not exact, for they were chosen at the distinct changes of gamma ray so they can be determined throughout the entire well log. Appendix 2 contains the entire gamma ray and sonic logs for Penobscot B-41, to examine where these figures were taken.

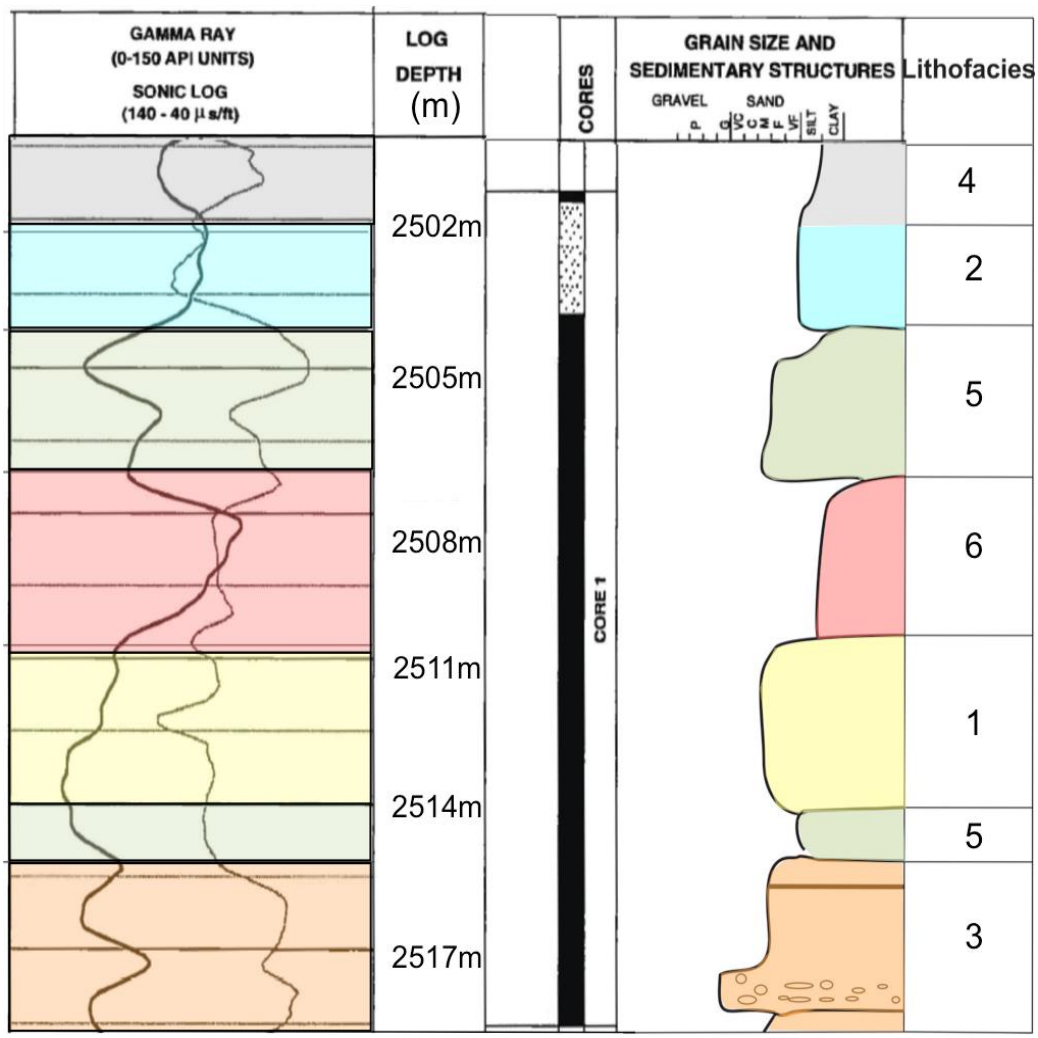

Figure 6.4 A: Gamma and sonic log response for Penobscot B-41 of core 1. The lithofacies identified from the stratigraphic log are correlated to the well logs, indicating what the petrophysical response looks like for each lithofacies (modified from Robertson, 2000).

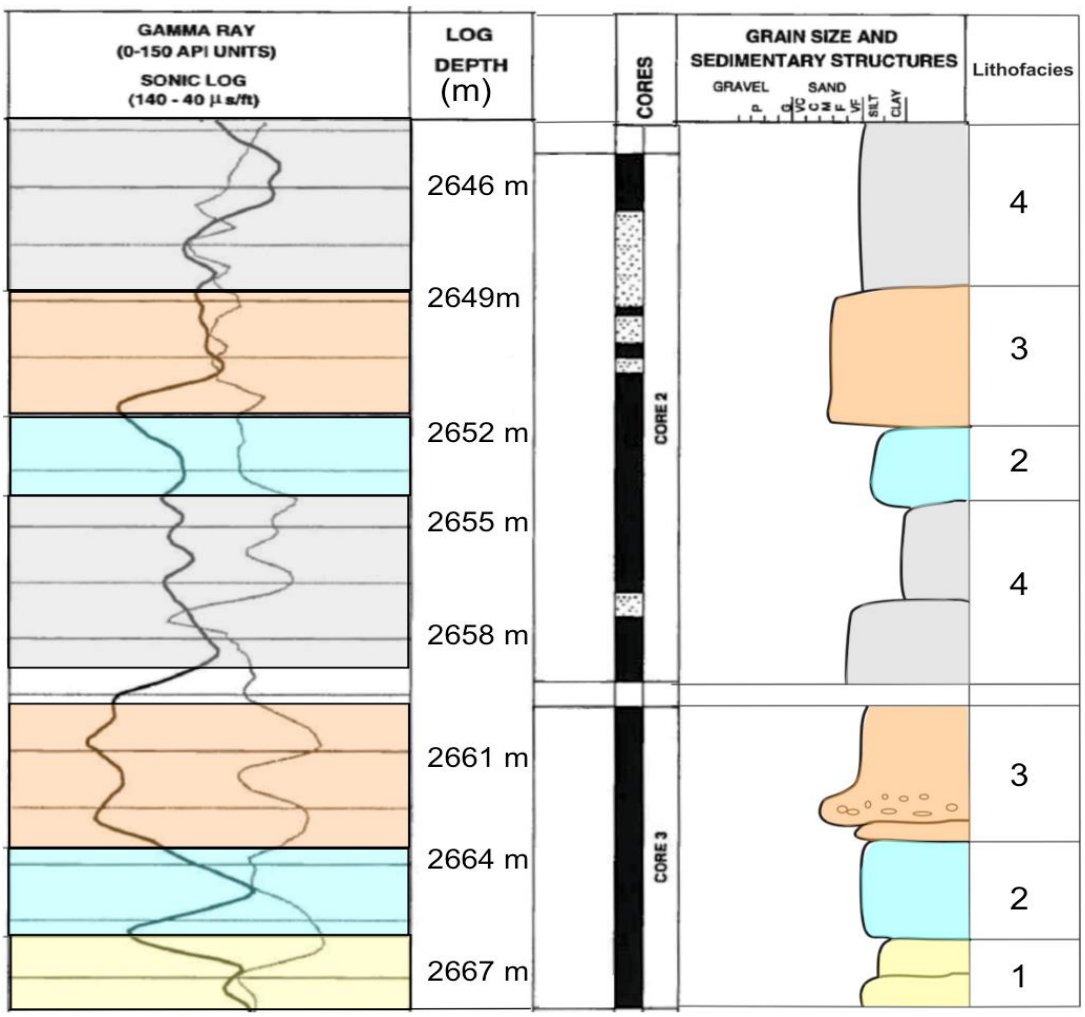

Figure 6.4 B: Gamma and sonic log response for Penobscot B-41 of core 2 and 3. The lithofacies identified from the stratigraphic log are correlated to the well logs, indicating what the petrophysical response looks like for each lithofacies (modified from Robertson, 2000).

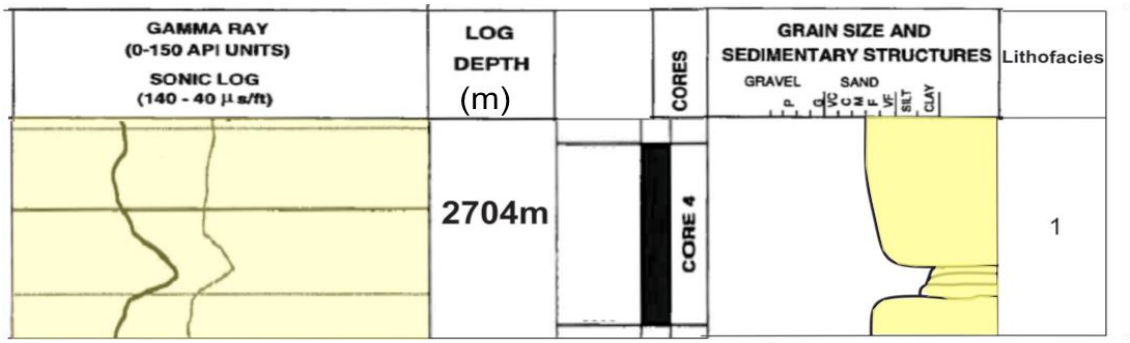

Figure 6.4 C: Gamma and sonic log response for Penobscot B- of the core 4. The lithofacies identified from the stratigraphic log are correlated to the well log, indicating what the petrophysical response looks like for each lithofacies (modified from Robertson, 2000).

Lithofacies 1:

The petrophysical facies for lithofacies 1 are generally represented by low gamma ray values. The sonic log trend appears to be low sonic, indicating a relatively fast velocity. The low gamma ray and relatively fast velocities responses are indicative of consolidated sandstone.

Lithofacies 2:

The gamma and sonic log response for lithofacies 2, have a gamma ray range of 75 API to 100 API, relatively high values. The increasing trend in gamma ray and decreasing trend in sonic, show the gamma increases as the velocity increases, since sonic is 1/velocity. These values are characteristic of organic-rich consolidated sandstone, representative of lithofacies 2.

Lithofacies 3:

Lithofacies 3 has low gamma ray and low sonic values. Lithofacies 3 and lithofacies 2, are similar, however lithofacies 3 contains little to no bioclastic material. In terms of the gamma ray response, this makes sense, low gamma ray indicating little organic material. The low sonic values represent a fast velocity, indicative of consolidated sandstone, like that of lithofacies 3.

Lithofacies 4:

The petrophsical facies for lithofacies 4 is difficult to determine. The gamma ray values range from approximately 70 API to 100 API. It is known from the lithofacies description, that this is fissile shale. This would typically infer that the gamma ray values would appear higher. The calcareous component of the shale may be altering the gamma ray value, generating smaller values than expected. The sonic log has spikes indicating higher sonic values, inferring slower velocities, again something that would not be expected for a compacted shale lithofacies. There some

intervals within both logs that demonstrate high gamma ray and low sonic, indicative of shale. The areas within the log that are creating the contradicting values potentially relate to the sandier parts of the lithofacies that have been intermixed the sand-rich lithofacies below.

Lithofacies 5:

Lithofacies 5, silty sandstone is denoted by a low gamma response and low sonic response. The gamma ray values appear to be slowly decreasing in both intervals, and the sonic values follow the shape of the gamma log, although first interval is too thin to extract an overall trend.

Lithofacies 6:

The petrophysical facies for lithofacies 6 is difficult to determine, due to one occurrence. The response has is a relatively high gamma value, and a low sonic value. Lithofacies 6, lenticular red shale, contains abundant organic materials and is well compacted, generating high gamma values and a fast velocity. An overall trend cannot be distinguished from only one occurrence.

Comparing the petrophysical responses to the lithofacies, helped confirm the characteristics each distinct lithofacies.

6.3 Inversion characteristics:

6.3.1 Introduction:

As discussed in Chapter 3 every reflection marks a change in amplitude of the returned wave. The property controlling this change at the interface is the contrast in impedance values, where impedance is the product of velocity and density. The seismic reflection amplitude information can then be used to invert for the relative impedances of the materials on either side of the interface. By correlating these seismically derived properties with the known measured

values from the borehole, the known properties at the wells can then be extended over the entire seismic volume (Barclay, 2008). It helps to fill the gaps in knowledge of formation properties between wells.

6.3.2 Lithologies determined from inversion:

The final inversion result can be observed in figure 6.5, with the black horizontal lines representing the five horizons that were input into the low frequency model, and the two purple vertical lines as Penobscot L-30 and Penobscot B-41. Figure 6.6 is associated with figure 6.5 and represents the seismic line from which figure 6.5 is showing and where it is located within the survey area. The seismic line that was chosen crosses both of the wells so the seismic-to-well correlation result can also be observed. The well logs in figure 6.5 begin to blend into the seismic P-impedance values at approximately 1.0s. The well logs are represented by P-impedance as well, and therefore should almost appear invisible if the seismic to well tie is accurate. Some areas within the well section fit very nicely with the P-impedance values of the seismic, demonstrating the seismic to well tie is good in those locations. The areas in which the colors do not match up imply that the seismic to well tie was poor due to inaccurate picks while correlating the actual seismic to the synthetic seismic, leading to poor wavelet estimation.

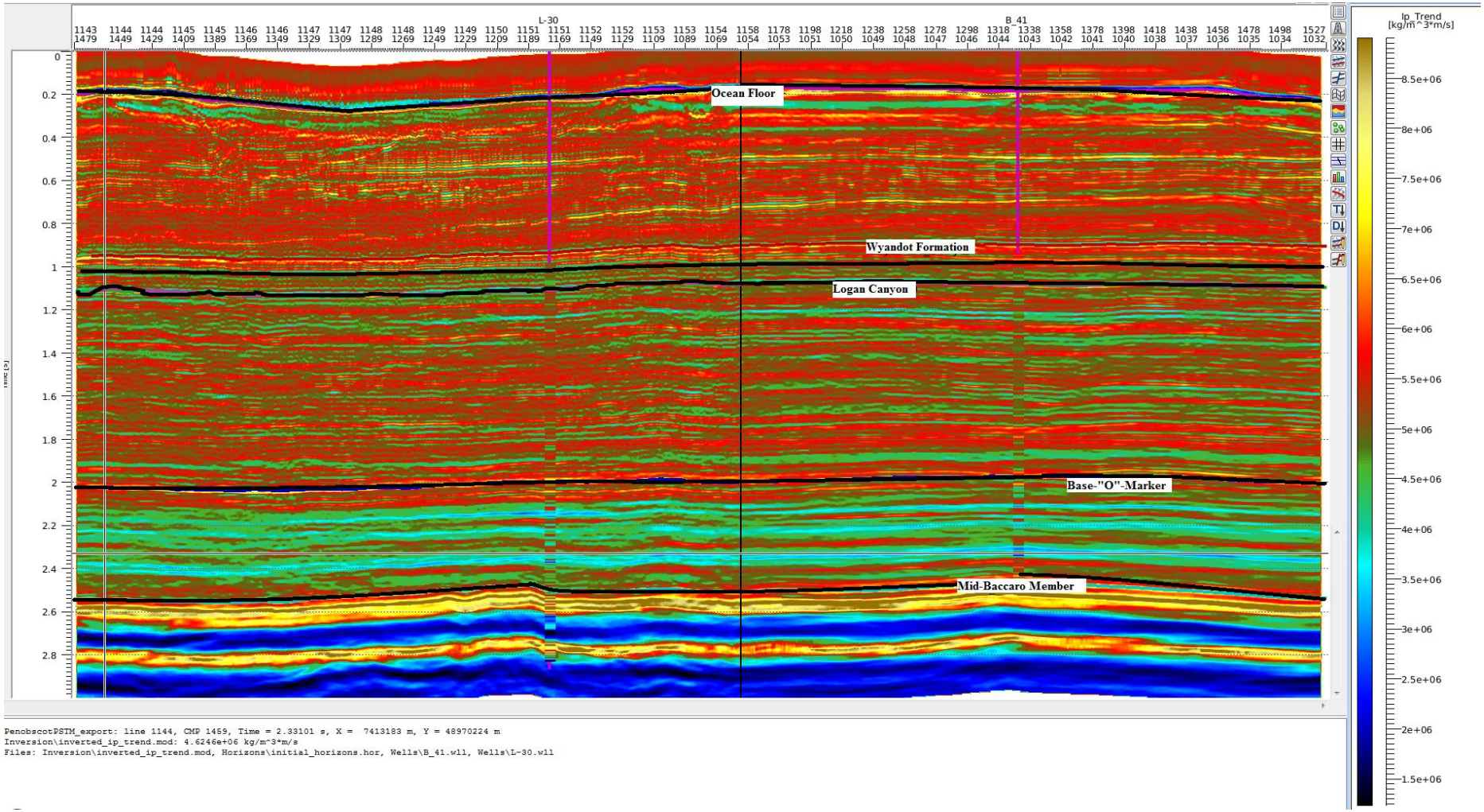

Figure 6.5: Final inversion result. Color representing P-impedance values. The vertical purple lines that blend into the P-impedance values represent the well logs demonstrated with P-impedance as well. The areas which match nicely, indicate good seismic to well ties, where the areas that do not match quite as nice, represent an inaccurate seismic to well tie.

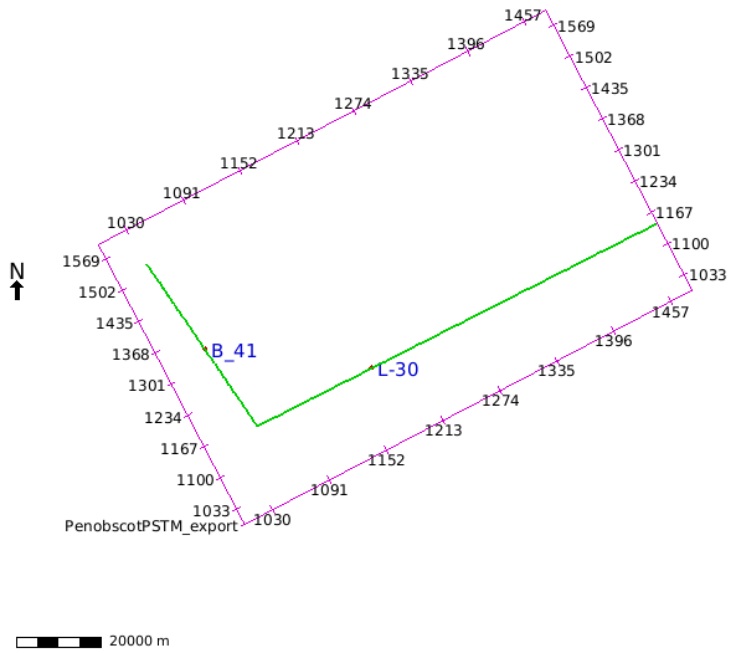

Figure 6.6: Seismic line chosen to represent Figure 6.3. It can be seen that the line crosses over the locations of both wells as indicated.

With the knowledge of the lithology of the area from the cored intervals, examination of well logs and from the interpreted seismic, the Baccaro and the Scatarie members of the Abenaki Formation are interpreted to be carbonate limestones. In the bottom section of figure 6.5, two blue packages can be observed, interpreted to be where the Baccaro and the Scatarie members are located. These carbonates are highly compacted, calibrated from the core descriptions of these units. The velocity of a wave increases within highly compacted material, specifically carbonate (Anselmetti and Eberli, 1993). This is also observed in the impedance log for Penobscot L-30, created from the density and the velocity logs. In the location of both of the carbonate units within the wells, the density is high and the velocity is high, giving a low impedance value. This can be confirmed in figure 6.5 where the blue-low impedance values from the wells match the blue impedance value within the entire survey. With the knowledge that there are shale units between each of the limestone members from the lithological logs and from the gamma ray logs, the yellow packages in between the blue packages in figure 6.5 represent shale. This can be confirmed with

the use of the density and sonic (1/velocity) logs from Penobscot L-30. In this location, the density is low and the sonic is low, giving a high impedance value, demonstrated by the color yellow. This also represents a strong contrast between the carbonate units and the shale units. The size of the packages can also be more easily seen than with seismic data. The results for the bottom section (blue and yellow) appear to be exaggerated compared to the rest of the inversion result. This could be due to the frequency content of the inversion. The data below the Baccaro Member was extrapolated further down in time than what was given, seen in the Solid Model in chapter 5 as the "Below All" horizon. This could be the source of exaggeration.

The formation overlying the Abenaki Formation is interpreted to be the sandstones, siltstones with minor carbonates of the Missisauga Formation. The member of the Missisauga Formation highlighted on figure 6.5 is the limestone "O" Marker. The Missisauga Formation is interpreted to have medium to medium-low impedance values corresponding to the values of the impedance logs from both of the wells as shown by the density and sonic logs. From the cored intervals from Penobscot B-41 taken from the Missisauga Formation, it is confirmed that the lithologies present have a carbonate influence with some intervals having higher concentrations of calcite and calcareous-rich sediments. Comparing the greenish blue intervals in figure 6.5 to the known blue carbonate layers of the Abenaki Formation it can be interpreted that the inversion result suggests there are calcareous rocks throughout the section, trending upwards to sandstones and siltstones, indicated by the red, medium impedance values indicating shallowing depositional conditions (Figure 6.7). The top view (Figure 6.7) of the Missisauga Formation represented by a time slice around the time interval of the "O" Marker shows many greenish-blue impedance values; again signifying carbonate or carbonate influenced lithologies, as well as red, indicating

sand-rich areas. The faint vertical lines cutting across the time slice represent artifacts created during the inversion process from the seismic data.

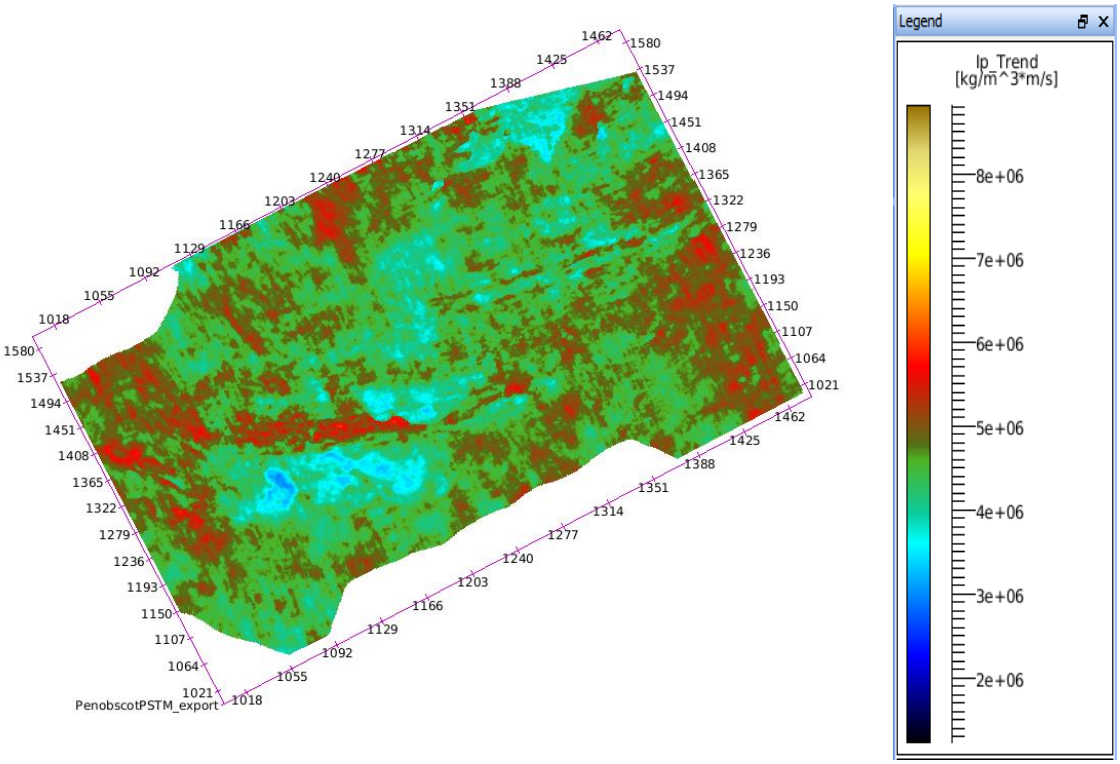

Figure 6.7: Time slice of the top of the "O" Marker, the color represents inverted P-Impedance values. Greenish-blue impedance values representing carbonate influenced lithologies dominating most of the time slice, although there is also higher impedance values (red) indicating sand-rich areas.

Sandstones and shales of the Logan Canyon Formation can be identified as having medium-low to medium-high impedance values. The impedance logs throughout the Logan Canyon Formation demonstrate medium impedance values, corresponding to the appropriate P-impedance colors. The shales however do not appear obvious on the 2D section of the inversion result in figure 6.5. With closer inspection, the top views of the Logan Canyon Formation do indeed have high impedance values indicating there is shale present, however the amounts are too minor to appear in the view of the entire area; this can be observed in figure 6.8. In this figure, both of the normal listric faults are outlined with high impedance values, indicating shale had in filled the space created by the offset of the faults. The red and green impedance values

represent calcareous-rich lithologies as well as sandstones. The faint vertical lines representing artifacts created during the inversion, from the seismic data.

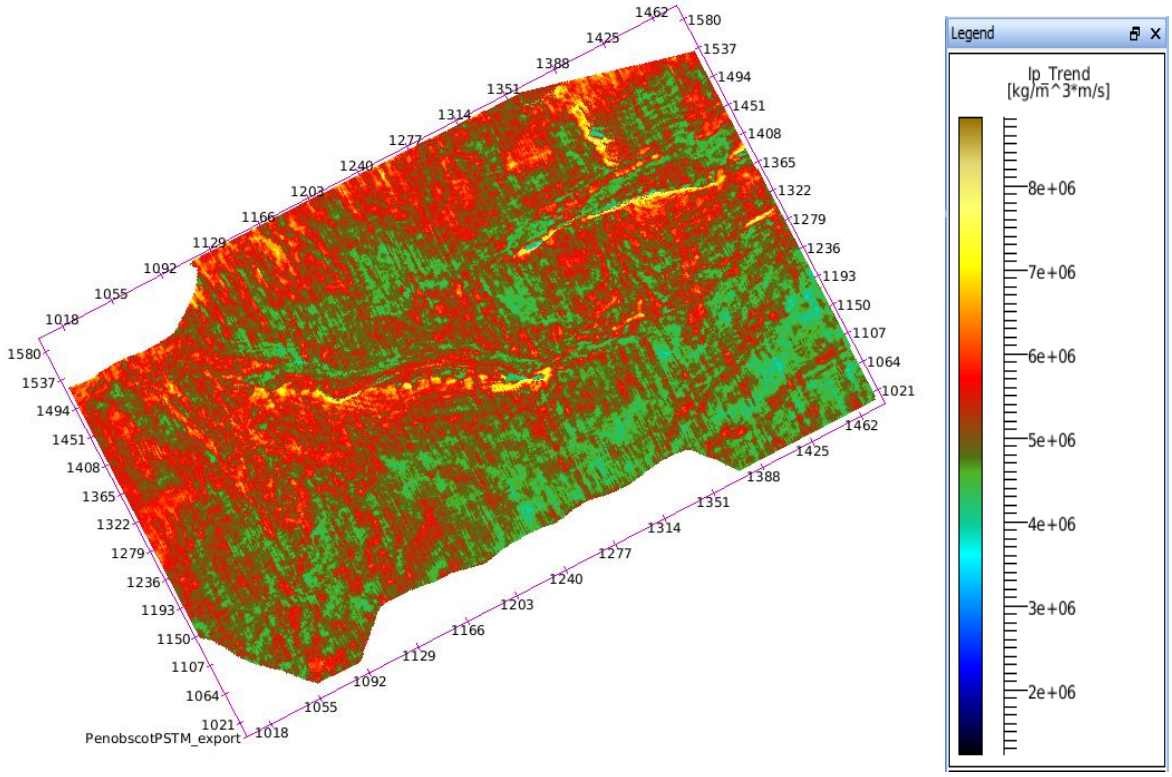

Figure 6.8: Time slice of the top of the Logan Canyon Formation, color indicating inverted P-impedance values. This time slice is dominated by green and red impedance values (medium values) representing carbonate-influenced lithologies, as well as sand-rich areas being present throughout the area.

The Wyandot Formation, composed mainly of chalk carbonate, can be interpreted to have medium-high to medium impedance values. This interpretation can also be confirmed by the impedance log for both of the wells, created from the sonic and density logs, which both demonstrate low to medium impedance values. The logs for both the density and the sonic log, however, only have data for the bottom half of the Wyandot Formation, potentially skewing the data. The colors of the impedance values correspond to carbonate by being greenish-blue, although there are also areas rich in sandstone. In figure 6.9, there are large polygonal shaped fractures throughout the chalk of the Wyandot, which appear to be filled with sand. The slight outline of the

faults can also be seen in the top view of the Wyandot Formation, and confirmed to contain minor amounts of shale within the offsets. Faint vertical lines are artifacts created during the seismic inversion process.

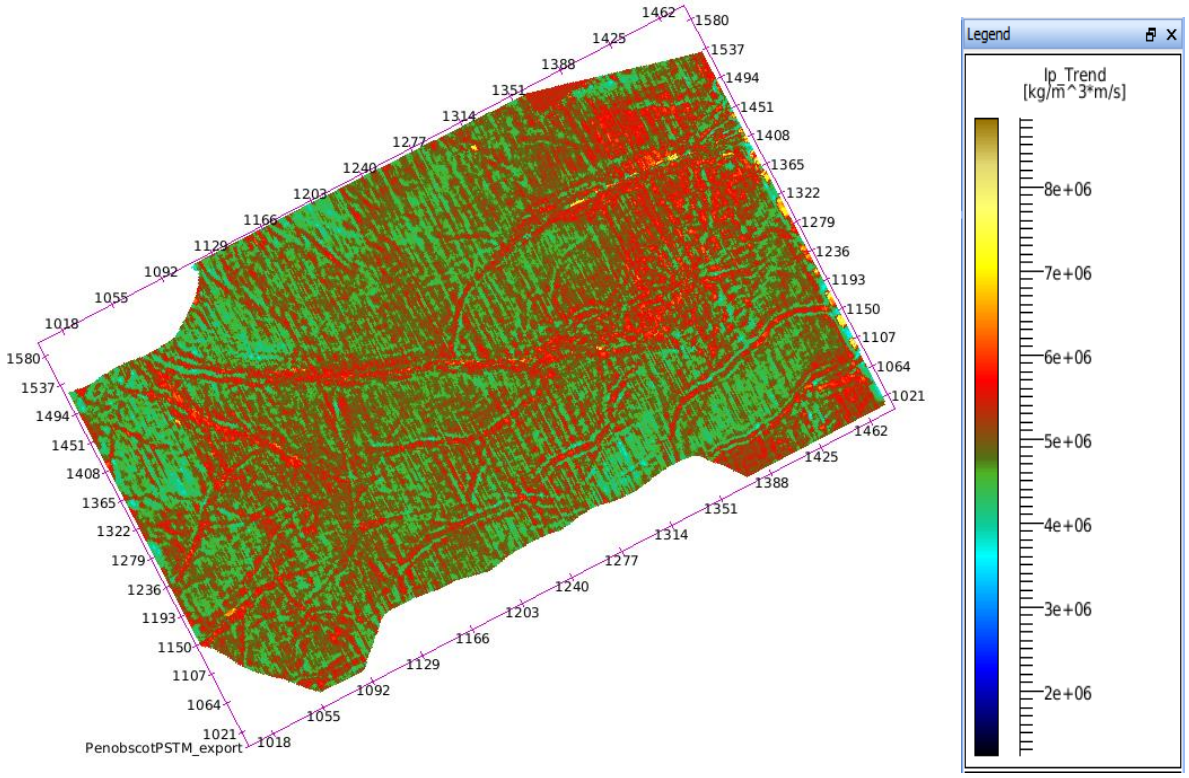

Figure 6.9: Time slice of the top of the Wyandot Formation, color represents inverted P-Impedance values. Primarily composed of greenish-blue impedance values, interpreted as carbonate-influenced lithologies, and sand-rich sediments infilling the large polygonal fractures represented by medium-high impedance values (red).

The last unit that can be observed in figure 6.5 is the Banquereau Formation, represented by high to medium-low impedance values. This formation has previously been interpreted as containing mainly shale beds and minor amounts of sandstone. The abundance of impedance values representing sandstone throughout this section could potentially have been skewed, due to the density log not extending through the Banquereau Formation, therefore giving improper results. Figure 6.10 represents the top of the Banquereau Formation containing carbonates with

the lowest impedance values, and the red and yellow intermixed sediments are composed of shale and sand. The slumped area within the Banquereau as previously described in Chapter 5 can be seen as the greenish-blue impedance values throughout the middle of figure 6.10. The Banquereau Formation has been eroded from this slumping feature down to carbonate-rich lithologies, potentially that of the Wyandot Formation.

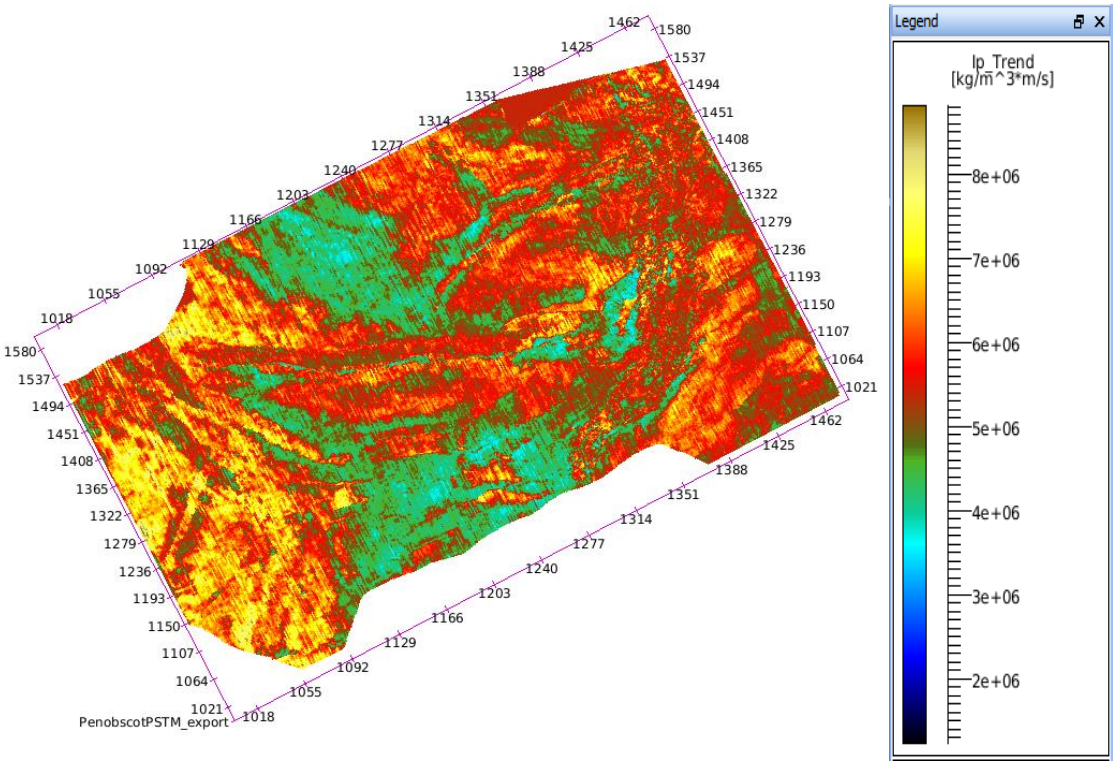

Figure 6.10: Time slice of the top of the Banquereau Formation, color represents inverted P-Impedance values. Impedance values representing primarily sand-rich lithologies and some carbonate influenced lithologies as a result of the slump feature in the middle of the figure being eroded.

CHAPTER SEVEN: CONCLUSIONS

7.1 Conclusions:

This study examined all components that comprise the Penobscot dataset; 3D seismic, two wells with accompanied wireline logs and cored intervals as well as minor horizon data. With the use of different methods and geological softwares, interpretations of seismic facies, petrophysical facies, structure, stratigraphy and lithology were made and correlated throughout the entire survey area. From this, an inversion was run, integrating all data analyzed from the Penobscot dataset. The seismic inversion that was performed for this study was the first non-proprietary analysis completed on the Scotian margin focusing on whether inverted acoustic impedance would aid in the distinction of lithology within the Scotian Basin. From interpreting the tops of the formations within the wells and then correlating those to the seismic, the approximate location and thickness throughout the Penobscot area of each formation was concluded, which allowed for the interpretation of seismic facies within the formations. Interpreting the seismic facies allowed for the lithologies to be better defined and understood. The core from both well also allowed in the distinction of lithofacies present within the Baccaro and Scatarie members of the Abenaki Formation, as well as the Lower Missisauga Formation. The description of lithofacies from these locations correlated appropriately with the lithology distinction made from the seismic facies as well as from the comparison to the petrophyiscal facies interpreted from the wireline logs. All this was done to confirm the lithology types and their distribution within the Penobscot area, before the inversion was run.

This study drew several conclusions about the strata of the Penobscot area.

1. The Penobscot cored intervals represent lithologies of the Abenaki Formation and of the Missisauga Formation, which can be further subdivided into nine lithofacies. The lithofacies examined from both wells indicate depositional environments in relatively shallow-water settings.
2. The interpreted lithofacies were able to be correlated to the wireline logs of both wells and petrophysical facies characteristic of the core intervals, where distinguished, identifying the lithologies present amongst both wells.
3. Identifying locations and approximate thicknesses of formations within the seismic data with the use of chosen well tops allowed for the interpretation of seismic facies, further confirming the lithologies present and their distinct characteristics within the survey area.
4. The inversion worked by identifying independent primary velocities and the densities in each cell of the 3-D stratigraphic grid. These velocities and densities were coupled during the inversion and yielded an accurate map of lithology with the additional help of selecting the correct wavelet scale and using a layered-based framework that was consistent with the seismic stratigraphy.
5. Inverted acoustic impedance allowed for proper thicknesses of formations to be determined and structural elements within the Penobscot area to be better understood.
6. The inversion result confirmed the correlation of the lithofacies to the petrophysical facies and enabled geological properties to be known within the entire survey area.
7. Inverted acoustic impedance allowed for the interpretation of lithologies based off of the velocity and density of the defined formations, although present knowledge of the lithology characteristics was needed to deduce the interpretations.

8. A proper seismic to well tie determines the inversion result, if the tie is good the exact locations of the formations can be known and the extent to which they extend throughout the area can be easily identified. If the tie is poor, the location of specific lithologies will not be known and the wavelet will be poor creating an inaccurate inversion.
9. Inverted acoustic impedance gives an accurate representation of the lithology present within the Penobscot area, and therefore can be used with further analysis within the Scotian Basin to distinguish locations of petroleum systems.

7.2 Recommendations for future work:

In order to fully understand the lithology present with the use of inverted acoustic impedance within the Scotian Basin the following measures should be taken:

1. Cross-plots of acoustic impedance versus porosity can be constructed, with the data points colored to represent specific formations, distinguishing where the porous zones are within the Penobscot area. This would help conclude which intervals are sandstones and which are shales.
2. From the cross-plot, a model can be made representing porosity, similar to that of figure 6.5 (P-impedance). This will indicate where in the Penobscot area the porous reservoirs are located.
3. Further petrophysical facies analysis of the entire length of both well logs (Penobscot L-30 and B-41) to correlate the log responses to the lithologies present within the Penobscot Area.

REFERENCES

Anselmetti, F. S., & Eberli, G. P. (1993). Controls on sonic velocity in carbonates. *Pure and applied geophysics, 141*(2-4), 288-290.

Barclay, Bruun et al. (2008). Seismic inversion: Reading Between the Lines. *Oilfield Review,* 42-44.

Bowman, Faber, J., & Harvey, P.J. (2003). Petroleum Systems of Deepwater Scotian Basin, Eastern Canada: Challenges for Finding Oil versus Gas Provinces. 2003 Offshore Technology Conference held in Houston, Texas, U.S.A., 5–8 May 2003.

Bjorlykke, K. (2010). Petroleum geoscience: From sedimentary environments to rock physics, 361-366.Oslo, Norway: Springer-Verlag Berlin Heidelberg.

Crane, P., & Clack, P. (1992). Final report on the 3-d seismic survey offshore Nova Scotia. CNSOPB.

Cummings D.C., & Arnott R.W.C. (2005). Growth-faulted shelf-margin deltas: a new (but old) play type, offshore Nova Scotia. *Bulletin of Canadian Petroleum Geology, 53*(3), 211-236.

CNSOPB. (2000). Canada-Nova Scotia Offshore Petroleum Board. Technical Summaries of Scotian Shelf Significant and Commercial Discoveries, Canada-Nova Scotia Offshore Petroleum Board, Halifax. p.257.

CNSOPB. (2008). Canada- Nova Scotia Offshore Petroleum Board Call for Bids 2007-2008. Retrieved September 2013 from http://www.callforbids.cnsopb.ns.ca/2007/01/regional_geology.html.

CNSOPB. (2010). Canada- Nova Scotia Offshore Petroleum Board.Exploration History. Retrieved September 2013 from http://www.cnsopb.ns.ca/geoscience/geoscience overview/exploration history.

Dunham. (1962). Dunham's Carbonate Rock Texture Classification. Modified by Embry & Klovan, (1971), and by Wright, (1992).

Fensome, R.A., & Williams, G.L. (2001). The last billion years. (pp. 135-139). *Atlantic Geoscience Society.* Halifax: Nimbus Meister, Semaphor Design Company.

Flügel, E. (2010.). *Microfacies of carbonate rocks*. (pp. 662-663). New York: Springer Heidelberg Dordrecht London New York.

Hansen, Møller, D., Shimeld, J.W., Williamson, M. A., Lykke-Anderse, H. (2004).

Development of a major polygonal fault system in Upper Cretaceous chalk and Cenozoic mudrocks of the Sable Subbasin, Canadian Atlantic margin. *Marine and Petroleum Geology 21*, 1205–1219.

Ings, Steven J. R., MacRae, A., Shimeld, J.W., & Georgia Pe-Piper. (2005). Digenesis and porosity reduction in the Late Cretaceous Wyandot Formation, Offshore Nova Scotia: a comparison with Norwegian North Sea chalks. *Bulletin of Canadian Petroleum Geology, 53*(3), 237-249.

ION Geophysical. (2009). Intelligent acquisition makes winning debut for ion. 27(1), Retrieved December 2013 from http://fb.eage.org/publication/content?id=28718.

Jansa, L.F. and Wade, J.A. (1975). Geology of the continental margin off Nova Scotia and Newfoundland: in Offshore Geology of Eastern Canada, Vol. 2, Regional Geology, Van der Linden, W.J.M. and Wade, J.A. (Eds.), *Geol. Sur. Can.*, Paper 74-30, 51-106.

Jansa, Lubomir F, & Noguera Urrea, V.H. (1990). Geology and Diagenetic History of Overpressured Sandstone Reservoirs, Venture Gas Field, Offshore Nova Scotia, Canada. *The American Association of Petroelum Geologist Bulletin, 74*(10) 1640-1658.

Jason- a CGG Company. (2013). Introduction to acoustic impedance inversion. Fugro Jason.

Kidston, A.G., Brown, D.E., Smith B.M., & Altheim, B. (2005). The Upper Jurassic Abenaki Formation Offshore Nova Scotia: A Seismic and Geologic Perspective. *Canada- Nova Scotia Offshore Petroleum Board.*

Kumar, D. (2013). Applying backus averaging for deriving seismic anisotropy of a long wavelength equivalent medium from well-log data. *Journal of Geophysics and Engineering*, *10*(5).

Mitchum, R.M., JR., P.R. Vail, S. Thompson (1977) Seismic Stratigraphy and Global Changes of Sea Level, Part 2: The Depositional Sequence as a Basic Unit for Stratigraphic Analysis. in Seismic Stratigraphy: Applications to Hydrocarbon Exploration (AAPG Memoir 26) Payton, Charles E.(ed) *American Association of Petroleum Geologists*, Tulsa, Oklahoma USA.

Mondol, N.H. (2010) in Bjorlykke, K. (2010). Petroleum geoscience: From sedimentary environments to rock physics, 361-366. Oslo, Norway: Springer-Verlag Berlin Heidelberg.

Mukhopadhyay (Muki), Prasanta K., Brown D.E, Kidston A.G, Bowman T.D, Faber J, Harvey P.J. (2003). Petroleum Systems of Deepwater Scotian Basin, Eastern Canada: Challenges for Finding Oil versus Gas Provinces. Offshore Technology Conference held in Houston, Texas, U.S.A.

Natural Resources Canada. (2010). Stratigraphic overview. Retrived December 2013 from http://www.nrcan.gc.ca/earth-sciences/energy-mineral/geology/marine geoscience/geology-of-scotian-margin/7013>.

Robertson. (2000). Frontier Reservoirs of the North Atlantic. *Canada Nova Scotia Offshore Petroleum Board, 1,* 270-271.

Sangree, J.B., and Widmier, J.M. (1979). Interpretation of depositional facies from seismic data. *Geophysics, 44,* 131-160.

Stoker, M.S., Pheasant, J.B., & Josenans, H. (1997). Seismic methods and interpretation. In, T.A. Davies, T. Bell, A.K. Cooper, H. Josenhans, L. Polyak, A. Solheim, M.S. Stoker, J.A. Stravers (Eds.), Glaciated Continental margins: An atlas of acoustic images, pp. 9-19.

Vail, P.R, R.M. Mitchum, JR; S. Thompson (1977) Seismic Stratigraphy and Global Changes of Sea Level, Part 3: Relative Changes of Sea Level from Coastal Onlap. in Seismic Stratigraphy: Applications to Hydrocarbon Exploration (AAPG Memoir 26) Payton, Charles E.(ed) *American Association of Petroleum Geologists,* Tulsa, Oklahoma USA.

Wade, J.A. and MacLean, B.C. (1990). Chapter 5 - The geology of the southeastern margin of Canada, Part 2: Aspects of the geology of the Scotian Basin from recent seismic and well data. In: M.J. Keen and G.L. Williams (Eds.), Geology of Canada No.2 - Geology of the continental margin of eastern Canada. *Geological Survey of Canada*, 190-238.

Wade, J.A, & MacLean, B.C. (1993). East coast basin atlas series: seismic markers and stratigraphic picks in Scotian Basin wells. *Atlantic Geoscience Centre, Geological Survey of Canada,* p. 276.

Wade, J.A., MacLean, B.C., and Williams, G.L. (1995). Mesozoic and Cenozoic stratigraphy, eastern Scotian Shelf: new interpretations. *Canadian Journal of Earth Sciences, 32,* 1462-1473.

Watson, N. (2013). Wireline logging, petrophysics lecture. Atlantic Petrophysics Ltd.

Appendix 1:

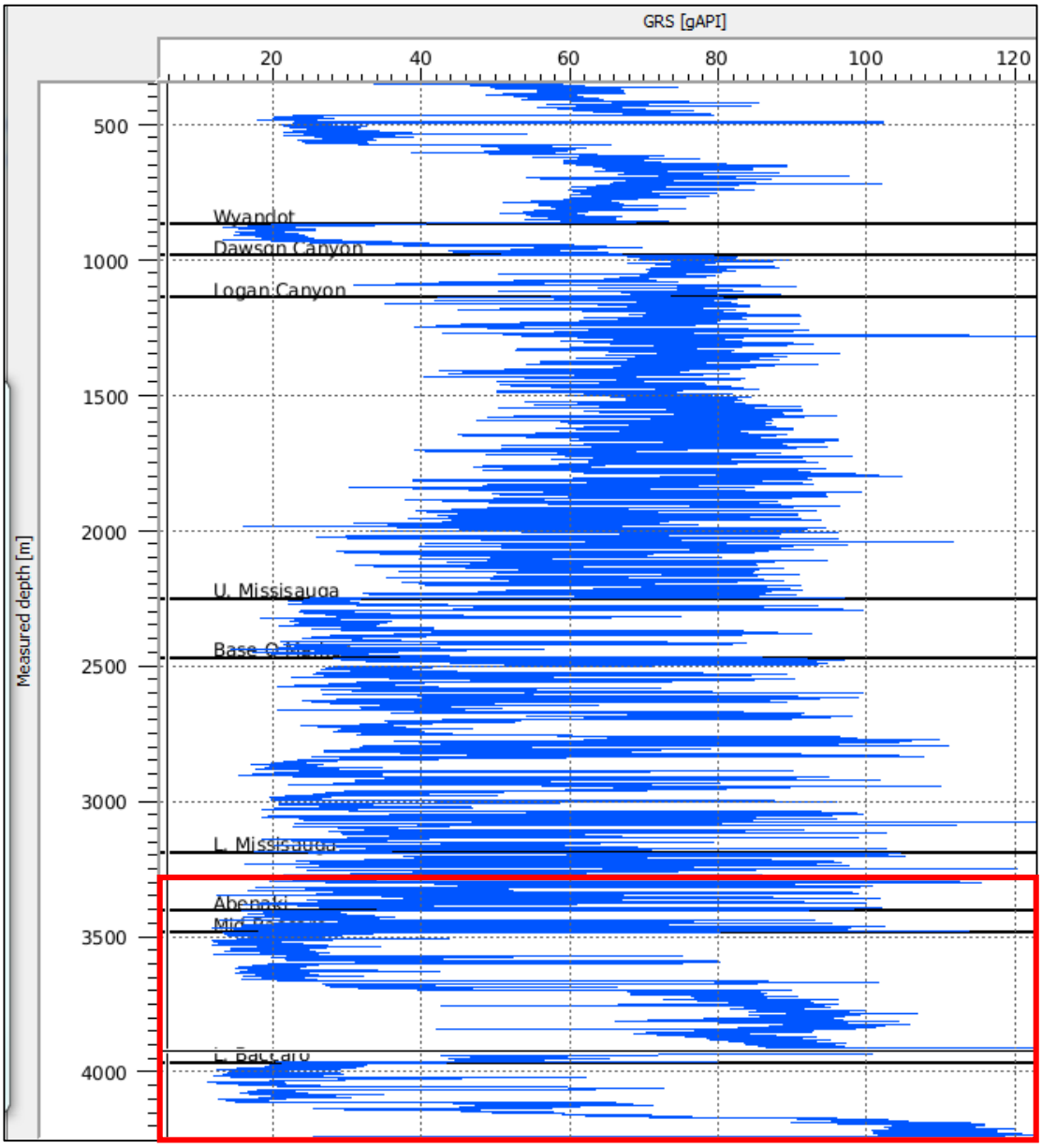

Appendix 1: Entire gamma ray log for Penobscot L-30. Red box indicates the zoomed in area for figure 6.3.

Appendix 2:

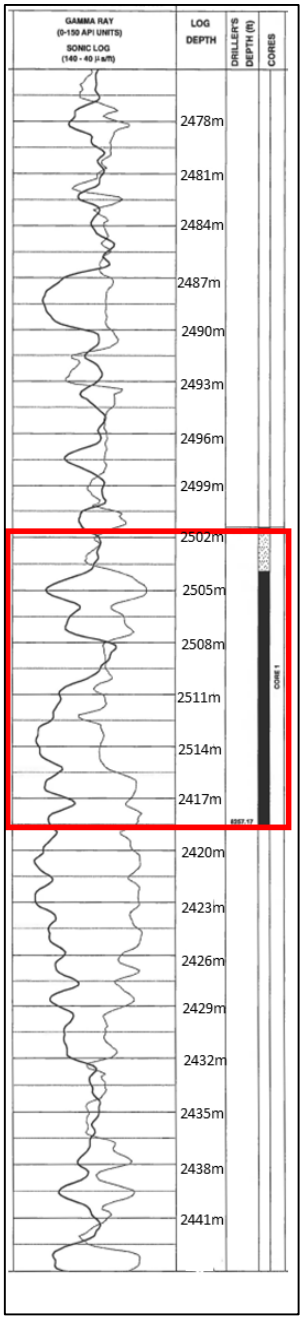

Appendix 2 A: Gamma and sonic log for Penobscot B-41, red box indicating the zoomed in area for figure 6.4 A (modified from Robertson, 2000)

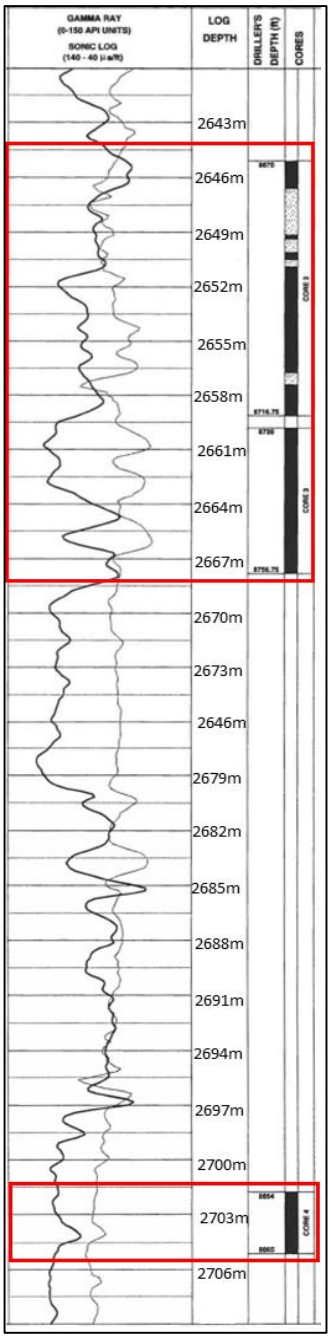

Appendix 2 B: Gamma and sonic log for Penobscot B-41, red box indicating the zoomed in area for figures 6.4 B and C (modified from Robertson, 2000).